DESIGN AND DEVELOPMENT OF AN AUTOMATIC STEERING SYSTEM FOR AGRICULTURAL TOWED IMPLEMENTS

A Dissertation
Submitted to the Graduate Faculty
of the
North Dakota State University
of Agriculture and Applied Science

By

Nadia Delavarpour

In Partial Fulfillment of the Requirements
for the Degree of
DOCTOR OF PHILOSOPHY

Major Department:
Agricultural and Biosystems Engineering

January 2022

Fargo, North Dakota

North Dakota State University
Graduate School

Title

DESIGN AND DEVELOPMENT OF AN AUTOMATIC STEERING SYSTEM FOR AGRICULTURAL TOWED IMPLEMENTS

By

Nadia Delavarpour

The Supervisory Committee certifies that this ***disquisition*** complies with North Dakota State University's regulations and meets the accepted standards for the degree of

DOCTOR OF PHILOSOPHY

SUPERVISORY COMMITTEE:

Sreekala G. Bajwa
Chair

Thomas A. Bon

John F. Nowatzki

Marisol Berti

Sulaymon Eshkabilov

Approved:

April 7th, 2022
Date

Leon Schumacher
Department Chair

ABSTRACT

While an auto steered tractor can improve the overall accuracy and efficiency of an operation, for operations that involve towing an implement, a significant portion of the efficiency reduction comes from uncontrolled motions of the towed implement. Therefore, there is a crucial need to study auto steering system for towed implement as well. In this study different requirements of an auto steering system for a towed implement were developed and studied. In this study the guiding performance of two local positioning sensors (Tactile and Ultrasonic sensors) under similar conditions were studied for reading different trajectories at different traveling speed. Furthermore, a fuzzy logic control algorithm was developed to continually generate correction steering signals and keep the tractor and towed implement within a certain boundary of the reference trajectory. Finally, the designed controller was implemented in a hardware-in-loop (HIL) system to analyze the performance of the controller in real world conditions.

The result of this study showed that although the local guidance sensors could locate the tractor or towed implement positions with respect to plant rows accurately, limitations to the performance of sensors were also observed in certain conditions. Sensors were prone to various noises and digital filters were required to apply to collected data. Data analysis showed that at lower speeds (less than 1.79 m/s) the accuracy of sensors was ±2 cm or better. The fuzzy logic controller improved the trajectory tracking accuracy at slow speeds (1-5 m/s) for following non-complex trajectories while no major improvements were achieved for complex trajectories at these speeds. Therefore, the controller had an acceptable accuracy following straight trajectory with negligible deviations at slow speeds. Moreover, experimental results showed that the hydraulic cylinder followed the controller signals with sufficient accuracy. During the

experiment the angular displacements remained in the range of ±10˚ and never hit the constraint of maximum achievable angle, which was ±30˚. The satisfactory results showed that the designed automatic steering control system has a good tracking performance with a fast response, thus meeting the navigation control requirement of agricultural equipment to a certain extent.

ACKNOWLEDGMENTS

I would like to express my deep and sincere gratitude to my research advisor, Dr. Sreekala Bajwa for giving me the opportunity to work on this research. I would like to express my sincere gratitude to Dr. Sulaymon Eshkabilov for his continuous guidance, motivation, enthusiasm, and immense knowledge. His expertise and wisdom have been invaluable throughout my graduate school career. He has taught me the methodology to carry out the research and to present the research works professionally. I am extremely grateful to Dr. Thomas Bon and Mr. John Nowatzki for their invaluable supports throughout this journey. It was a great privilege and honor to work and study under their guidance. I would also like to thank Dr. Marisol Berti. Her dynamism, vision, passion, and motivation have deeply inspired me.

This research was possible thanks to the funding provided by the North Dakota State University Agricultural Experimental Station project ND 01557, the USDA-NIFA award No. 2016-69004-24784, "CropSys—A novel management approach to increase productivity, resilience, and long-term sustainability of cropping systems in the northern Great Plains". In addition, I would like to say thanks to the personnel of Reichhardt Electronic Innovations, Mr. Jayme Paquin, Mr. Josh Kistner, and Mr. Chad Braaten for providing required technical tools and equipment to conduct the experiments of this study. The completion of this project could not have been accomplished without their support.

I am extremely grateful to my parents for their unconditional love, caring, and sacrifices for educating and preparing me for my future. A very special word of thanks goes for my sister and brother, whose blessing and guidance are with me in whatever I pursue.

Finally, I would like to thank my caring, loving, and supportive husband, Amin Vedadi. His encouragement when the times got rough are much appreciated and duly noted.

DEDICATION

To my beloved family

Mom, Dad, Kimia, Kaivan

and to my love,

Amin

Thank you all for your unconditional love, support, and encouragement.

TABLE OF CONTENTS

LIST OF TABLES

LIST OF FIGURES

LIST OF APPENDIX FIGURES

1. INTRODUCTION

1.1. Motivation

Autosteering system for agricultural machines is considered a key factor that can significantly improve the accuracy and efficiency of agricultural operations. Without an accurate autosteering system, an operator has to adjust the position of the vehicle with respect to boundaries of driving path while performing other tasks including tilling, planting, and applying fertilizer and pesticides. In these situations, even the most experienced drivers can make mistakes such as damaging crops by running over plant rows, skipping areas between passes, and over-applying inputs through overlaps between passes. Autosteering systems not only could reduce the human errors but also improve efficiency of field operations by avoiding overlaps or skips, reducing excess maneuvers of vehicles in fields, reducing fuel and chemical consumption, reducing the pressures on an operator, and decreasing the operator's fatigue.

The artificial intelligence (AI) used in autosteering agricultural machines should be flexible to adapt operating parameters of the machine to suit their operating environments. Compared with the working environments of on-road vehicles, agricultural fields are considered unstructured and uncertain environments that require higher machine intelligence to achieve adequate precision in operations. Therefore, on-road autosteering system concepts and designs are not suitable for agricultural machines that work on complex and dynamic conditions of agricultural fields. In order to develop the autosteering systems for these environments accurate models and designs of agricultural autosteering systems are required.

Moreover, towed implements are commonly used in major agricultural operations, and there is no guarantee that the towed implements attached to an autosteered tractor will follow the tractor path correctly because of the high nonlinear dynamics of the implement motion and

running environment, especially at headlands and turns. A towed implement that does not accurately follow the tractor path could easily damage plants and reduce the efficiency of agricultural operations conducted in fields with standing crops. Therefore, an autosteering system for a towed implement is also necessary to minimize damages to plants during field operations.

The major challenges in designing agricultural autosteering systems comes from the nonlinear behaviors of the tractor and towed implement, sensor and steering system capabilities, and uncontrollable noises and disturbances. The techniques explored for system control are valid locally, meaning their functions highly depend on a limited range of running speeds and environments and are restricted to a certain size of the tractor or towed implement. Consequently, there is still a need for additional research to improve the functionality of the tractor and towed implement autosteering systems with acceptable performance at an affordable cost.

1.2. Hypothesis and Objectives

The main goal of this project was to develop an autonomous steering system for a tractor and towed implement to keep them from running over plants while driving between rows. The project was divided into three objectives:

Objective 1: Determine the success of local guidance sensors in positioning a vehicle with respect to plant rows

Hypothesis 1: Local guidance sensors provide sufficient accuracy for positioning a vehicle in a field with respect to plant rows

Objective 2: Analyze a fuzzy logic control algorithm to steer a tractor and towed implement autonomously

Hypothesis 2: A fuzzy logic controller provides sufficient accuracy to steer a tractor and its towed implement autonomously

Objective 3: Develop a hydraulic actuator system to analyze the performance of the fuzzy logic controller in real world conditions

Hypothesis 3: Design of a hydraulic actuator and its characteristics affect the performance of the fuzzy logic controller.

2. LITERATURE REVIEW

Autosteering systems employ three major steps to steer vehicles automatically. The first step is to accurately determine the position of machines with respect to the reference driving path in real time using a guidance sensor. Without a guidance system, it becomes an operator task to observe the position of the vehicle and continuously adjust the steering angle. In the second step, a steering command is generated based on the sensor output, which is then sent to a controller unit to determine the best traveling speeds and steering angles that keep the tractor and towed implement on the correct trajectory. A qualified control system requires high control accuracy, good reliability, and quick response to achieve accurate and prompt steering control on an automated agricultural machine. The last step is the execution of the steering commands that were generated by the control algorithm in the previous step to follow an optimal trajectory. A compact electric motor or hydraulic actuator is directly mounted to a vehicle steering wheels to accurately adjust the position of tractor and towed implement with respect to the boundaries of the trajectory. Each of these three steps are executed by the guidance sensors, control system, and steering mechanism respectively and can significantly affect the steering accuracy and efficiency of agricultural operations.

Sensor type and placement on vehicles are the parameters that initially define the accuracy of a guidance sensor. Several types of sensors and positioning technologies have been used to provide absolute or relative positions of tractor and towed implements, but many of these sensors are vulnerable to the outside disturbances. This vulnerability can result in inaccuracies in positioning the tractor or towed implement (Hodo et al., 2007). Also, the location of sensor on the vehicle could improve or degrade the accuracy of sensors in reading a correct trajectory.

Therefore, sensor types and their placements should be selected wisely to minimize inaccurate measurements and provide better steering for tractor and towed implements.

When a towed implement runs over plant rows, it has real implication on crop yield. It is very common for a towed implement to follow a different trajectory than the tractor because of the diverse, complex, and non-smooth field environment, as well as the limited maneuverability of the vehicles. In order to minimize errors in following a trajectory, accurate steering control algorithms should be used on a tractor and its towed implement to ensure this combined unit follow a defined trajectory and to control the lateral and longitudinal movements of the combined unit. Due to the vehicle's dynamic variables, tractor and towed implements are basically nonholonomic constraint systems. Therefore, traditional control methods cannot directly be employed to design these controllers.

After receiving generating the correction signal using a proper control algorithm, it is necessary to have a steering linkage between a tractor and the towed implement (called actuation system) that has high control accuracy, good reliability, and real-time response. As the actuation system transfers power from a tractor to the towed implement, the hitch control dictates the performance of tractor and towed implement combination (Bhondave et al., 2017). The hitch control should prevent unwanted and excess movements of the combined unit. The accuracy, control stability, and response speed of the tractor and towed implement actuation are affected by hitch controller performance and the hitch system design. The actuation system also affects the maximum steering rate (Oksanen & Backman, 2013). Thus, the actuation systems for agricultural vehicles require precise design and analysis of the performance.

Many research studies on autonomous agricultural vehicles, are reviewed based on navigation and control viewpoints in this study. I discussed the technical characteristics of

different guidance sensors, control algorithms, and steering actuation mechanisms developed for agricultural purposes. Also, I analyzed advantages and disadvantages of each system.

2.1. Guidance and Positioning Sensors

There are specific criteria for ensuring accuracy of positioning systems in agricultural environments, include independency from weather condition and light intensity, real-time response to fast changes in trajectory, and having a simple structure at a reasonable cost. Not all sensor types meet these criteria at the same time (Gray, 2002). Combining different technologies could remarkably improve the performance of agricultural positioning sensors but could increase the complexity of the system at the same time. The review of some of the most common agricultural guidance system is presented in this section.

2.1.1. Mechanical Guidance System

Mechanical guidance sensors consist of feelers or mechanical arms, that provide a linkage between crop row trajectory and the vehicle. The arm senses the trajectory and sends correction signals to a controller to change the position of the vehicle with respect to boundaries of a desired route. These sensors could be classified into different types based on their installation locations on vehicle, their feeler type, or their method of finding the correct trajectory.

Mechanical guidance sensors have benefits and capabilities of successfully locating/identifying row patterns. These sensors are cost-effective because their costs are restricted to sensing and controlling devices, a simple structure, and easy maintenance (Tillett, 1991). However, there are several factors that could limit the performance of mechanical sensors. These factors include high susceptibility to multiple sources of noises like internal sensor noises and uncontrollable environmental disturbances. To reduce the inconsistency of a sensor output

due to noises and disturbances, internal/external (analogue or digital) filtering may be required. Because the feelers of the sensor should touch the plants to locate the position of the vehicle with respect to the plant rows, these sensors might not have acceptable performance in fields with small, thin, or delicate plants (Delavarpour et al., 2019). Damages to plants could be worse at higher tractor speeds. Another key challenge for mechanical guidance sensors could be skips in plant population or a bare region encountered in the contact environments. These situations lead to interference between the feeler and the crop (Subramanian, 2005). Although, multiple mechanical contacts could be used to overcome this limitation, it could also increase the potential for contact to damage the crops. Considering the benefits and limitations of mechanical guidance sensors, these sensors are only applicable for guiding the vehicles in some agricultural fields at certain stages of crop growth.

2.1.2. Global Positioning Guidance System (GPS)

Global positioning system (GPS) is the only commercialized guidance sensor for agricultural machines that is offered by the agricultural companies as a guidance option on tractors. These systems provide absolute position measurements to increase pass-to-pass accuracy of navigation regardless of environmental factors.

Accuracy levels of GPS guidance depend on availability and reliability of correction signals, quality of GPS receiver, receiver position, and mounting height on vehicles (Gomez-Gil et al., 2011; M. Min et al., 2008). Positioning signal availability and reliability are affected by obstructions next to fields such as trees and buildings (Oksanen & Backman, 2013). These obstructions block satellite signals to the GPS receivers, and GPS cannot effectively navigate a machine (Li et al., 2009). In these environments, accuracy expectation for guidance can be met either by additional means for positioning e.g. integrating GPS with cameras, laser range,

ultrasonic sensors, or by selecting more precise GPS receivers, e.g. employing differential correction signals. However, these integrated systems could increase the complexity and total cost of a guidance system.

Other factors affecting the accuracy of GPS in fields include satellite position in orbit (ephemeris), geometry of the GPS satellites, minimum elevation angle above the horizon (elevation mask), receiver clock timing, receiver type, antenna mounting height, ionospheric and atmospheric delays, and multipath effects (Alonso-Garcia et al., 2011; Chosa et al., 2011). To counter these limiting factors, many researchers develop autosteering navigation systems in agricultural environments without using GPS as a primary sensor for navigation.

2.1.3. Machine Vision Guidance System

The basic concept of machine vision uses navigation sensors, computational methods, and navigation control strategies for measuring the relative position of a vehicle concerning a landmark to estimate the vehicle heading.

Several factors affect the application of machine vision guidance systems that lead to shortcomings in overall performance. Vision sensors may not work properly under heavy weed, dust, and fog conditions. Due to the effects of light source, shadow interference on a target could be a main reason affecting the image accuracy of measurement and segmentation that cause a machine vision system to fail. Because of the many steps involved in image processing required for machine vision systems and the large quantity of information in images, machine vision sensors could be computationally demanding. Thus, computational speed of a machine vision system plays a crucial role in real-time vehicle guidance. Camera location has a number of practical and theoretical effects on performance of a machine vision navigation system. Camera location should be adjusted according to field of view of the sensor, geometric relationship

between image sensors and a vehicle, plant height, etc. Cameras that view additional rows as a result of a larger field of view provide robustness against crop damage. Traveling speed is also considered as a factor that limits navigational accuracy. Basically, traveling speed is estimated based on image processing methods and calculation speed of a system. A majority of the field experiments with machine vision guidance sensors (Guerrero et al., 2017; Meng et al., 2018) were conducted at very low speeds. Image processing methods have significant effects on extracting the correct trajectory, performance, and reliability of these systems.

Researchers have developed methods to successfully eliminate or reduce the negative effects of one or more factors affecting machine vision navigational system. However, reducing the impact of one factor does not necessarily guarantee the improvement of overall performance of guidance systems because the performance may still be under the influence of other uncontrolled factors. Thus, these guidance systems usually integrate multiple sensors (e.g., GPS, laser radar) as complementary tools in order to enhance precision of navigation.

2.1.4. Ultrasonic Guidance Sensor

The working principle of ultrasonic guidance sensors is to calculate the distance of a sensor to a desired object by measuring the time delay between sending and receiving reflected sound signals. Due to relatively simple measuring concepts and a non-destructive method of positioning vehicles, ultrasonic sensors are considered suitable for outdoor areas with mature trees and orchards, where performance of common systems such as GPS and machine vision degrade. Ultrasonic sensors are also perfect options for indoor applications like greenhouses because they operate independent of light intensity and signal receiving. An ultrasonic sensor can provide good accuracy at distances of 15-215 cm and angles of 0-30 degrees (Masoudi et al., 2009).

Performance of ultrasonic sensors is affected by several parameters. Since these sensors locate crops by sensing the reflected ultrasonic signals it emits, any objects in its field of view that reflects the signal could be interpreted as crops. To reduce mischaracterization errors, only the reflected signals from the nearest objects are considered. Also, it is important to avoid other objects, e.g. stray foliage, from coming between the sensor and target. Uncontrollable environmental background noises could negatively impact the performance of ultrasonic sensors. Built-in hardware filters can remove some of these noises, but if they could not remove undesired noises from the sensor readings entirely, digital filters should be applied before analyzing the data (Delavarpour et al., 2020a).

When vehicles operate in confined or narrow spaces, specular reflection can prevent the ultrasonic beam from returning back to the receiver. In these environments, the ultrasonic beam is bounced away from the target object, and after a critical angle of specular reflection, the ultrasonic sensor will not receive the correct response from the object. Also, the target angle (perpendicular and non-perpendicular) also affects the real-time navigation with ultrasonic sensors (Thamrin et al., 2013).

2.1.5. Laser Range Guidance System

The general concept of laser radars is to emit laser radiations or light beams that are capable of working where GPS signals or machine vision guidance systems perform poorly. There are two main types of laser radar sensors, pulsed radiation sensor and continuous radiation sensor. Distance measurement in pulsed radiation is based on radiation flight time, and continuous radiation is based on the modulation phase or frequency of the returned radiation. To guide an agricultural vehicle using laser sensors, at least three reflectors or landmarks around the field are needed to use a triangulation method to define the location of the vehicle. Laser range

radars have the benefits of high resolution and large field of view. These sensors are capable of working individually or as complementary tools to other sensors such as GPS and machine vision guidance systems.

Although laser sensors are fast, able to work in different lighting conditions, and not affected by background noises, the accuracy of these systems could be significantly affected by dirt, dust, fog, and precipitation. Dust, precipitation, or fog can reflect part of the energy of the laser signal, creating echoes. This would demand specific precautions for dust, fog, and precipitation, such as the use of a laser sensor capable of detecting multiple echoes of each measurement pulse.

2.1.6. Sensor Fusion

Because no navigational sensor is perfect for agricultural localization, combining different guidance principals can help to compensate for shortcomings of a certain sensor type and guide vehicles with higher accuracy. The outputs of different individual sensor types are prone to be corrupted by a variety of noises and errors due to spatio-temporal changes in the agricultural environment. Most of these sensors are restricted to a certain type of operations or certain running speed. They might need extensive and expensive preparations in or around the field and some of them require bulky and hindering structures on the tractor or implements. Integrating the inputs of multiple sensors is an effective practice to reduce the amount of uncertainty that may be involved in a guidance sensor. Fusion of sensors bring significant benefits including higher accuracy, versatility, and reliability, in cases of trees or crops missing in the alleyway, navigating close to headlands, or limited field of view.

With regard to the output integration of different sensors, Durrant-Whyte (1990) categorized the fusion sensor configuration in three groups of complementary fusion,

competitive fusion, and cooperative fusion. A sensor configuration is called complementary if sensors do not directly depend on each other but can be combined in order to give a more complete image of the phenomenon under observation. This resolves the incompleteness of sensor data. An example for a complementary configuration is the employment of multiple cameras (Hoover & Olsen, 2000). Generally, fusing complementary data is easy, since the data from independent sensors can be appended to each other (Brooks & Iyengar, 1997). Sensors in a competitive configuration have each sensor delivering independent measurements of the same target (Visser & Groen, 1999). Competitive configurations are used for fault-tolerant and robust systems. An example would be the reduction of noise by combining two overlaying camera images. A cooperative sensor network uses the information provided by two independent sensors to derive information that would not be available from the single sensor. An example for a cooperative sensor configuration is stereoscopic vision – by combining two-dimensional images from two cameras at slightly different viewpoints, a three-dimensional image of the observed scene is derived (Galar & Kumar, 2017).

Although sensor fusion has many advantages to autosteering of agricultural machines, it is not widely used in real world applications. The total cost of integrating several sensors, incorporating technologies for data fusion, and many additional electronic components make these systems complex and unaffordable for the majority of end-users. The reliability of these systems highly depends on their component systems. In terms of algorithm interpretation, data resolution, the amount of data produced, and processing time, conflicting situations can arise because of combination of heterogeneous data (Lin & Lal Tummala, 1994). In order to make sensors fusion guidance systems reliable and affordable, its hardware and software components as well as data integration need to be simplified.

2.2. Control Algorithm

Designing a simple real time steering control system for a tractor and towed implement could be a challenging process due to the inherent characteristics of the system. One of the main challenges is modeling the system in such way the model represents the tractor and towed implement behaviors under various conditions. The model should be simple enough to allow accurate, robust, and/or adaptive control system design. It also should be computationally fast enough to generate the corresponding signal orders with the minimum time delay. Due to the inherent nonlinearities such as non-negligible longitudinal velocity and tire lateral force of a tractor and towed implement system model, it is not always feasible to consider a simple linear model for a system.

A vehicle could be represented with a geometric, kinematic, or dynamic model. Geometric models consider the vehicle's dimension and radius of a road's curvature. Due to the complexity of tractor and towed implements, this method has not been widely applied by researchers. For kinematic models, position, velocity, and acceleration of the vehicle are being considered (Cariou et al., 2010a, 2010b; Delavarpour et al., 2020a; Lee et al., 2004; Leng & Minor, 2017; Nakamura et al., 2000; Zhao et al., 2012). Kinematic models can only have reliable performance for low speeds (< 7 m/s) when the vehicle satisfies pure rolling constraints. Dynamic models consider the position, velocity and acceleration, internal forces from tires, and the vehicle mass, energy, and momentum at high-speeds (Astolfi et al., 2004; Keymasi Khalaji & Moosavian, 2014; Ryu et al., 2008; Zhou et al., 2019). Complex system of equations in dynamic modeling requires identification of complex parameters like, tire vertical force and coefficient of friction for the road surface. These factors are not easy to measure and model.

At low velocities (less than 7 m/s), it is very common to adopt a bicycle model to represent a tractor and towed implement system that does not consider the changes in dynamics of the system. In the bicycle model, vehicle models are reduced to a two-tire configuration at the front and rear axles by assuming similar behavior for left and right tires on the same axle. At these velocities, the effect of lateral load transfer on overall cornering force could be considered small for operations with small steering angles. In this study the most common control systems are briefly reviewed and discussed.

2.2.1. Classical Controller

A classical controller refers to the common controller in industrial applications with simple linear designs. It is considered as a convenient choice for single-input single-output (SISO) systems. In classical motion control laws, the slippage effect is considered as negligible.

Classical controllers, Proportional (P)-Integral (I)-Derivative (D) [PID] may be the most popular classical control algorithms for SISO systems (T. Wu, 2017). PID is model-independent, and effective for many field situations and environments. However, careful tuning is a prerequisite for applying PID control algorithms. Automatic adjustment of the optimal PID steering controller parameters is required in order to avoid the need for frequent offline adjustment. PID controller tuning for a wide range of integrating processes with varying time-delays can optimize the closed-loop performance with respect to certain robustness constraints while providing robustness to delay variance (Eriksson et al., 2009). The integral part (I) of the PID controllers could oscillate the system easily and cause an excessive response that would push the system output beyond the acceptable range. The settling time may also become longer than expected (Franklin et al., 2019). Additionally, the cumulative errors in the control may

saturate the actuator, causing the control effort to be ignored until the saturation is offset (Ang et al., 2005).

The PID classical controllers may not perform satisfactorily for tractor and towed implement systems even when the system is near the reference trajectory. The main reason is that PID controllers do not have any information about the tractor heading angle that is critical to the direction of the implement.

Fuzzy logic controls that mimic human-like behavior are another widely-used classical controllers. A fuzzy logic controller usually works based on human experience/knowledge and does not require a precise mathematical model. Fuzzy logic controllers offer incomparable advantages over other algorithms because of their unique capabilities to combine mathematical equations with knowledge-based linguistic variables by applying simple fuzzy membership functions to control electrohydraulic system in an intelligent way. These controller types eliminate the requirement of the detailed and complicated models for controllers (Delavarpour et al., 2020b; Meng et al., 2015; S. I. Cho & N. H. Ki, 1999; Subramanian et al., 2009; Xue et al., 2012). In a fuzzy logic system, an input is expressed by a combination of variables in a fuzzy set with a membership function via fuzzification (Cheung et al., 2005). Because the fuzzy logic controllers usually are built based on the operator knowledge, several trials and errors are required in order to design the system and more importantly, different controller designs could result with different designers.

2.2.2. Optimal Controller

Optimal controllers use a vehicle model and a simulation process to compute the control commands that will lead to the best tracking of the trajectory (Pradalier & Usher, 2007). The required control trajectory can be optimized over time to determine the minimum time, minimum

control effort, or a combination of these and other relevant costs. This method requires accurate models of the vehicle behavior and a heavy reliance on computational resources. Inputs to these controllers are generally obtained by the combination of feedback and feedforward actions, but feedback probably would not be necessary for most controlled systems unless there are uncertainties and disturbances to the systems.

2.2.3. Adaptive Controller

Self-adaptability and robustness are crucial key factors for the navigation decision-making in agricultural environments due to various unknown, or unpredictable, and irregular features. Because of unavoidable diversity and complexity in operating environments of agricultural vehicles, automatic navigation of a tractor and towed implement might be influenced by the modeling errors, parameter perturbations, external disturbances, and other uncertainties (Liu et al., 2016). Robustness to uncertainties and insensitivity to disturbances for control algorithms are essential in actual applications. To overcome the drawbacks of individual algorithm methods, robust adaptive controllers combine several algorithms to maximize the controlled behavior of tractor and towed implement (Chen et al., 2013; Engeberg & Meek, 2013; Zhang et al., 2013). Adaptive control techniques are advantageous because controllers can be adjusted to match changes in the control modelling they are trying to regulate.

In agricultural environments, repetition of a specific task and varying initial conditions are two important factors that could affect the performance of a system and should be considered in designing an adaptive controller.

2.2.4. Model Based Controller

Model-based controllers were suggested as an evolution of optimal control approaches to deal with constraints on the states and inputs (Kayacan et al., 2016), as well as actuator

saturations. Model-based controller design uses a system model (linear or non-linear model) to represent the controller. A general requirement of these controllers is the minimization of a quadratic cost function with respect to constraints of a system inputs and outputs. The cost function is compounded by the error between the predicted and reference output. The real-time path tracking of model-based controllers depends on their computational capacities.

Model-based controllers could be classified into two major groups, Linear Model Predictive Controller (LMPC) and Non-Linear Model Predictive Controller (NMPC). The LMPCs are generally designed based on trajectory tracking error-based models. For the LMPC techniques, the controlling processes stay around fixed operating-points in most of the applications to allow linearization of the process model. In these applications, vehicles are not capable of staying on-track on a curvilinear path because LMPC depends on fixed operating points for linearization of the process model (Kayacan et al., 2016). Because the model mismatch increases when the system is far away from the actual pattern, it can generate large prediction errors causing instability of the closed-loop system (Falcone et al., 2007). In these cases, a centralized NMPC is a better alternative to the LMPC. The NMPC are computationally heavy and require a clear feasible path to work. Thus, they might not be reliable in curvatures or tight corners.

2.3. Actuation System Design

Non-negligible and varying friction in agricultural environments produce unpredictable sideslip that affects steering performance of a vehicle. The design of an actuation system should account for variations in operating state and operating environments.

Major principal actuator technologies for tractor and towed implements used to convert electronic control signals into useful control outputs in steering include direct current (DC)

motor, electro-mechanical actuators, and hydraulic valves. Direct current motor systems have a short response time in a controllable system with real-time functionality, and they offer the highest precision. The total cost of DC motor actuator is usually expensive, and they might not be suitable for all agricultural operations where holding a constant force for a period of time is required (Hatten Electric Service & Bak-Vol, 2016). Electro-mechanical actuators have force generation limits. Hydraulic systems provide a cost-effective alternative without force generation limits and are commonly used in agricultural environments (Hatten Electric Service & Bak-Vol, 2016).

For the tractor and towed implement applications, where high actuating forces are required, hydraulic piston-cylinder systems are the most popular actuators (Lindner, 2018). In hydraulic systems, the pressurized fluid is supplied by a pressure compensated or load–sensing pump to a valve-controlled piston-cylinder. These steering systems are limited in adaptability and applicability. The control valves of these systems can unload in the neutral position and could lead to hydraulic leakage over long operation periods. Due to leakage in bypass valves (hydraulic pump) and throttle loss at control valves, hydraulic systems may not work with their optimum energy efficiency (Gupta et al., 2019). Reduced energy efficiency might particularly happen during long-time operations that require high-pressure fluid and large energy consumption. High pressure fluid could result in a temperature rise. Therefore, auxiliary methods are required to overcome the shortcoming of each of these actuator technologies.

Combining the electric and hydraulic methods (electro-hydraulic control or EHC) leads to taking advantage of both systems simultaneously. However, new challenges arise when these two methods are combined. EHC systems provide a higher continuous output power compared with DC motor control systems and hydraulic systems. An electrohydraulic servomechanism is

theoretically a good fit for controlling hydraulic pressure electronically. These methods are expensive and have a slow response time and system lag (*Electro-Hydraulic Systems, Potentialities and Limits - Power Transmission World*, 2018).

Designing and developing an EHC system for steering a tractor and towed implement have several challenges including nonlinear behavior. The non-linearity of an EHC steering system is influenced by the valve, cylinder, and control system characteristics as well as by the wheel-ground interactions (Stombaugh, 1997). The nonlinearities of valve switching induce pressure and flow rate oscillations through the hydraulic system with relatively high frequency. These nonlinearity characteristics include deadband, saturation, asymmetry, and hysteresis. Although all these parameters could result in lag and/or unstable responses, deadband is the most influential characteristic that contributes to time-delay and inaccuracy of steering control ((D. Wu et al., 2001). Deadband is caused by system pressure, valve spool overlap, and fluid temperature. Positive overlap in spool valve causes minimal amount of translation to open the valve in each direction that could compromise the safety. Therefore, developing an EHC actuator that accounts for the contribution of each of these characteristics is a challenging process.

3. PERFORMANCE ANALYSIS OF TWO LOCAL POSITIONING SENSORS FOR AGRICULTURAL EQUIPMENT[1]

3.1. Abstract

Cover crops have been gaining popularity in the Northern Great Plains as an effective practice to improve soil health. Field observations showed that the towed implement often trample on plant rows, indicating a need for the development of an accurate guidance strategy for the farm equipment during field operations. An accurate guidance system when planting cover crops between rows of standing corn (*Zea mays* L.) requires a precise navigation tools to avoid damaging standing crop. In this study, the capabilities of two guidance sensors, an ultrasonic sensor and a tactile sensor, were evaluated for automatic local guidance of a tractor and towed implement. The objective of this study was to determine the performances of these two navigation sensors to guide a tractor and towed implement between crop rows under different operating conditions (e.g., speed, tracking trajectory). For this purpose, a test unit was designed in order to capture the performances of sensors at the same simulated conditions viz. different patterns of plant rows (reference trajectories) and different operating speeds. The output of sensors (voltage [V] for tactile sensor and distance [mm] for ultrasonic sensor) varied as the distance of plants to sensors changed. The sensor outputs were collected to analyze the performance of sensors for reading five different reference trajectories (left side, right side, sinusoidal, step, zigzag) at five different speeds (0.45, 0.9, 1.34, 1.79, and 2.23 [m/s]). The initial

[1] The material in this chapter was co-authored by Nadia Delavarpour, Sulaymon Eshkabilov, Thomas Bon, John Nowatzki, and Sreekala Bajwa. Content in this chapter was published in Design, Simulation, Manufacturing: The Innovation Exchange, 541-551, Springer, and 2019 ASABE Annual International Meeting. Nadia Delavarpour had primary responsibility for preparation and performing of the tests. Nadia Delavarpour also drafted and revised all versions of this manuscript. Sulaymon Eshkabilov and Thomas Bon helped in conducting the experiments, data processing, and interpreting the results. Sreekala Bajwa and John Nowatzki supervised the project and served as proofreaders (Delavarpour et al., 2019, 2020a).

analyses of collected data showed that the output of sensors was too noisy and inconclusive; thus, several digital filters for both sensors were tested and applied to find the best digital filter for each sensor. A Low-Pass Butterworth filter and a Gaussian filter were considered as best options to smooth the data collected with the tactile and ultrasonic sensors, respectively. Analysis of the smoothed data showed that the outputs of both sensors were in the expected range. However, due to the difficulties in adjusting the sensitivity of the ultrasonic sensor and similarity of the sensor outputs in reading the distance to the rows on left and right sides, outputs of this sensor were unreliable and were not used for further data analyses. The performance of tactile sensor was evaluated in terms of time delay in generating output signals and accuracy of measuring the distance to the plant rows. The performance of the tactile sensor was acceptable in reading all reference trajectories at lower speeds (0.45 and 0.9 m/s). At higher speeds (1.34 and 1.79 m/s), the performance of the tactile sensor decreased significantly for reference trajectories with sharp changes (sinusoidal and zigzag). A considerable time delay in generating the output signals was observed at 1.79 and 2.23 m/s regardless of reference trajectory pattern. The performance of tactile sensor at 2.23 m/s for all the tested trajectories were not acceptable. Thus, it was concluded that the ultrasonic sensor requires a substantial revision regarding the sensitivity adjustment and the tactile sensor only should be used for low speed operations (less than 1.5 m/s).

3.2. Introduction

Increased and sustained agricultural productivity is a key to meeting increasing global demands for food and energy. Automation of agricultural machinery is one of the ways to improve the efficiency and productivity of various field operations, such as tillage, planting, chemical application, and harvesting. Accurate and optimal navigation of agricultural machinery

will result in reduced operation time and energy inputs. Subsequently, it will reduce production costs and improve the timeliness of field operations. The goal of autonomous navigation or guidance in agriculture is to control the trajectory traced by the vehicle and keep it within a constant distance to the adjacent driving line (Backman et al., 2012). A driver does not need to manually steer a vehicle with an autonomous navigation system. These guidance systems improve the precision of farming by minimizing the swath overlaps or skips. Also, they reduce the amount of inputs delivered to the field, crop damage, soil compaction, and soil rutting.

In the northern Great Plains and Midwest, interseeding or fertilizing between the rows of planted crops is done in the early stages of crop growth. The purpose of interseeding is to plant cover crops. During cover crop planting, crop plants can be run over by a tractor and towed implement. This problem was reported by farmers and machinery companies, and validated during our own field experiments in 2017. This indicates a need for an accurate navigation system to control movements of the towed implements and to steer it exactly between the planted crop rows. Therefore, this study was undertaken with the goal of identifying and validating navigation ability of two local guidance sensors, tactile and ultrasonic sensor.

3.3. Materials and Methods

Three major tasks were conducted to accomplish the objective of this study, including developing a system to monitor performances of the guidance sensors, simulating the vehicle dynamics in laboratory conditions, and analyzing the performances of sensors in different conditions. For this purpose, a flexible test unit was built from two-sets of snowmobiles, a hydraulic hitch, and a hydraulic power pack to analyze the guiding performance of the sensors in controlled situation of the laboratory. Two local positioning sensors, ultrasonic and tactile (Hall Effect) sensors (Reichhardt ® Electronic Innovation), were selected for the lab evaluation.

3.3.1. Sensors

3.3.1.1. Tactile Sensor

The tactile sensor (PSR TAC, Reichhardt®Electronic Innovation, Hungen, Germany) used in this study consists of two yellow rod-shaped arms (paddles) with flexible sensing ends called the feeler (Figure 3.1.a). Also, in the centerline of the sensor shown in Figure 3.1.b, there is a hall-effect sensor that generates electrical signals when feelers are flexed (Figure 3.1.b). The output of the hall-effect sensor (for each side of the sensor) is between 0.5 V to 4.5 V, depending on how far the yellow paddle is flexed. As a paddle gets closer to the centerline, the output voltage gets higher. Conversely, if the plant is far off the centerline and touches the far end of a paddle, the output voltage value gets lower. Output voltages were converted to the physical distance from the sensor centerline to plants using calibration models.

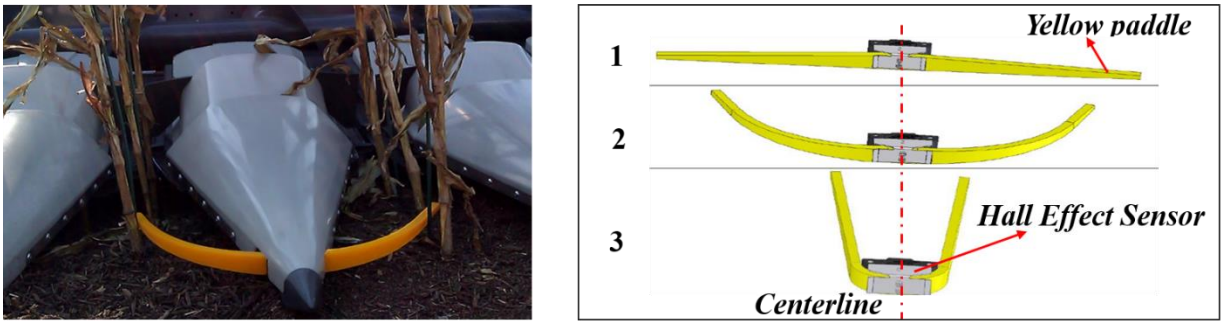

(a) (b)

Figure 3.1. (a) Tactile sensor for measuring the distance between the plants, (b) 1. Tactile sensor with stretched paddles, 2. Tactile sensor with middle range deflected paddles, 3. Tactile sensor with minimal scope of paddle deflection.

3.3.1.2. Ultrasonic Sensor

The ultrasonic sensor (PSR SONIC, Reichhardt®Electronic Innovation, Hungen, Germany) used in this study consists of a sound frequency emitter and a receiver. The sensor measures distance to plants by measuring the time required to emit and reflect back the sound frequency from the plant (Figure 3.2). Because of the dynamic environment in agricultural fields,

an emitted signal might be disturbed and returned back from a number of objects or obstructions other than the desired plant. Objects and obstructions include soil clumps, weeds, or adjacent plant leaves. These obstructions may introduce errors or noises into the sensor reading. To reduce the effect of these misreading, the sensitivity of the signal receiver was set in such a way to record the responses only from the nearest objects. For a better reading of the row patterns, two ultrasonic sensors were used side-by-side (Figure 3.2. a), one of each to read the plant row on the right side (sensor 1) and the other for the left plant row (sensor 2). The outputs of these sensors were the distance of the sensor to plants on left and right sides (mm).

(a) (b)

Figure 3.2. Ultrasonic sensor for measuring the distance to the plants.

3.3.2. Test Unit Design

A test unit (Figure 3.3) was designed to simulate the vehicle's movements in the field. It was composed of seven major components: (1) three-phase motor (WEG Electric, Jaraguá do Sul, Santa Catarina, Brazil) to run the system, (2) a power supply (Delta Electronics/Industrial Automation, Taipei City, Taipei, Taiwan), (3) sensors to find the path based on positions of plants, (4) an analogue to digital (ADC) convertor to make the sensor signals readable to an actuator, (5) two snowmobile tracks to simulate the movement of vehicle between the rows, (6) a

hydraulic power pack as a source of hydraulic power (Dayton Electric MFG. CO. Chicago, IL, USA), and (7) a hitch or hydraulic actuator (ProTrakker Guidance Systems, Odebolt, IA, USA) for the actuation section.

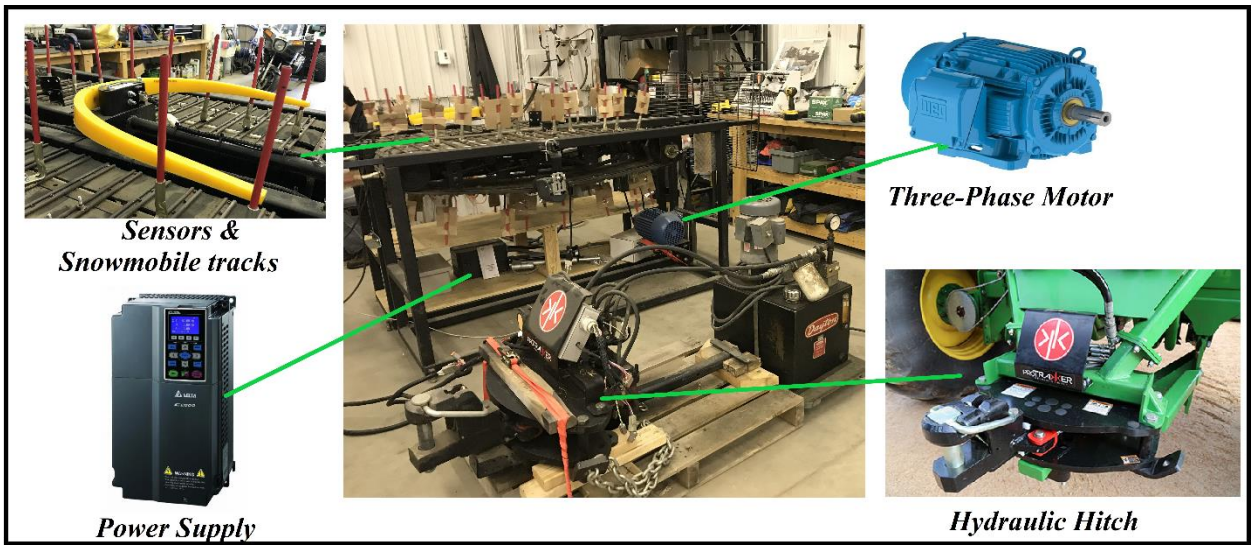

Figure 3.3. The main components of the test unit developed to test auto-guidance sensors.

A pair of snowmobile sets (Figure 3.4) were used to simulate the movement of tractor and towed implement between the crop rows. The total length of the snowmobiles was 304.8 cm. Plants in early stage of growth were simulated on the snowmobile set using 20 small bars (on each side) at 14-cm spacing. The distance between left and right rows was 76 cm. The rotation of the snowmobiles simulated the tractors movement through the plant rows. Sensors were installed in the centerline of the snowmobile tracks to guide the vehicle between the plant rows (Figure 3.4).

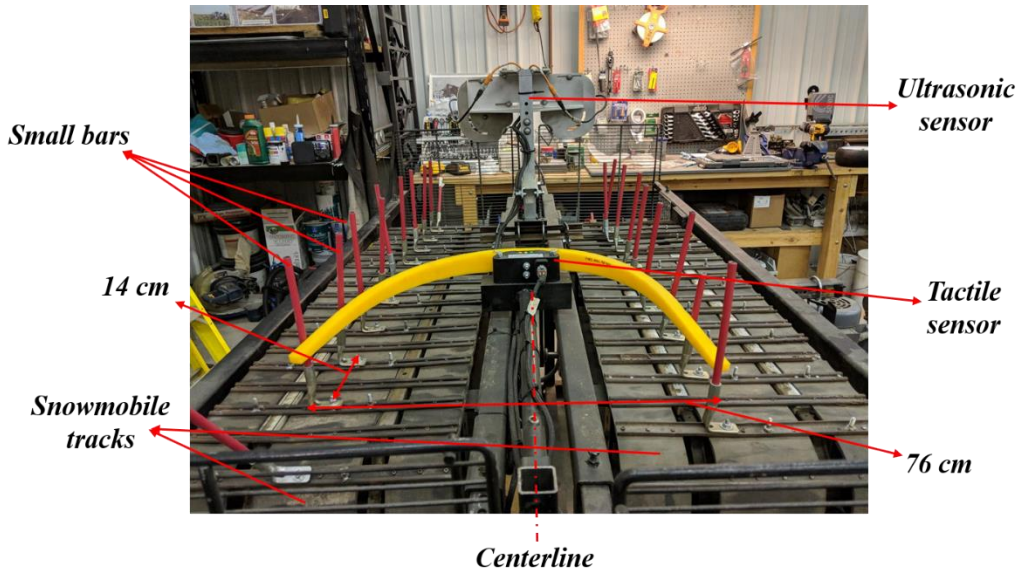

Figure 3.4. Snowmobile tracks and small bars used to simulate the movement of tractor and towed implement between the crop rows.

3.3.3. Conversion Equations

The reference trajectory (also mentioned as the row pattern in this study) was the actual physical distance of the small bars (also mentioned as plants) to the sensors. The sensor outputs were collected in millivoltage for the tactile sensor and centimeter for the ultrasonic sensor. Conversion equations were developed to convert the outputs of sensors to their respective distances.

To develop the conversion equation for the tactile sensor, the output voltages of the left and right sensors were recorded for several defined distances between yellow paddles. The minimum and maximum output voltage of the tactile sensor were 5 and 450 mV for 120-cm and 20-cm distances between paddles respectively.

The relationship between the output of sensors (voltage) and the physical distance between small bars was produced using trend line mathematical equation. The best model fitted into collected data was derived as the conversion equation. The second order polynomial regressions with R^2= 0.9788 for the hall-effect sensor on the right side (Figure 3.5) and

R^2=0.9756 for the hall-effect sensor on the left side (Figure 3.6) were selected as models that fits the data best (Equation 3.1 and Equation 3.2). Although with the third order trendlines the calculated R^2 for left and right sensors were 0.9964 and 0.9967 respectively, the improvement of the prediction was not significant and the second order was decided as the fit model for both left and right sides. In Figure 3.5 and Figure 3.6, solid line shows the collected data and blue dots is the regression model fitted into the data. The x variables in Equation 3.1 and Equation 3.2 are output voltage of tactile sensor (mV) and the y variables are the distance between the yellow paddles of the tactile sensor (cm).

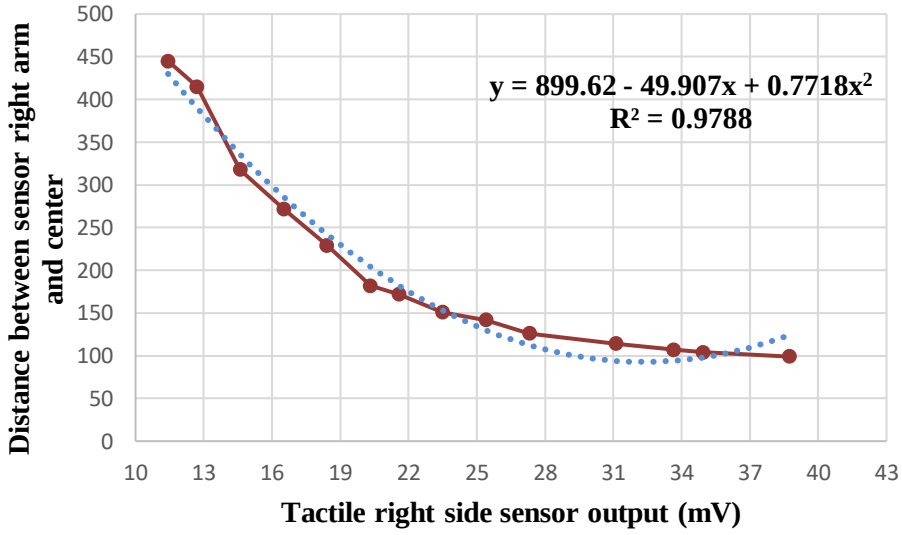

Figure 3.5. The second order polynomial regression model fitted into right side tactile sensor data, solid line: the collected data, blue dots: the regression model fitted into the data.

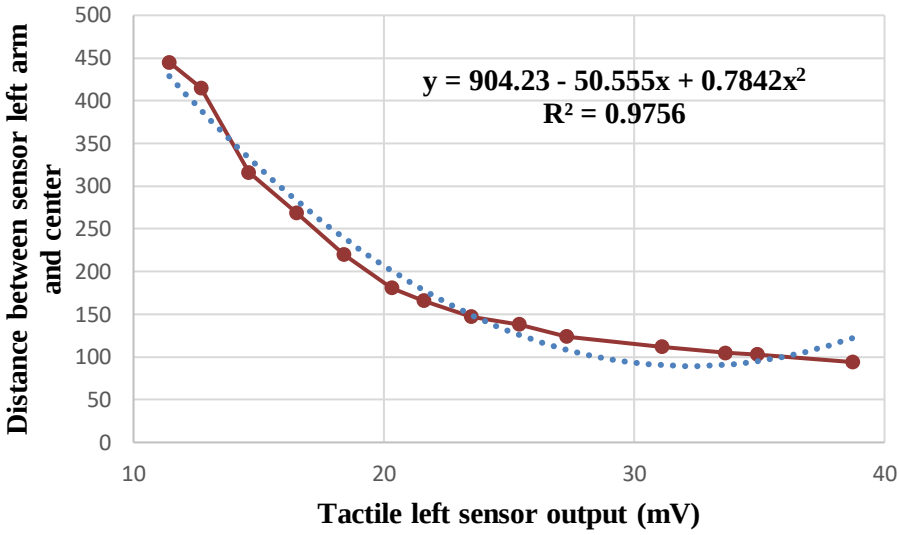

Figure 3.6. The second order polynomial regression model fitted into left side tactile sensor data, solid line: the collected data, blue dots: the regression model fitted into the data.

$$y = 899.62 - 49.907x + 0.7718x^2 \quad \text{(Equation 3.1)}$$

$$y = 904.23 - 50.555x + 0.7842x^2 \quad \text{(Equation 3.2)}$$

For the ultrasonic sensor, the emitters emitted the sound frequencies at $\alpha = 37°$ (Figure 3.7). The distance (cm) of the sensor to the small bars was converted to the distance of the small bars (plants) to the center line of the path (leg C in Figure 3.7) using the cosine equation:

$$C = d\cos\alpha \quad \text{(Equation 3.3)}$$

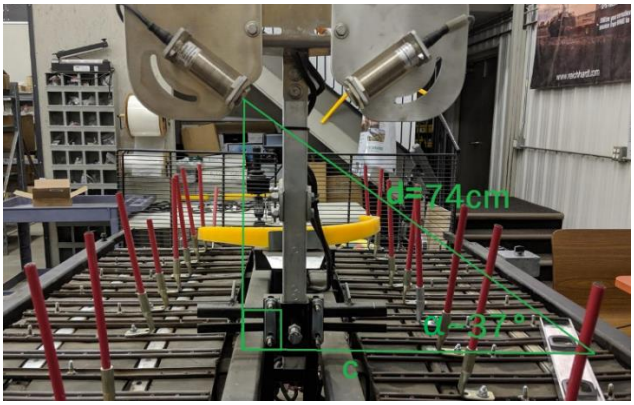

Figure 3.7. Adjusted angle of ultrasonic sensor to emit the sound frequency.

3.3.4. Experimental Design

The laboratory tests were designed to analyze the performances of the two sensors in measuring the distance to crop rows. Tests were conducted in the laboratory to limit many uncertainties present in a field experiment, while allowing to control factors affecting sensor performance, such as reference trajectory and traveling speed. Experimental test study cases are presented in Table 3.1.

Table 3.1. Experimental test study cases

Type of sensors	Tactile and Ultrasonic
Velocity	5 Constant velocities (0.45, 0.9, 1.34, 1.79, and 2.23 [m/s])
Reference trajectory	5 patterns (left side, right side, sinusoidal, step, zigzag)
Sampling duration	2 min. (each test)
Sampling frequency	100 Hz

To simulate the field conditions, five different reference trajectories (left side, right side, sinusoidal, step, zigzag) were created by changing the pattern and spacing of small bars on the snowmobile tracks. Figure 3.8 shows bolts attached to snowmobile tracks used to change the position of small bars on snowmobile tracks and simulate different reference trajectory. The five created trajectories (left side, right side, sinusoidal, step, and zigzag) are shown in Figure 3.9. These trajectories were considered as the boundary that should be followed by sensors. Also, the snowmobile tracks were rotating at five different speeds (0.45, 0.9, 1.34, 1.79, and 2.23 [m/s]) to simulate the traveling speeds of a tractor in the field.

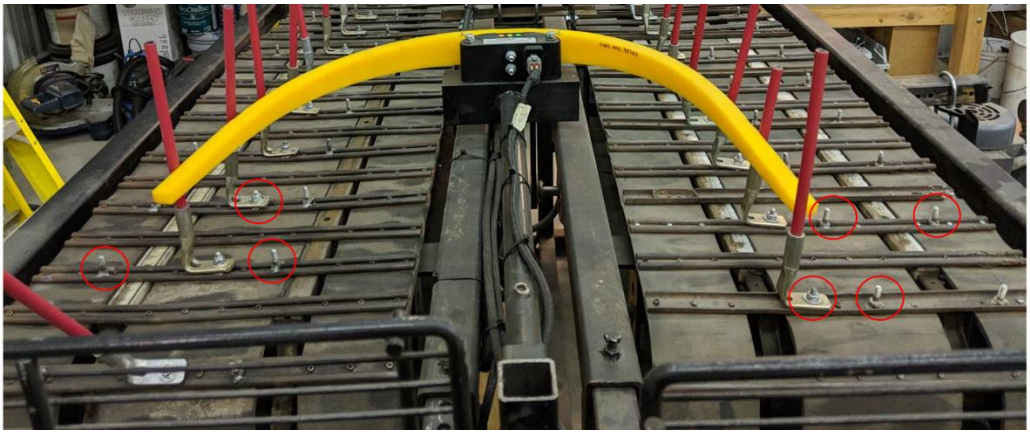

Figure 3.8. Bolts on snowmobile tracks used to change the positions of small bars and simulate various trajectories.

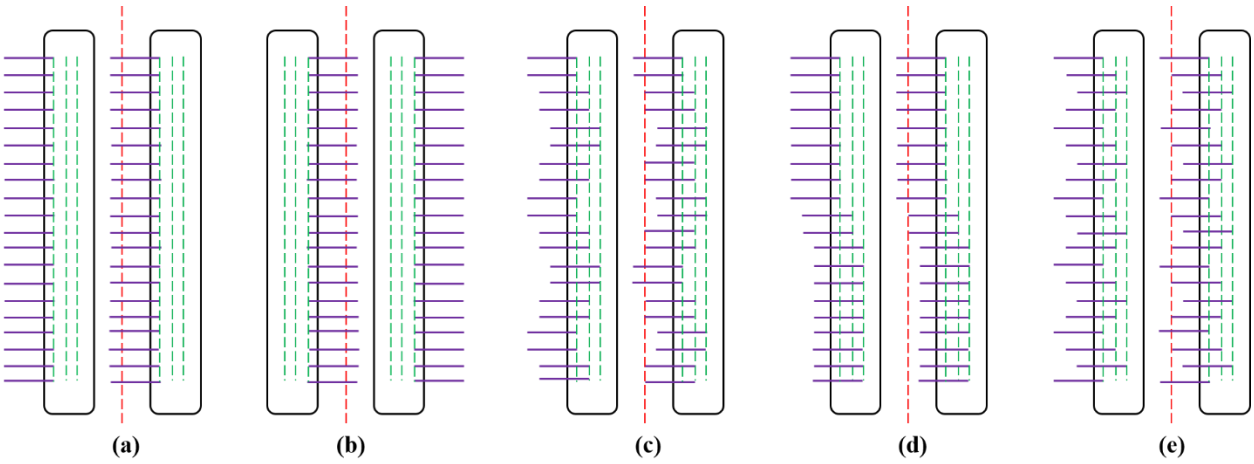

Figure 3.9. Different trajectories created by various arrangements of small bars on snowmobile tracks, (a) left side, (b) right side, (c) sinusoidal, (d) step, and (e) zigzag.

3.3.5. Accuracy Assessment of Sensors

The combinations of five different speeds and five different trajectories were repeated three times for each sensor. A total number of 75 experiments were conducted for each sensor. The sampling frequency of each test was 100 Hz and the duration of running each test was two minutes.

To analyze the accuracy of sensors in measuring the distance to plants, the time delay in generating an output signal (τ) and the lateral error in measuring the distance to the small bars (ε)

were calculated. The time delay (τ) in generating the output signals was calculated as the difference between the time when the sensor sees a small bar and the time when the sensor generates the output signal. This time delay (τ) was calculated using cross-correlation method [Dudáček, 2015]. In this method the time delay (τ) is computed by comparing the time difference between a peak in the reference trajectory and the immediate maximum output of a sensor after the peak. The permissible time delay for each experiment depends on the traveling speed and the distance between plants in a row. In this study the distance between the small bars (plants) in row was fixed (14 cm). The rational for the distance between the small bars is that the common seed spacing for corn in different states is between 8 to 25 cm (Golden Harvest, n.d.). In this study an average of this interval was considered. Thus, for tested speeds of 0.45, 0.9, 1.34, 1.79, and 2.23 [m/s] the permissible time delays were 0.31, 0.15, 0.1, 0.08, and 0.063 s respectively. The average sensor time delay (τ) was calculated for each experiment. The average sensor time delay (τ) and the permissible time delay at different speeds were compared using one-tailed t-test to test an alternate hypothesis that the sensor time delays (τ) are significantly different from the permissible time delays at the 95% level of confidence. The summary of sensor time delay testing hypothesis at different speeds is:

$$\begin{aligned} H_0 &: \tau \le 0.31s \\ H_A &: \tau > 0.31s \end{aligned}$$ At 0.45 m/s

$$\begin{aligned} H_0 &: \tau \le 0.15s \\ H_A &: \tau > 0.15s \end{aligned}$$ At 0.9 m/s

$$\begin{aligned} H_0 &: \tau \le 0.1s \\ H_A &: \tau > 0.1s \end{aligned}$$ At 1.34 m/s

$$\begin{aligned} H_0 &: \tau \le 0.08s \\ H_A &: \tau > 0.08s \end{aligned}$$ At 1.79 m/s

$H_0 : \tau \leq 0.063s$
$H_A : \tau > 0.063s$ At 2.23 m/s

Also, the mean absolute error (MAE) in the sensor reading (ε) from a reference trajectory was calculated for each experiment. The method that was used to calculate the MAE from a reference trajectory is shown in Figure 3.10. Considering the dimension of the tractor and towed implement and the spacing between the rows, an offset of ±2 cm was selected as the permissible MAE in following the centerline between rows. The MAE of sensor readings and reference trajectory were compared using one-tailed t-test to test an alternate hypothesis that the lateral errors in the sensor readings were significantly higher than ±2 cm at an alpha value of 0.05. The summary of testing the lateral errors in the sensor reading hypothesis is:

$H_0 : \varepsilon \leq \pm 2cm$
$H_A : \varepsilon > \pm 2cm$

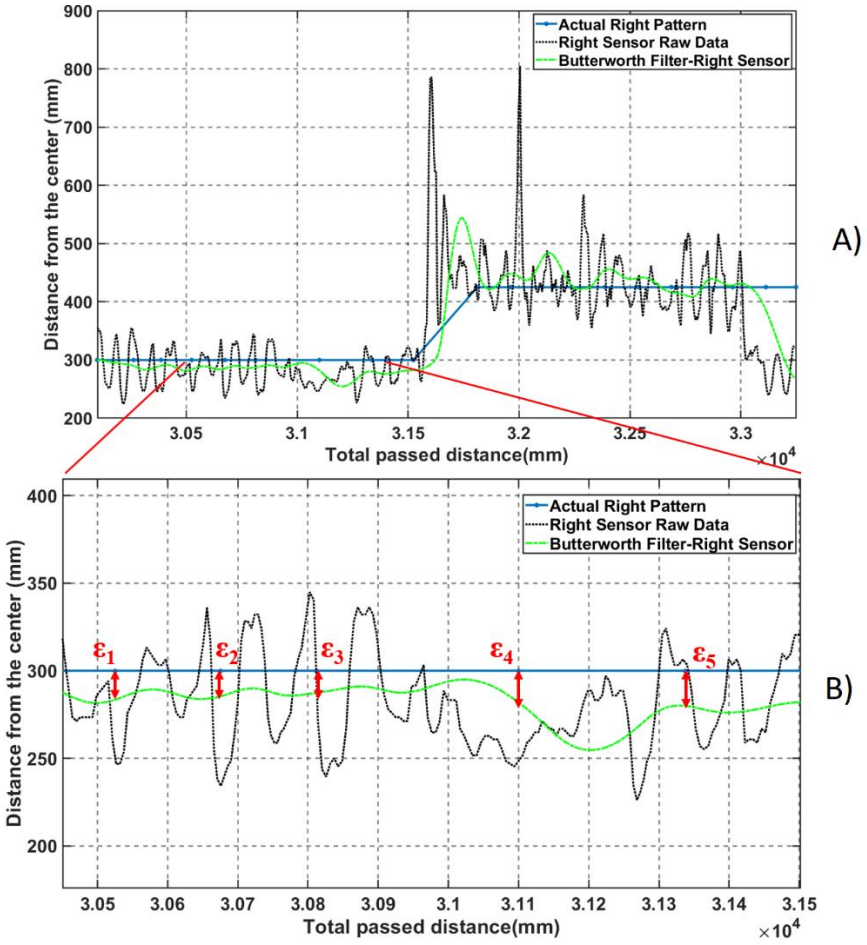

Figure 3.10. Mean absolute error (MAE) measurement between the A) sensor reading (ε) and B) the actual row pattern.

3.3.6. Sensor Signal Processing

Although sensors had built-in data filtering systems, the initial analyses of data showed that outputs are too noisy. The built-in filters were not sufficient to remove all the undesired noises and disturbances from the recorded signals. The noisy raw data collected from the tactile and ultrasonic sensors for the whole period of running the experiment are shown in Figure 3.11 and Figure 3.12 (top graphs). For better illustration of noises, 10 seconds of the plots were zoomed-in and shown in bottom of Figure 3.11 and Figure 3.12. In these figures, the *x* axis is the time in which the data were captured by the sensor and *y* axis is the distance of plants to the centerline of the trajectory.

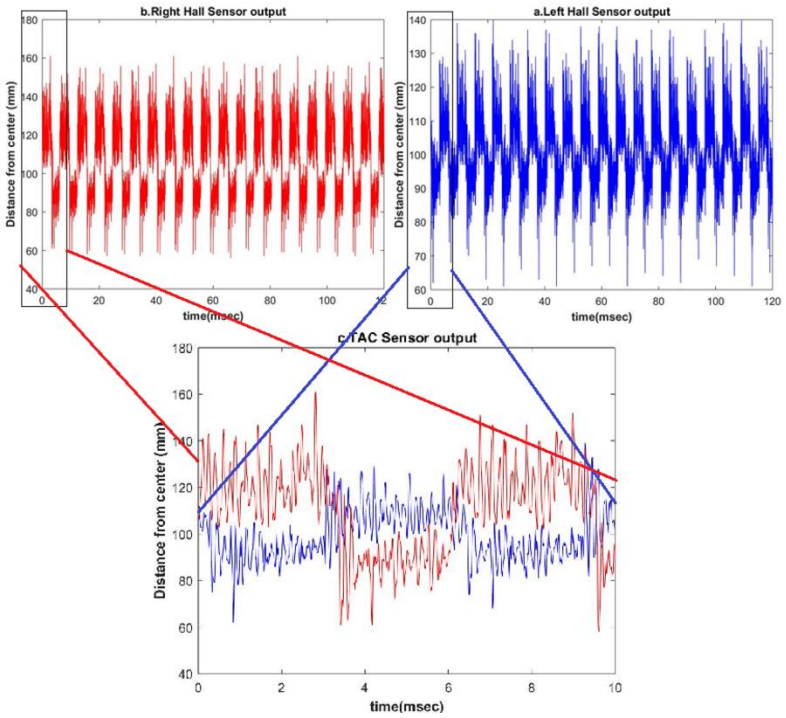

Figure 3.11. Initial observation of noisy raw data collected by the tactile sensor.

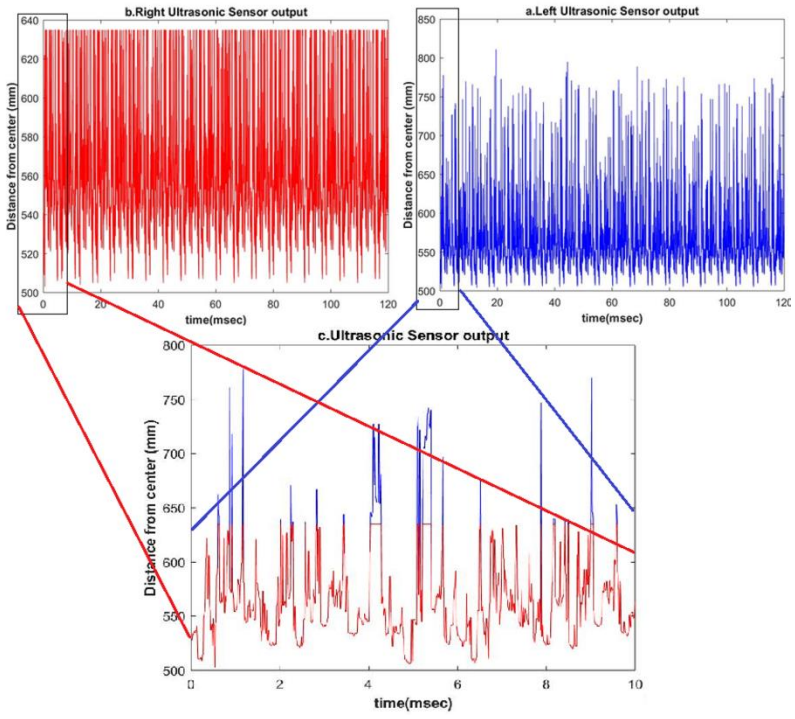

Figure 3.12. Initial observation of noisy raw data collected by the ultrasonic sensor.

Since the collected data contained various frequencies, magnitudes, and fluctuations of noises, analyzing the collected raw data and drawing conclusions based upon it was not feasible. Therefore, an additional digital filter was needed to remove unwanted parts of the data, such as random noise, and to extract useful parts of the signal, such as the components lying within a certain frequency range. Different digital filters were applied to the collected data, including Exponential, Butterworth, Bandpass, Savitzky-Golay, Kalman, and Gaussian. These filters are commonly used for signal processing and filtering the data acquired from sensors in different engineering domains. To find the most appropriate filters for each sensor, the lateral errors between the sensor measurements and the reference trajectory were compared after applying the filters. The result of this comparison is presented in Table 3.2 and Table 3.3 for the tactile and the ultrasonic sensors respectively. Low-Pass Butterworth filter was found to be the best fit to remove noises and disturbances from the tactile sensor data; the best filter for the ultrasonic sensor readings was the Gaussian filter. Two examples of filtered data from tactile sensor and ultrasonic sensor are presented in Table 3.13 and Figure 3.14. The *x* axis in Table 3.13 and Figure 3.14 is the distance traced by the snowmobile tracks during the two minutes of the experiment and the *y* axis is the plant distance to the centerline of the trajectory.

Table 3.2. Comparison of lateral error between the tactile sensor measurements and actual row patterns for different filters at V=0.45 m/s.

	Error reduction after applying filters (%)					
Patterns	Exponential	Butterworth	Bandpass	Savitzky-Golay	Kalman	Gaussian
Left side	32	61	33	46	48	52
Right side	30	66	30	46	48	49
Sinusoidal	21	56	27	36	45	43
Step	36	68	28	43	47	48
Zigzag	24	57	26	38	46	44

Table 3.3. Comparison of lateral error between the ultrasonic sensor measurements and actual row patterns for different filters at V=0.45 m/s.

	Error reduction after applying filters (%)					
Patterns	Exponential	Butterworth	Bandpass	Savitzky-Golay	Kalman	Gaussian
Left side	35	31	48	41	55	67
Right side	33	36	44	41	57	63
Sinusoidal	20	30	46	39	53	60
Step	31	34	48	42	59	61
Zigzag	22	31	43	35	51	63

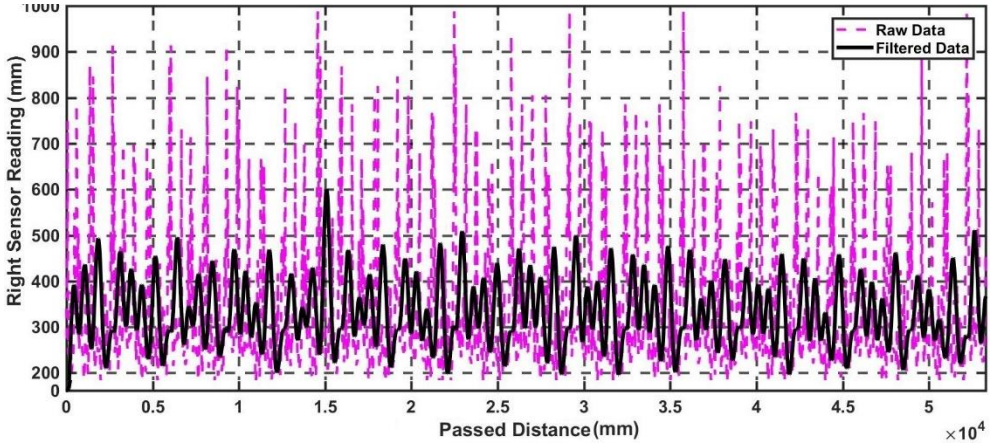

Figure 3.13. The tactile sensor filtered data using Low-Pass Butterworth filter.

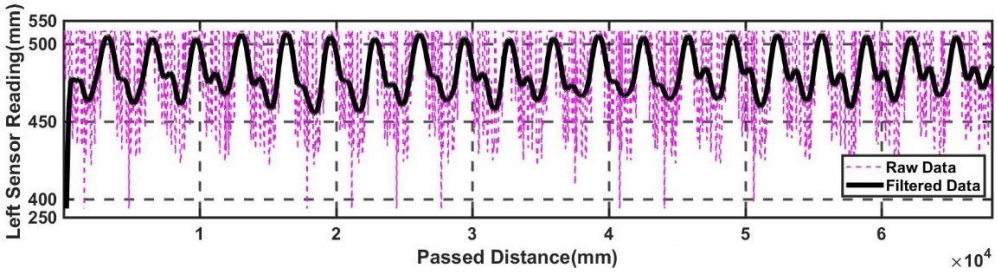

Figure 3.14. The ultrasonic sensor filtered data using Gaussian filter.

3.4. Test Results and Discussion

The filtered datasets were used to analyze the guiding performance of sensors. After filtering the data, outputs of tactile sensors were in the range of 0.8-4.3 V and the outputs of ultrasonic sensors were in the range of 36-80 cm. Outputs of sensors were in the desired range

with respect to the physical distances between sensors and small bars on the snowmobile tracks shown in Figure 3.9.

3.4.1. Time Delay in Tactile Sensor's Measurements

The distances measured by tactile sensors for reading the zigzag, sinusoidal, and step patterns are shown in Figure 3.15-Figure 3.17. The solid blue and red lines in these figures indicate the physical patterns of small bars on the snowmobile tracks (reference trajectory). The centerline of the snowmobile tracks is shown as y=0. The small asterisks and circles on the solid blue and red lines show the exact locations of small bars (plants) with respect to the centerline of the snowmobile tracks.

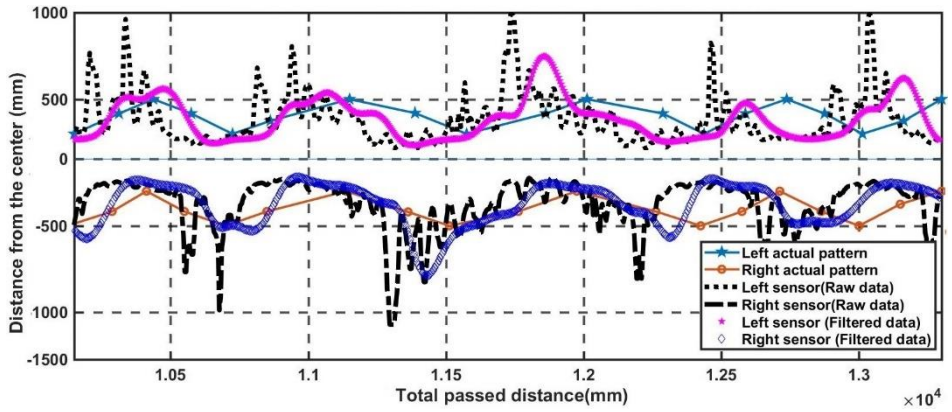

Figure 3.15. Comparison of the zigzag reference trajectory and distances measured by tactile sensor at 0.45 m/s.

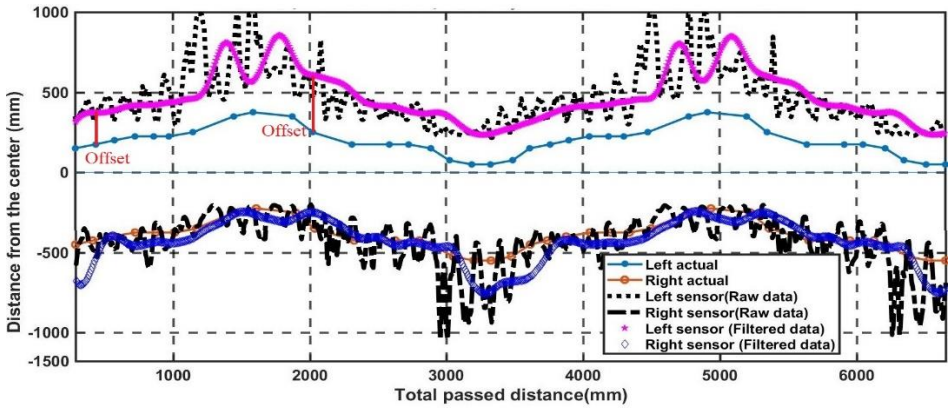

Figure 3.16. Comparison of the sinusoidal reference trajectory and distances measured by tactile sensor at 0.9 m/s.

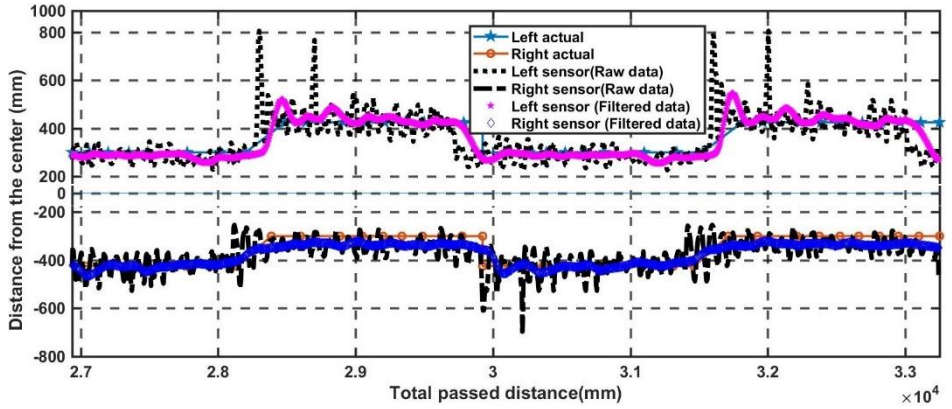

Figure 3.17. Comparison of the step reference trajectory and distances measured by tactile sensor at 1.34 m/s.

Disturbances due to the paddle fluctuations caused a considerable constant lateral offset between the reference trajectory and the sensor readings. This lateral offset is shown in Figure 3.16 for tracking sinusoidal trajectory. For further data analysis the constant offsets in sensor readings were removed from the collected data by adding a constant value to the whole datasets. The sensor readings after applying the observed offset in Figure 3.16 is shown in Figure 3.18.

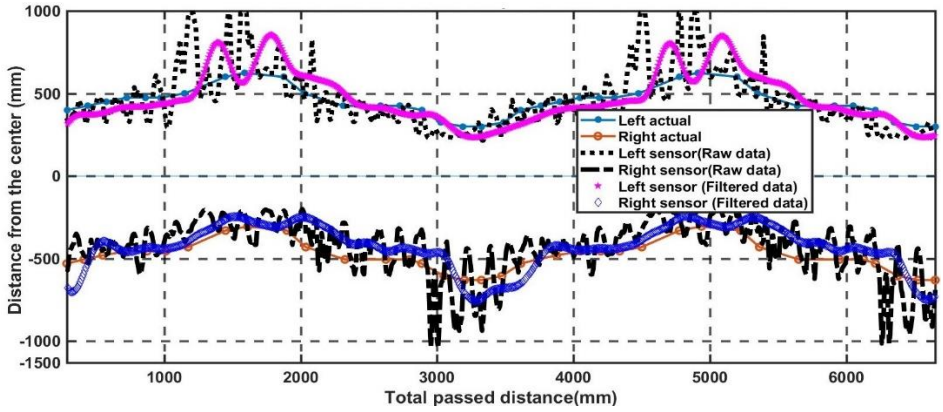

Figure 3.18. Comparison of the sinusoidal reference trajectory and distances measured by tactile sensors at 0.9 m/s after applying the offset observed in Figure 3.16.

The average sensor time delay (τ) was calculated for each trajectory at different speeds. The average sensor time delay (τ) and the permissible time delay at different speeds were compared using one-tailed *t-test* to test an alternate hypothesis–whether the sensor time delays (τ) are significantly different from the permissible time delays at each speed at the 95% level of confidence. According to Table 3.4-Table 3.6 the tactile sensor time delay was not significantly different from the permissible time delay at 0.45 m/s, 0.9 m/s, and 1.34 m/s at the 95% level of confidence. Table 3.7 shows at V=1.79 m/s the tactile sensor time delays were not significantly different from the permissible time delay only for left side, right side, and step trajectories at the 95% level of confidence. Table 3.8 shows at V=2.23 m/s the tactile sensor's time delay was significantly different from the permissible time delay for all tested patterns at the 95% level of confidence.

Table 3.4. One-tail *t-test* results to test tactile sensor time delay $(H_0 : \tau \leq 0.31\ \text{s})$ at V= 0.45 m/s at 95% level of confidence for df=∞.

Patterns	n	Mean	Standard deviation	*t-calculated*	Decision
Left side	12013	0.090	0.0348	-845.5	Fail to reject H_0
Right side	12034	0.065	0.0318	-843.8	Fail to reject H_0
Sinusoidal	12008	0.105	0.0374	-599.4	Fail to reject H_0
Step	12021	0.069	0.0229	-1145.5	Fail to reject H_0
Zigzag	12010	0.105	0.0318	-704.7	Fail to reject H_0

Table 3.5. One-tail *t-test* results to test tactile sensor time delay $(H_0 : \tau \leq 0.15\ \text{s})$ at V= 0.9 m/s at 95% level of confidence for df=∞.

Patterns	n	Mean	Standard deviation	*t-calculated*	Decision
Left side	12002	0.095	0.0489	-121.5	Fail to reject H_0
Right side	12015	0.110	0.0464	-94.0	Fail to reject H_0
Sinusoidal	12006	0.124	0.0436	-63.7	Fail to reject H_0
Step	12011	0.100	0.0406	-134.4	Fail to reject H_0
Zigzag	12018	0.119	0.0405	-81.7	Fail to reject H_0

Table 3.6. One-tail *t-test* results to test tactile sensor time delay $(H_0 : \tau \leq 0.1\ \text{s})$ at V= 1.34 m/s at 95% level of confidence for df=∞.

Patterns	n	Mean	Standard deviation	*t-calculated*	Decision
Left side	12014	0.100	0.0407	0.683	Fail to reject H_0
Right side	12004	0.100	0.0405	0.002	Fail to reject H_0
Sinusoidal	12002	0.100	0.0404	0.413	Fail to reject H_0
Step	12012	0.099	0.0402	-0.601	Fail to reject H_0
Zigzag	12023	0.099	0.0288	1.4	Fail to reject H_0

Table 3.7. One-tail *t-test* results to test tactile sensor time delay $(H_0 : \tau \leq 0.08 \text{ s})$ at V= 1.79 m/s at 95% level of confidence for df=∞.

Patterns	n	Mean	Standard deviation	*t-calculated*	Decision
Left side	12012	0.082	0.0347	1.29	Fail to reject H_0
Right side	12018	0.085	0.0345	0.72	Fail to reject H_0
Sinusoidal	12020	0.087	0.0345	1.49	Reject H_0
Step	12006	0.087	0.0347	0.70	Fail to reject H_0
Zigzag	12003	0.089	0.0344	1.76	Reject H_0

Table 3.8. One-tail *t-test* results to test tactile sensor time delay $(H_0 : \tau \leq 0.063 \text{ s})$ at V= 2.23 m/s at 95% level of confidence for df=∞.

Patterns	n	Mean	Standard deviation	*t-calculated*	Decision
Left side	12007	0.08	0.0347	54.4	Reject H_0
Right side	12001	0.08	0.0345	55.2	Reject H_0
Sinusoidal	12016	0.08	0.0344	54.5	Reject H_0
Step	12019	0.07	0.0346	53.0	Reject H_0
Zigzag	12002	0.07	0.0346	53.5	Reject H_0

The observed time delay in generating output voltage signals at the highest speed created considerable longitudinal offsets between the actual row pattern and the sensor measurements. Time delays of generating an output signal at V=2.23 m/s are shown in Figure 3.19-Figure 3.21.

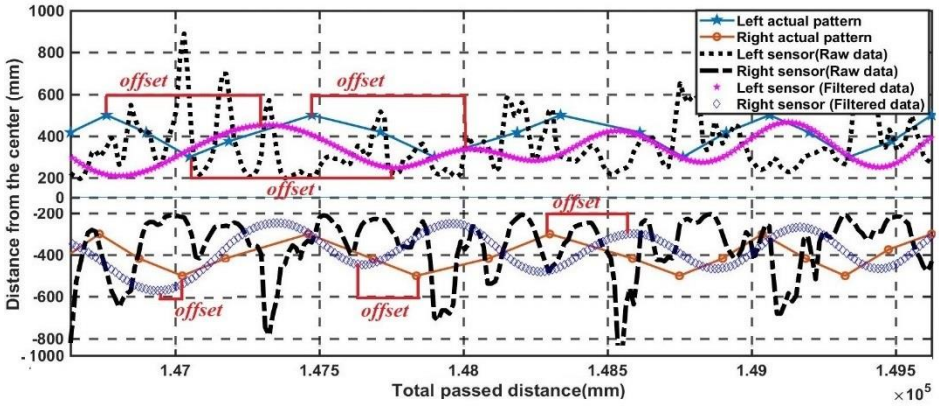

Figure 3.19. Significant longitudinal offsets due to the tactile sensor time delay in generating output signals at 2.23 m/s for zigzag trajectory.

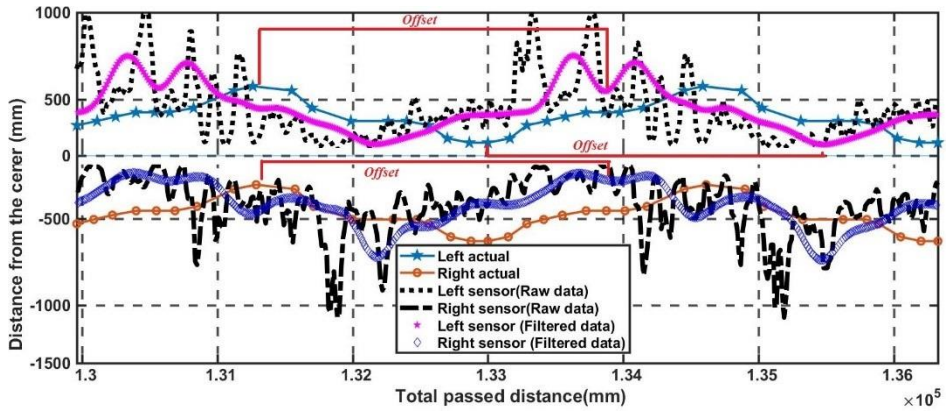

Figure 3.20. Significant longitudinal offsets due to the tactile sensor time delay in generating output signals at 2.23 m/s for sinusoidal trajectory.

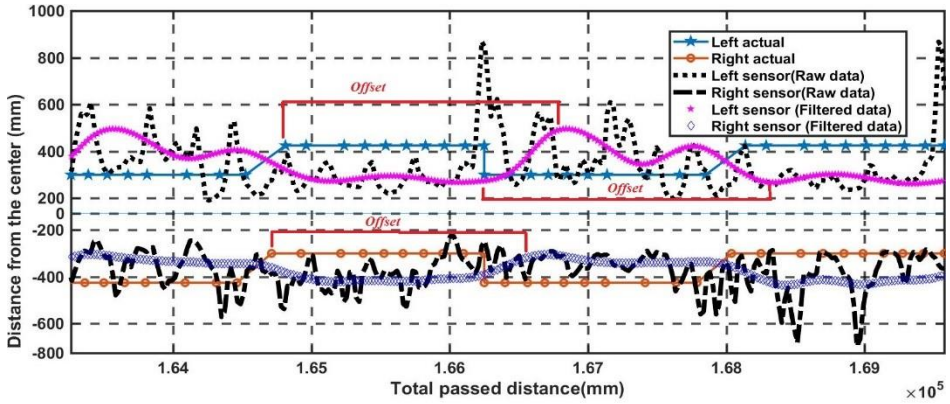

Figure 3.21. Significant longitudinal offsets due to the tactile sensor time delay in generating output signals at 2.23 m/s for step trajectory.

3.4.2. Lateral Errors in Tactile Sensor Readings

One-tailed *t-tests* were conducted to analyze the accuracy of the tactile sensor in measuring the distance to the small bars (plants). MAE in the sensor readings (ε) from a reference trajectory was calculated for all experiments. The permissible error in following the centerline between rows without damaging plants was defined as ±2. According to

Table 3.9 and Table 3.10 the sensor lateral errors in measuring the distance to small bars (plants) were not significantly different from the permissible error at 0.45 m/s and 0.9 m/s at the 95% level of confidence. Table 3.11 shows that at V=1.34 m/s the accuracy of the sensor's

measurement for zigzag pattern, which is the most complex pattern, was beyond the ±2 cm range. Running experiments at higher speed decreased the accuracy of the sensor reading measurement in complex patterns. The MAE for zigzag and sinusoidal trajectories were different from the permissible error at V=1.79 m/s (Table 3.12). Table 3.13 shows at V=2.23 m/s, the sensor lateral errors were significantly different from the permissible error for all tested patterns. This was caused by the considerable time delay in generating the output signals at higher speeds.

Results of these experiments show that at all operating speeds, except V=2.23 m/s, the sensor was successful in following a trajectory. At lower speeds (V=0.45 and 0.9 m/s) the tactile sensor was able to read the reference trajectory with the highest accuracy of 1.9 cm. At higher speeds (V=1.79 and 2.23 m/s), as the trajectory became more complex with more sharp changes, the accuracy of sensor readings decreased substantially. The accuracy of the tactile sensor dropped to 5.5 cm at V=2.23 m/s. Also, during these experiments it was observed that after the yellow paddles were released, they were prone to whip the adjacent small bars (plants) that could damage the plants at their early stage of growth.

Table 3.9. One-tail *t-test* results to test the lateral errors in tactile sensor reading $(H_0 : \varepsilon \leq \pm 2 \text{ cm})$ at V= 0.45 m/s at 95% level of confidence for df=∞.

Patterns	n	Mean	Standard deviation	*t-calculated*	Decision
Left side	325	2.043	1.1318	0.699	Fail to reject H_0
Right side	319	2.027	1.1010	0.453	Fail to reject H_0
Sinusoidal	323	2.019	1.0855	0.326	Fail to reject H_0
Step	327	1.9	1.1621	-1.5	Fail to reject H_0
Zigzag	315	2.006	1.1446	0.106	Fail to reject H_0

Table 3.10. One-tail *t-test* results to test the lateral errors in tactile sensor reading $(H_0 : \varepsilon \leq \pm 2 \text{ cm})$ at V= 0.9 m/s at 95% level of confidence for df=∞.

Patterns	n	Mean	Standard deviation	*t-calculated*	Decision
Left side	635	2.046	1.1751	0.987	Fail to reject H_0
Right side	642	2.049	1.1883	1.2	Fail to reject H_0
Sinusoidal	637	2.057	1.1647	1.2	Fail to reject H_0
Step	648	1.953	1.1684	-1.4	Fail to reject H_0
Zigzag	634	2.046	1.1303	1.3	Fail to reject H_0

Table 3.11. One-tail *t-test* results to test the lateral errors in tactile sensor reading $(H_0 : \varepsilon \leq \pm 2 \text{ cm})$ at V= 1.34 m/s at 95% level of confidence for df=∞.

Patterns	n	Mean	Standard deviation	*t-calculated*	Decision
Left side	963	2.023	1.1636	0.614	Fail to reject H_0
Right side	955	2.038	1.1743	1.0	Fail to reject H_0
Sinusoidal	954	2.043	1.1722	1.2	Fail to reject H_0
Step	967	2.001	1.1851	0.037	Fail to reject H_0
Zigzag	962	2.073	1.1538	1.9	Reject H_0

Table 3.12. One-tail *t-test* results to test the lateral errors in tactile sensor reading $(H_0 : \varepsilon \leq \pm 2 \text{ cm})$ at V= 1.79 m/s at 95% level of confidence for df=∞.

Patterns	n	Mean	Standard deviation	Standard error	*t-calculated*	Decision
Left side	1291	2.002	1.168	0.032596	0.061	Fail to reject H_0
Right side	1286	2.014	1.204	0.033471	0.438	Fail to reject H_0
Sinusoidal	1294	2.084	1.151	0.032029	2.6	Reject H_0
Step	1293	2.036	1.157	0.032278	1.1	Fail to reject H_0
Zigzag	1284	2.079	1.177	0.032873	2.4	Reject H_0

Table 3.13. One-tail *t-test* results to test the lateral errors in tactile sensor reading $(H_0 : \varepsilon \leq \pm 2 \text{ cm})$ at V= 2.23 m/s at 95% level of confidence for df=∞.

Patterns	n	Mean	Standard deviation	Standard error	*t-calculated*	Decision
Left side	1610	2.117	1.2201	0.030408	3.8	Reject H_0
Right side	1612	2.18	1.2225	0.030448	5.9	Reject H_0
Sinusoidal	1606	2.136	1.2147	0.030311	4.4	Reject H_0
Step	1609	2.185	1.2299	0.030662	6.0	Reject H_0
Zigzag	1615	2.173	1.2018	0.029904	5.7	Reject H_0

3.4.3. Ultrasonic Sensor Performance

Data analyses for the ultrasonic sensor indicated that the sensor readings on the right and left sides were mirroring each other and the measured distances to the small bars on both sides were equal. The space-domain plot of analyzing ultrasonic data for the zigzag pattern at 0.45 m/s is shown in Figure 3.22. Due to this problem, the reading from the ultrasonic sensor were not entirely reliable for further processing. This problem was due to the high sensitivity of the ultrasonic sensor receiver. The high sensitivity of the signal receiver did not grant enough time for the sound signals to bounce back from the small bars.

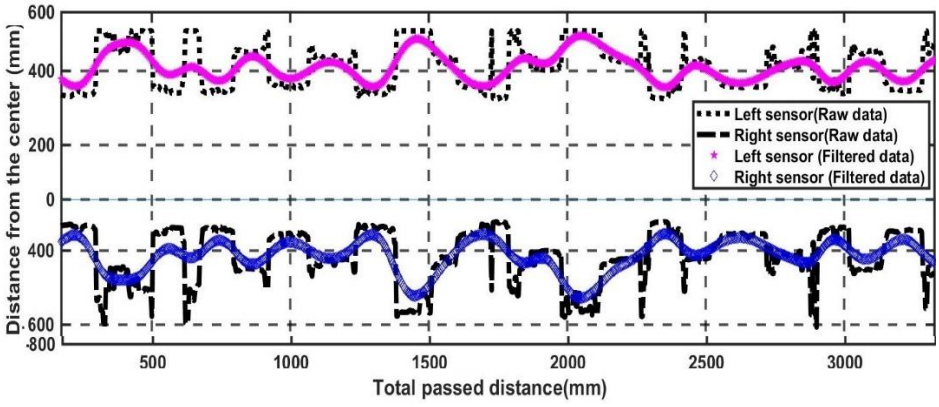

Figure 3.22. The ultrasonic sensor measured the same distances to the small bars on the left and right sides (0.45 m/s, zigzag pattern).

3.5. Conclusion

In this chapter, the capabilities of two navigation sensors, the ultrasonic and tactile sensors, were evaluated for automatic local guidance of agricultural machines. An important advantage of both sensors was independency from GPS signals, light intensity of the environment, and weather conditions. Also, the distances measured by sensors could be used directly by the steering system of a vehicle, with no further data analyses required to extract meaningful information from them. However, the outputs of both sensors were too noisy and required applying different digital signals. Noises and disturbances caused inconsistency in the distance measurements and consequently in steering the machine. Butterworth low-pass and Gaussian digital filters were selected as the best filters to remove noises from the signals collected using tactile and ultrasonic sensors respectively. The outputs of both sensors after filtering were in the expected ranges of 0.8-4.3 V for the tactile sensor and 36-80 cm for the ultrasonic sensor. Due to the potential sudden sharp whipping movements of the tactile sensor feeler arms, this sensor might not be the best option for small, thin, and delicate plants such as soybean in VE to V2 stages of growth. Also, the sound signals generated by the ultrasonic sensor are prone to hitting a surface other than the desired object. Thus, it should not be fields with heavy weed pressure or field with long leaves of plants such as corn filed after V8 stage of growth. Adjusting the sensitivity of the ultrasonic sensor could help to reduce this effect. However, in this experiment it resulted in false measurements. Due to this reason, data collected from the ultrasonic sensor was unreliable, and stopped the author from further analyses of the performance of this sensor. At higher speeds (e.g. V=1.79 and V=2.23 m/s) the tactile sensor had a considerable time delay in generating the output signals. This time delay resulted in significant longitudinal offsets between the reference trajectory and sensor measurements.

Regardless of pattern complexity, the tactile sensor showed an acceptable accuracy at lower speeds (V=0.45 and V=0.9 m/s). At higher speeds (V=1.34 and V=1.79 m/s), the accuracy of the tactile sensor decreased for row patterns with sharp changes. At V=2.23 m/s the sensor was no longer able to measure distances correctly for all tested row patterns.

4. DESIGN AND DEVELOPMENT OF A FUZZY LOGIC BASED CONTROLLER FOR AUTOMATIC STEERING OF A TRACTOR AND TOWED IMPLEMENT[2]

4.1. Abstract

In post-planting operations (e.g., fertilizing, cover crop planting), keeping the tractor and towed implement within a certain boundary region to avoid crop damage could be challenging. An automatic steering system on the tractor is a possible solution to this challenge; however, an auto steering system only on the tractor does not guarantee that the implement will follow the tractor accurately. An active control system that is able to control the position of the implement could significantly reduce crop damage due to running these vehicles in a field. In this study, a fuzzy-based automatic controller was designed to adjust lateral and longitudinal positions of a tractor and towed implement with respect to a reference trajectory. The controller measured the lateral and longitudinal positions of the tractor and towed implement using a kinematic bicycle model. The effects of tractor tire slip-angle were considered in the kinematic bicycle model to improve the accuracy of the controller in measuring the positions. The lateral and longitudinal deviations from the reference trajectory ($[e_{t,x}, e_{t,y}], [e_{c,x}, e_{c,y}]$) and the changing rate of these deviations ($[\dot{e}_{t,x}, \dot{e}_{t,y}], [\dot{e}_{c,x}, \dot{e}_{c,y}]$) were considered as inputs to the fuzzy logic control system. The controller predicted a heading angle for the tractor (δ) and an angular displacement for the implement ($_{\alpha}$) by comparing the inputs to the controller and the reference trajectory. A hydraulic

[2] The material in this chapter was co-authored by Nadia Delavarpour, Sulaymon Eshkabilov, Thomas Bon, John Nowatzki, and Sreekala Bajwa. Content in this chapter was published in Applied Sciences journal. Nadia Delavarpour had primary responsibility for preparation and performing of the tests. Nadia Delavarpour also drafted and revised all versions of this manuscript. Sulaymon Eshkabilov and Thomas Bon helped in conducting the experiments, data processing, and interpreting the results. Sreekala Bajwa and John Nowatzki supervised the project and served as proofreaders (Delavarpour et al., 2020b).

hitch actuation system was developed to change the position of the tractor and implement according to the generated angles. The performance of the fuzzy logic controller was analyzed in MATLAB/Simulink environment for following four different reference trajectories (zigzag, sinusoidal, step, and mixed) at running speeds of 1-10 m/s. The results of the simulation demonstrated that in conventional speed of agricultural operations (less than 7 m/s) the controller improved the trajectory tracking of the tractor and towed implement by at least 58%. However, as the speed increased the performance of the controller degraded significantly, particularly for complex pattern trajectories. At the highest speeds (9 and 10 m/s) of experiments, the accuracy of tracking a trajectory using the fuzzy logic controller was not different from trajectory tracking without the controller.

4.2. Introduction

Recently automatic steering of tractors has been the research focus of several industrial companies and academic studies. However, many agricultural operations are performed after crop emergence and include a hitched implement behind a tractor or planter. Although improving the path tracking accuracy of a tractor along the desired trajectory is important, it cannot guarantee the implement to follow the tractor's trajectory accurately. Unbalanced movements of the towed implement can easily increase crop damage and reduce yield efficiency. Feng et al., (2005) showed that the differences between the trajectories followed by a tractor and an implement often changed according to the tractor steering angle and running velocity. Therefore, there is a crucial need for a steering controller to control the movements of a towed implement with respect to the tractor steering angle and running velocity. Lack of sufficient studies on automatic steering for a towed implement was the main motivation behind this study. The ultimate objectives of this study are to increase the precision of agricultural post-planting

procedures and reduce crop damage and yield loss. These objectives were achieved by designing an accurate fuzzy logic controller for a tractor and towed implement system to minimize viable position errors of the whole system while driving between plant rows.

Due to simplicity and adaptability to varying conditions, fuzzy logic-based controller has been used widely for different control systems (Allou et al., 2017; Delavarpour et al., 2019; Yin et al., 2019; Zhou et al., 2019). Fuzzy logic controller is an alternative to conventional and classical controller (Gouda et al., 2000). Fuzzy logic controller is a heuristic approach that embeds the knowledge and key elements of human perception in the design of nonlinear controllers (Omega Engineering, n.d.). Fuzzy logic control is based on the fact that an experienced human operator can control a process without knowledge of its dynamics (King & Mamdani, 1977). Developing fuzzy logic controller is usually easier and cheaper than PID controller and fuzzy logic controllers are more robust and can cover a wider operation range (Gouda et al., 2000). Moreover, Qualitative and heuristic considerations cannot be handled by classical controller such as PID. Not only fuzzy logic controllers do not require accurate mathematical models or precise inputs, but also can handle nonlinearity, and can present disturbance insensitivity greater than the most nonlinear controllers. Fuzzy logic controllers usually outperform other controllers in complex, nonlinear, or undefined systems for which a good practical knowledge exists (Silva & Pinto, 2018). Also, fuzzy logic controls have the capability of handling non-linearities to control complex systems such as hydraulic systems. Thus, a fuzzy logic algorithm was developed to design an adaptive controller for a tractor and towed implement steering system. Mathematical models of the tractor and towed implement were developed based on a kinematic bicycle model. Moreover, a hydraulic hitch design along with its mathematical model formulation and numerical simulations were developed to control

the implement position with additional steering torques actuated by a pair of hydraulic cylinders. Finally, the performance of the fuzzy logic control algorithm was validated via numerical simulations in the MATLAB/Simulink environment.

4.3. Materials and Methods

4.3.1. Tractor and Towed Implement Modeling

Understanding steering kinematics and motion dynamics of a tractor and towed implement in various field conditions are crucial to design an automatic guidance system. Traveling speed of a tractor defines the complexity level of modeling equations. Conventionally, the average traveling speed in agricultural fields is 6.5 m/s (15 mile per hour) (Thelen, 2014). For vehicles with low traveling speeds (less than 7 m/s) the kinematic bicycle model is a viable and simple modeling option. According to the assumptions of this model at low speeds, the sideway slippage of tires is negligible, the inertia of the system is not significant, and air-drag acting on the vehicle does not influence the system dynamics. The tractor and towed implement were modeled according to the assumptions of the kinematic bicycle model.

Two different situations were studied to provide a better understanding of the performance of the fuzzy logic controller: (1) the towed implement freely followed the tractor without any active controller over its motion; (2) the towed implement was actively guided by the controller independently from the tractor. Equations related to each case study were developed separately.

The schematic of the tractor and towed implement is presented in Figure 4.1 and the definitions of parameters in Figure 4.1 are provided in Table 4.1

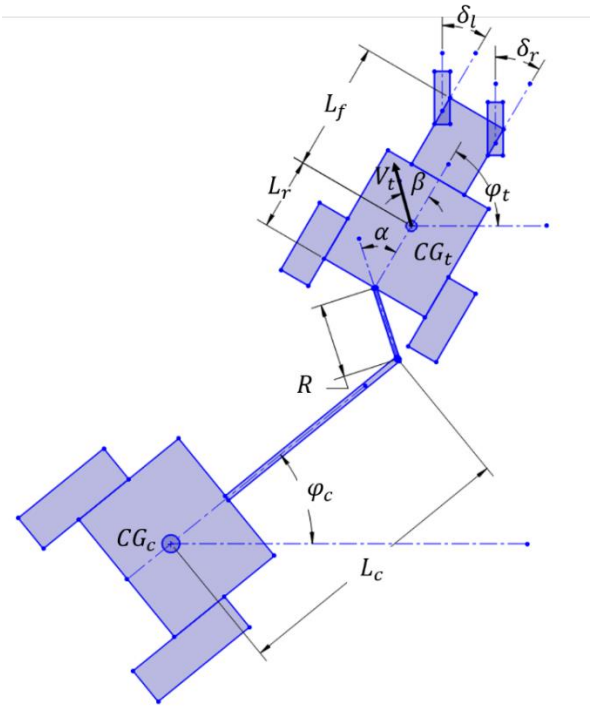

Figure 4.1. Schematic representation of tractor and towed implement system.

Table 4.1. Tractor and towed implement kinematic bicycle model parameters definition shown in Figure 4.1.

Parameter	Definition
CG_t, CG_c	Tractor's center of gravity (t), towed implement's center of gravity (c)
δ_f, δ_r	Steering angles of the tractor's front wheels (f: front, r: rear)
V_t	Operating speed of tractor
φ_t, φ_c	Heading angles of tractor and towed implement
$\dot{\varphi}_t, \dot{\varphi}_c$	Yaw rate of tractor and towed implement
α	Angular displacement of the hitch arm
$\dot{\alpha}$	Angular velocity of the hitch arm
β	Slip angle at the tractor's center of gravity
L_f, L_r	Distance from tractor's center of gravity to the front (f) and rear (r) axels
L_t	Tractor's wheel-base distance ($L_f + L_r$)
L_c	Distance from the hitch to the implement's center of gravity
R	Hitch arm length

The kinematic bicycle model, which is a simplification of the model in Figure 4.1, is presented in Figure 4.2. In this model (Figure 4.2), the left and right front wheels of the tractor are represented by one single wheel. The same concept was used to represent the tractor rear wheels and the implement wheels. In this model developed for the tractor and towed implement it was assumed:

- The front wheels are the only steering wheels and rear wheels are followers (front-wheel-only steering).
- The rear tire steering angle δ_r is zero.
- Tractor velocity is constant.
- The velocity vector at the front and rear axles of the tractor are in the same directions as their respective wheels.
- The implement's center of gravity CG_c resides on the middle of its axel.

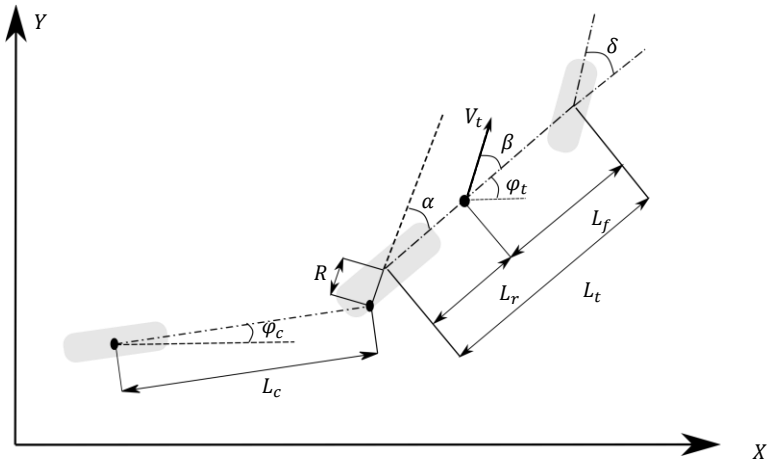

Figure 4.2. Kinematic bicycle model of the tractor and towed implement system.

According to the assumptions stated above, equations of motion for the tractor are expressed in Equation 4.1 and Equation 4.2. The angular velocity equation of the towed

implement without an active controller is presented in Equation 4.3. The angular velocity equation of the towed implement with an active controller is presented in Equation 4.4.

$$\begin{bmatrix} \dot{X}_t \\ \dot{Y}_t \\ \dot{\varphi}_t \end{bmatrix} = \begin{bmatrix} V_t \cos[\varphi_t + \beta] \\ V_t \sin[\varphi_t + \beta] \\ \dfrac{V_t \cos\beta \tan\delta}{L_t} \end{bmatrix} \quad \text{(Equation 4.1)}$$

$$\beta = \arctan\left(\frac{L_r \tan\delta}{L_t}\right) \quad \text{(Equation 4.2)}$$

$$\dot{\varphi}_c = \frac{V_t \cos\beta \sin(\varphi_t - \varphi_c) - R\dot{\varphi}_t \cos(\varphi_t - \varphi_c)}{L_c} \quad \text{(Equation 4.3)}$$

$$\dot{\varphi}_c = \frac{V_t \cos\beta \cos\alpha \sin(\varphi_t - \alpha - \varphi_c) - R\dot{\alpha} \cos(\varphi_t - \alpha - \varphi_c)}{L_c} \quad \text{(Equation 4.4)}$$

4.3.2. Fuzzy Logic Control Algorithm Design

The controller was designed to control the steering angle of the tractor (δ) as well as the angular displacement of the implement hitch arm (α) with respect to coordinates of the reference trajectory. The flow chart of the fuzzy logic controller is presented in Figure 4.3. the lateral and longitudinal errors from the reference trajectory were calculated. The errors—$(e_{t,x}, e_{t,y})$ and $(e_{c,x}, e_{c,y})$ for the tractor and towed implement—and their change rate—$(\dot{e}_{t,x}, \dot{e}_{t,y}), (\dot{e}_{c,x}, \dot{e}_{c,y})$—were used as the inputs to the controller to estimate the steering angle for the tractor (δ) and the angular displacement for the implement (α). The new positions of the tractor and towed implement were calculated with respect to the generated δ and α. These new positions were fed into the system as feedbacks and updated the inputs to the controller.

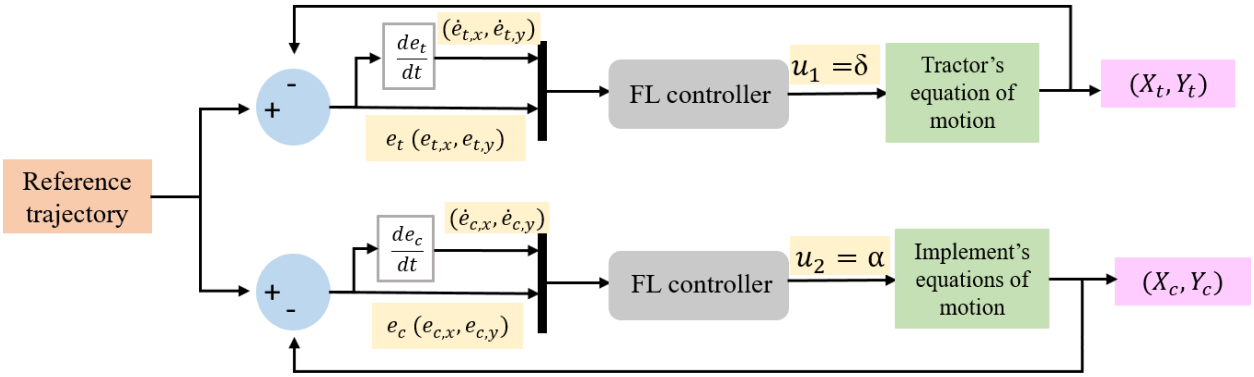

Figure 4.3. The control algorithm designed to control the position of the tractor and towed implement with respect to reference trajectory.

The trajectory tracking concept of the controller is to find the closest reference points of the reference trajectory and determine the desired steering angle for the tractor (δ) and an angular displacement for the implement (α) to reach the reference point. It should be noted that small angles would result in oscillations during the trajectory tracking. In the design of the controller it was attempted to minimize the tracking error with minimal oscillation around the reference trajectory. Thus, the optimum design of the controller with lowest fluctuations for δ and α was determined by trial and error method. For designing the fuzzy logic controller, Mamdani reasoning and centroid methods for de-fuzzification were used. A triangular function was adopted to define membership functions. The reason for choosing this membership function was to reduce the computational burden and easily tune the controller. Membership functions for inputs and outputs of the tractor and towed implement steering controllers are shown in Figure 4.4 and Figure 4.5. In these figures the error signals—$(e_{t,x}, e_{t,y}), (e_{c,x}, e_{c,y})$—were represented via three membership functions, NF, VC, PF, and the error change rates—$(\dot{e}_{t,x}, \dot{e}_{t,y}), (\dot{e}_{c,x}, \dot{e}_{c,y})$—were represented via N, Z, P. Linguistic terms of these membership functions are presented in Table 4.2. Each controller was composed of total number of 81 rules to cover all the possible

conditions of tractor and towed implements with respect to the reference trajectory. Table 4.3 shows the designed fuzzy logic rules used for both controllers.

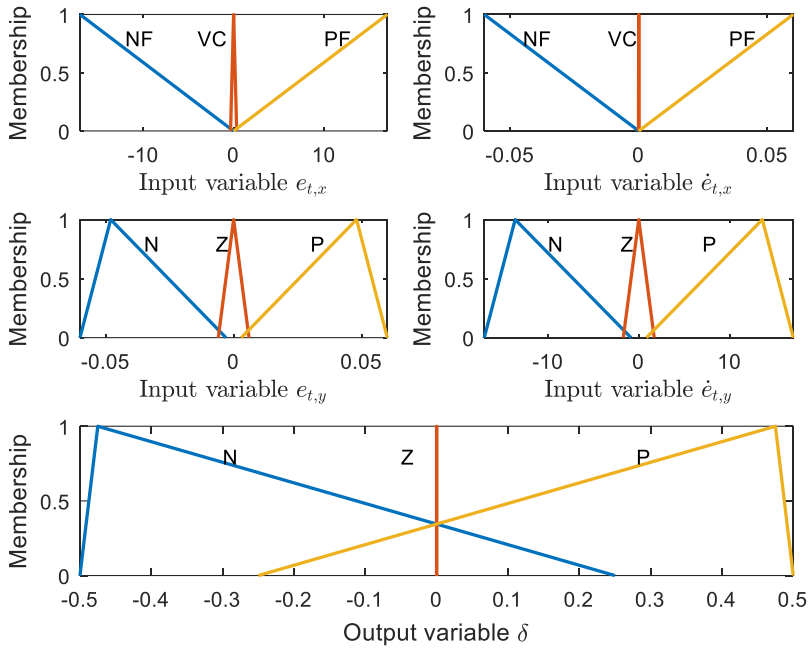

Figure 4.4. Input and output membership functions for the tractor controller.

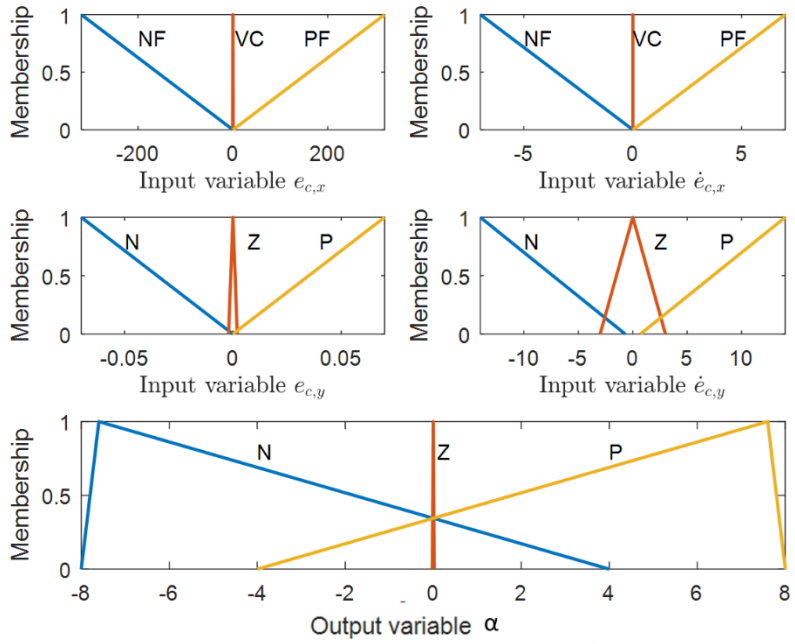

Figure 4.5. Input and output membership functions for the implement controller.

Table 4.2. Linguistic terms used in inputs and outputs membership function of the designed controllers.

Linguistic term	Definition
N	Negative
Z	Zero
P	Positive
NF	Negative Far
VC	Very Close
PF	Positive Far

Table 4.3. Fuzzy logic rules for the tractor and its towed implement controllers.

	$e_y / \dot{e}_y$								
$e_x / \dot{e}_x$	Z/Z	Z/N	Z/P	N/Z	N/N	N/P	P/Z	P/N	P/P
VC/VC	Z	P	P	N	P	P	P	P	N
VC/NF	N	N	N	P	N	N	N	N	P
VC/PF	P	P	P	N	P	P	P	P	N
NF/VC	P	P	P	N	P	P	P	P	N
NF/NF	P	P	P	N	P	N	N	N	P
NF/PF	N	N	N	P	N	P	P	P	N
PF/VC	P	P	P	N	P	P	P	P	N
PF/NF	N	N	N	P	N	P	N	P	N
PF/PF	P	P	P	N	P	P	P	N	N

4.3.3. Tractor and Towed Implement Equations of Motion

The controller was designed to minimize unbalanced movements of a tractor and towed implement and make them follow the reference path as closely as possible. Inputs to the controller were the errors between the current positions of the tractor and its towed implement with the reference trajectory. The outputs of this controller were a steering angle for the tractor ($\delta = u_1$) and an angular displacement for the towed implement ($\alpha = u_2$). Models of the tractor and towed implement were modified with respect to the inputs of the controller by substituting δ and α in Equation 4.1, Equation 4.2 and Equation 4.4 with u_1 and u_2 . The tractor and towed

implement equations of motion (Equation 4.5-Equation 4.7) were developed by discretizing the tractor and towed implement models and integrating them with respect to the sampling frequency ($f_s = \frac{1}{\Delta t}$, f_s : sampling frequency). The tractor equation of motion after receiving a correction signal from the controller is given in Equation 4.5, while Equation 4.6 and Equation 4.7 are the towed implement equations of motion with and without an active controller, respectively. In Equation 4.6 $\sigma = \varphi_t - \alpha - \varphi_c$.

$$\begin{bmatrix} X_t \\ Y_t \\ \varphi_t \end{bmatrix} = V_t \Delta t \begin{bmatrix} \cos[\varphi_t(t) + \beta(t)] \\ \sin[\varphi_t(t) + \beta(t)] \\ \frac{\cos\beta(t)\tan u_1(t)}{L_t} \end{bmatrix} \quad \text{(Equation 4.5)}$$

$$\begin{bmatrix} X_c(t) \\ Y_c(t) \\ \varphi_c(t) \end{bmatrix} = \begin{bmatrix} X_t(t) - L_r\cos\varphi_t(t) - R\cos(\varphi_t(t) - \alpha(t)) - L_c\cos\varphi_c(t) \\ X_t(t) - L_r\sin\varphi_t(t) - R\sin(\varphi_t(t) - \alpha(t)) - L_c\sin\varphi_c(t) \\ \frac{V_t\Delta t\cos\beta(t)\cos u_2(t)\sin\sigma(t) - R\Delta t\dot{u}_2(t)\cos\sigma(t)}{L_c} \end{bmatrix} \quad \text{(Equation 4.6)}$$

$$\begin{bmatrix} X_c(t) \\ Y_c(t) \\ \varphi_c(t) \end{bmatrix} = \begin{bmatrix} X_t(t) - L_r\cos\varphi_t(t) - L_c\cos\varphi_c(t) \\ X_t(t) - L_r\sin\varphi_t(t) - L_c\sin\varphi_c(t) \\ \frac{V_t\Delta t\cos\beta(t)\sin(\varphi_t(t) - \varphi_c(t))}{L_c} - \frac{RV_t\Delta t\cos\beta(t)\tan u_1(t)\cos(\varphi_t(t) - \varphi_c(t))}{L_tL_c} \end{bmatrix} \quad \text{(Equation 4.7)}$$

4.3.4. Implement Hydraulic Hitch Drive

A hydraulic hitch drive (Figure 4.6) was developed to mount on the rear axle of the tractor to provide an active control over the implement movements. The hydraulic hitch drive

changed the angular displacement (α) of the hitch arm via changing the position of cylinder rod. Table 4.4 shows the definitions of different parameters in Figure 4.6.

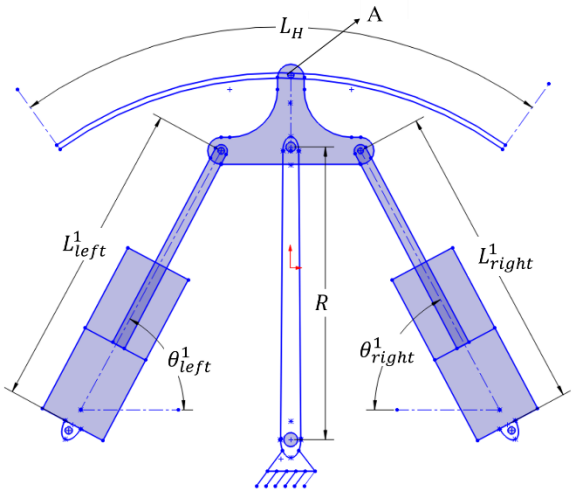

Figure 4.6. Hydraulic hitch design and its parameters.

Table 4.4. Definition of parameters in Figure 4.6 and the initial values of angle in the figure.

Parameters	Definition
A	Hitch point
R	Hitch arm
L_H	Hitch arc
L^1_{left}	Left cylinder length
L^1_{right}	Right cylinder length
θ^1_{left}	Left cylinder angle
θ^1_{right}	Right cylinder angle

The hydraulic drive was designed with respect to the dimensions of a Case IH Magnum 310 tractor (380 hp, 44 GPM), an AmityST250 Air Cart towed implement, and 76-cm spacing between the rows (Table 4.5). Considering these, the acceptable range of the implement angular displacement was ±30˚, the initial condition of the hitch arm in Figure 4.6.

Table 4.5. The dimensions of tractor and towed implement used for the design of the hydraulic hitch.

Parameters	Dimension
L_f	1.8 m
L_r	1.2 m
L_c	7.77 m
L_H	80 cm, 60˚
L^1_{left}	50 cm
L^1_{right}	50 cm
θ^1_{left}	45˚
θ^1_{right}	45˚
R	0.6 m

Figure 4.7 shows the situation of hitch point (A), left and right hydraulic cylinders (L_{left}, L_{right}), and the hitch angular displacement (α) after applying a certain value of angular displacement. In Figure 4.7, L_P is the changes in the hitch point (A) position compared with its initial condition in Figure 4.6. Table 4.6 lists the rod position at three hitch angular displacements: 1. when $\alpha = 0^\circ$ and hitch arm (R) is in the middle of the hitch arc (L_H); 2. when $\alpha = 30^\circ$ and hitch arm (R) is in the left end of the hitch arc (L_H); 3. when $\alpha = -30^\circ$ and hitch arm (R) is in the right end of the hitch arc (L_H).

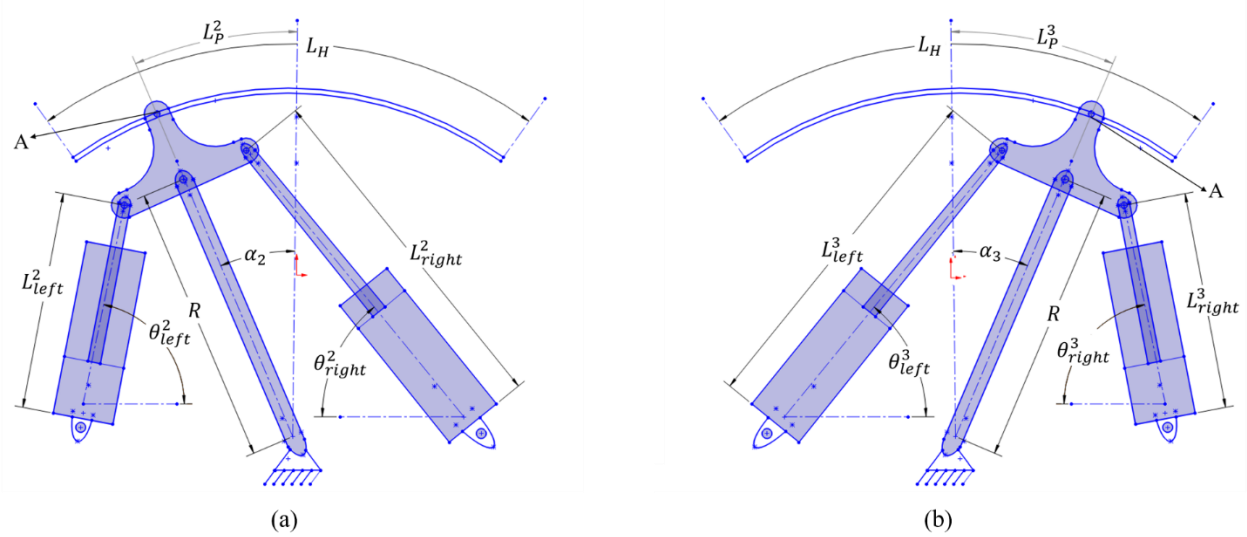

Figure 4.7. Relationship between the hydraulic cylinder position and the angular displacement of the hydraulic hitch arm (α).

Table 4.6. Values left cylinder angle (θ_{left}) and right cylinder angle (θ_{right}) at three different hitch angular displacements: $\alpha = 0^\circ$, $\alpha = 30^\circ$, $\alpha = -30^\circ$.

Angular displacement	Left cylinder angle/length	Right cylinder angle/length
$\alpha = 0^\circ$	$\theta_{left}^1 = 45^\circ, L_{left}^1 = 50$ cm	$\theta_{right}^1 = -45^\circ, L_{right}^1 = 50$ cm
$\alpha = 30^\circ$	$\theta_{left}^2 = 30^\circ, L_{left}^2 = 41.2$ cm	$\theta_{right}^2 = -75^\circ, L_{right}^2 = 56.5$ cm
$\alpha = -30^\circ$	$\theta_{left}^3 = 75^\circ, L_{left}^3 = 56.5$ cm	$\theta_{right}^2 = -30^\circ, L_{right}^3 = 41.2$ cm

4.3.5. Experimental Design

In order to evaluate the proposed algorithm based on the fuzzy logic rules to control the motion of the tractor and cart, computer simulations were performed in MATLAB/Simulink environment. For this purpose, four different trajectories (Figure 4.8) were designed to test the performance of the fuzzy logic controller in steering the tractor and towed implement at 10 different speeds (1-10 m/s). In Figure 4.8, the *x*-axis represents the longitudinal direction (or the forward direction) and the *y*-axis represents the lateral direction (or sideways direction) of motion. The total longitudinal length of each trajectory was 150 m and 1500 navigation points on

the reference trajectory were selected as the reference points. Trajectory tracking was conducted by considering the given geometric path between two consecutive navigation points. This is the best approach when a machine has to drive very accurately along a seeding lane. To analyze the performance of the controller in steering the tractor and towed implement, the lateral and longitudinal deviations of CG_t and CG_c from navigation points were measured after receiving the correction signals from the controller.

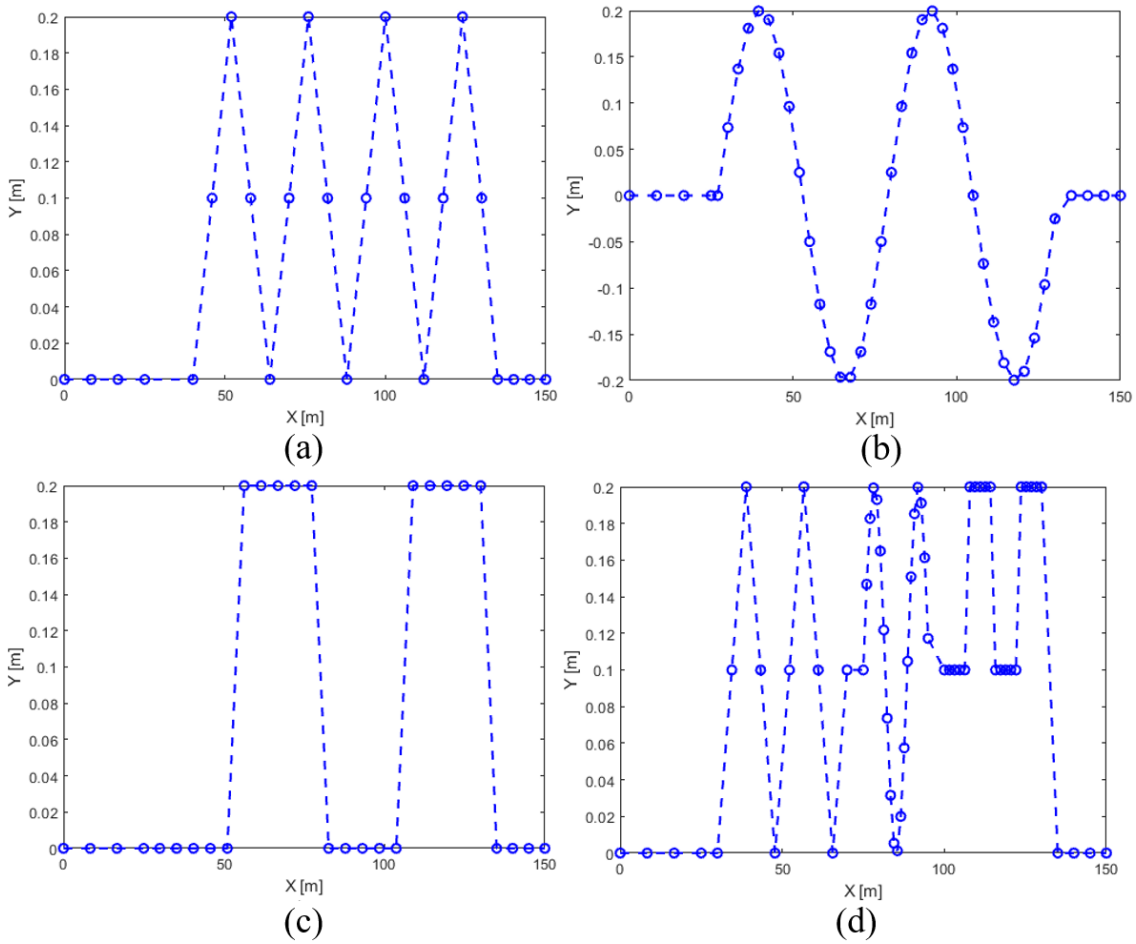

Figure 4.8. Designed trajectory in MATLAB/Simulink environment to test the performance of the fuzzy logic controller, (a) zigzag trajectory, (b) sinusoidal trajectory, (c) step trajectory, and (d) mixed trajectory.

4.3.6. Statistical Analysis of the Fuzzy Logic Controller Performance

Figure 4.9 shows the method that was used in this study to measure the tractor and towed implement lateral and longitudinal deviations from of CG_t and CG_c. In this figure RP_t and RP_c are the reference navigation points for tractor and towed implement respectively. The lateral and longitudinal errors—$[e_{t,x}, e_{t,y}], [e_{c,x}, e_{c,y}]$—were measured for all 1500 navigation points of the reference trajectory.

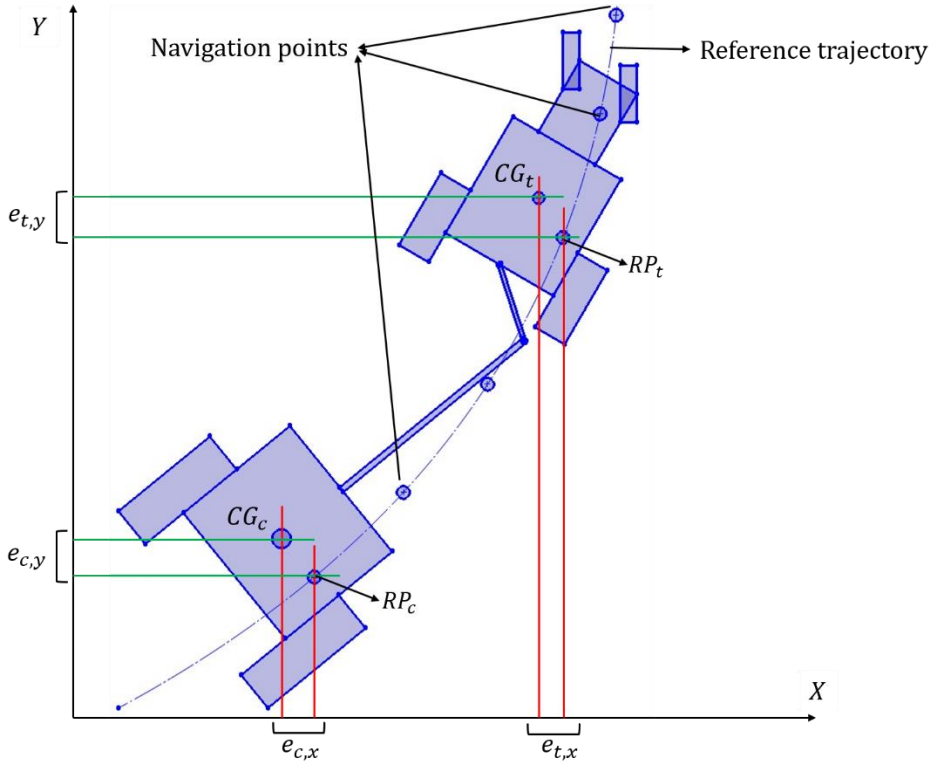

Figure 4.9. Tractor and towed implement lateral and longitudinal deviations $([e_{t,x}, e_{t,y}], [e_{c,x}, e_{c,y}])$ from navigation points on the reference trajectory.

The average lateral and longitudinal deviations of tractor and towed implement—$[Avg.(e_{t,x}), Avg.(e_{t,y})], [Avg.(e_{c,y}), Avg.(e_{c,y})]$—were calculated for tracking all trajectories at various speeds. Considering the dimensions of the hydraulic hitch drive and the 76-cm spacing between the rows, the permissible longitudinal and lateral deviations without damaging the crops

were ± 4 cm and ± 3 cm respectively. One-tailed *t-tests* were conducted to test whether the accuracy of the controller in steering the tractor and towed implement is significantly less than the given permissible ranges for lateral and longitudinal directions at the 95% level of confidence. The summary of controller accuracy testing hypothesis is:

$H_0 : Avg.(e_{t,x}) \leq \pm 4$ cm, $Avg.(e_{t,y}) \leq \pm 3$ cm
H_A : Either $e_{t,x}$ or $e_{t,y}$ greater than the permissible errors — for the tractor

$H_0 : Avg.(e_{c,x}) \leq \pm 4$ cm, $Avg.(e_{c,y}) \leq \pm 3$ cm
H_A : Either $e_{c,x}$ or $e_{c,y}$ greater than the permissible errors — for the implement

4.4. Test Results and Discussion

The performance validation of the controller was conducted in MATLAB/Simulink environment for following four different trajectories at different speeds from 1 to 10 m/s. The movements of the towed implement were evaluated and compared in two conditions: 1. When there is no active control over the towed implement (passive control of the implement); 2. When the controller actively steers the towed implement (active control of the implement). In the first condition, the towed implement followed the tractor freely and the movement of the towed implement was affected by forces from soil friction, tire stiffness, terrain, etc. In the second condition, the movement of the towed implement was controlled by the controller. For brevity, the results of the implement's behavior are only illustrated at 1, 3, 5, 7, and 9 m/s.

4.4.1. Analysis of the Fuzzy Logic Controller for Tracking a Zigzag Trajectory

The results of simulation experiments for tracking a zigzag trajectory in both active and passive conditions at various speeds are displayed in Figure 4.10-Figure 4.14. The result of the simulations with the active controller, the traced trajectory by the tractor overlaid the reference zigzag trajectory (Table 4.7). Without the controller, the trajectory tracking accuracy of the implement decreased significantly and overstepped the permissible error limits (Table 4.8),

which results in running over crop rows and damaging plants. Compared with passive control condition, the controller kept implement errors within the acceptable range at all speeds (Table 4.9). Although the actively controlled implement had an acceptable performance at all speeds, increasing the traveling speed did negatively affect the performance of the controller. At higher speeds (7 and 9 m/s) the controller struggled to follow the defined trajectory with considerable fluctuations and overshoots during the initial sections (Figure 4.13 and Figure 4.14). The fluctuations and overshoots were due to either insufficient accuracy of the kinematic bicycle model at high speeds (> 7m/s) or insufficient time to follow the correction signals. According to the Figure 4.10-Figure 4.14 the most inaccuracies in tracking the zigzag trajectory occurred on peaks and valleys of the path, where sharp changes in the direction of motion were required. These sharp changes might happen due to digging holes and making mounds in fields by gophers or other animals. Also, skipping a seed while planting them is another reason that could cause these sharp changes in a field. A dynamic model might help to improve these types of inaccuracies in following the reference trajectories.

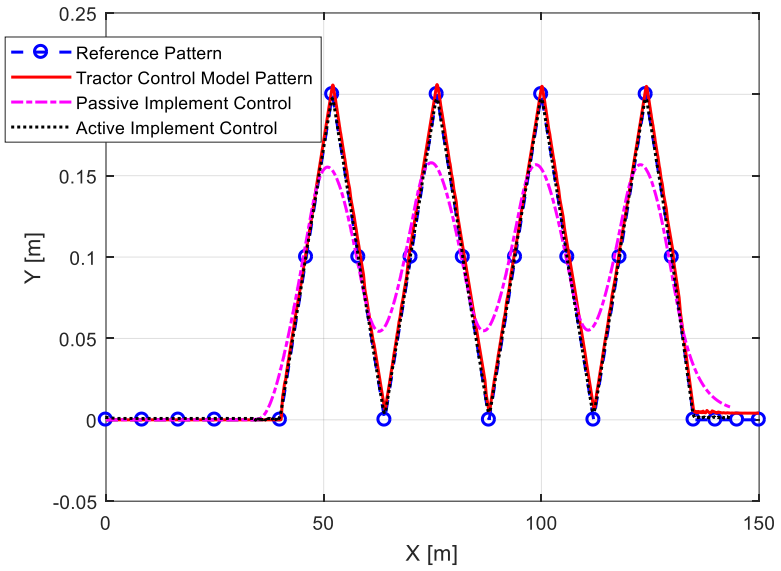

Figure 4.10. Tractor and towed implement behaviors in tracking a zigzag trajectory in passive and active control conditions at 1 m/s. X: the longitudinal direction and forward motion of the tractor and towed implement, Y: The lateral direction of motion.

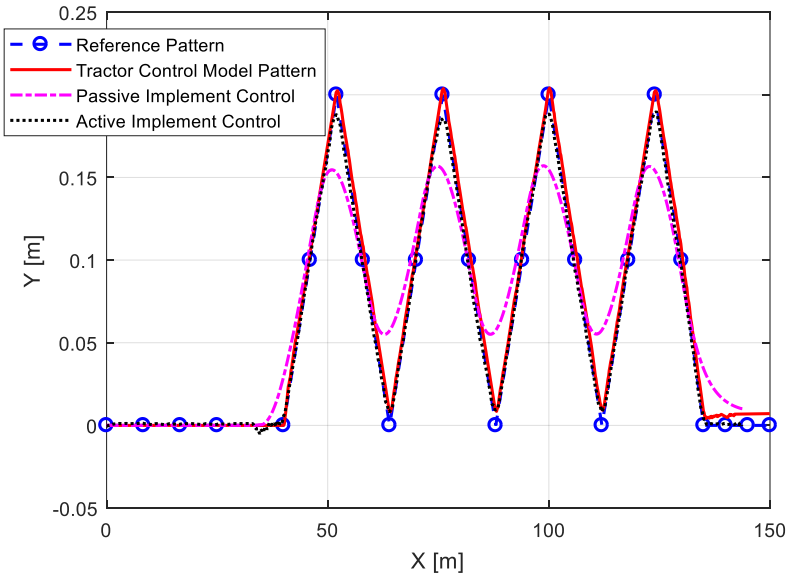

Figure 4.11. Tractor and towed implement behaviors in tracking a zigzag trajectory in passive and active control conditions at 3 m/s. X: the longitudinal direction and forward motion of the tractor and towed implement, Y: The lateral direction of motion.

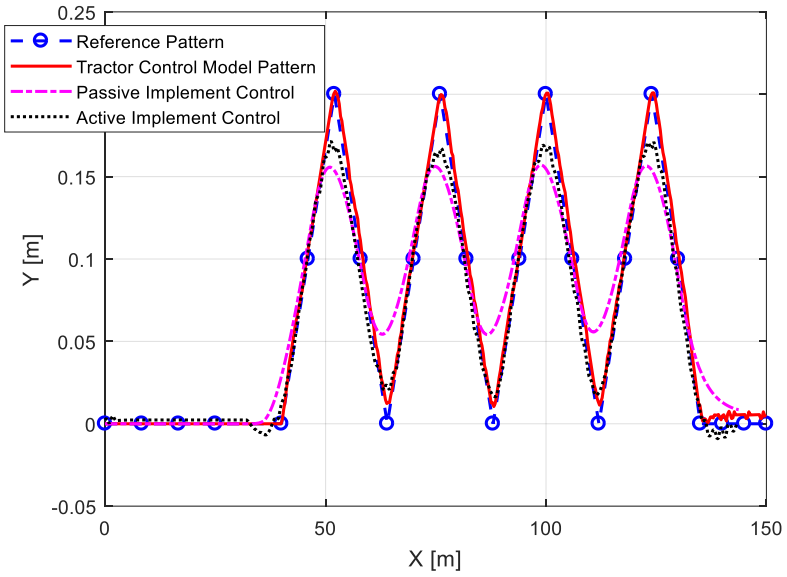

Figure 4.12. Tractor and towed implement behaviors in tracking a zigzag trajectory in passive and active control conditions at 5 m/s. X: the longitudinal direction and forward motion of the tractor and towed implement, Y: The lateral direction of motion.

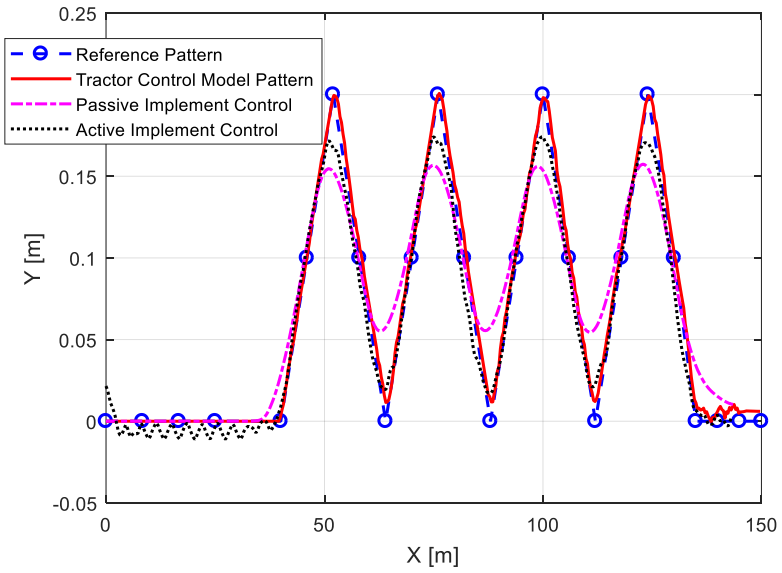

Figure 4.13. Tractor and towed implement behaviors in tracking a zigzag trajectory in passive and active control conditions at 7 m/s. X: the longitudinal direction and forward motion of the tractor and towed implement, Y: the lateral direction of motion.

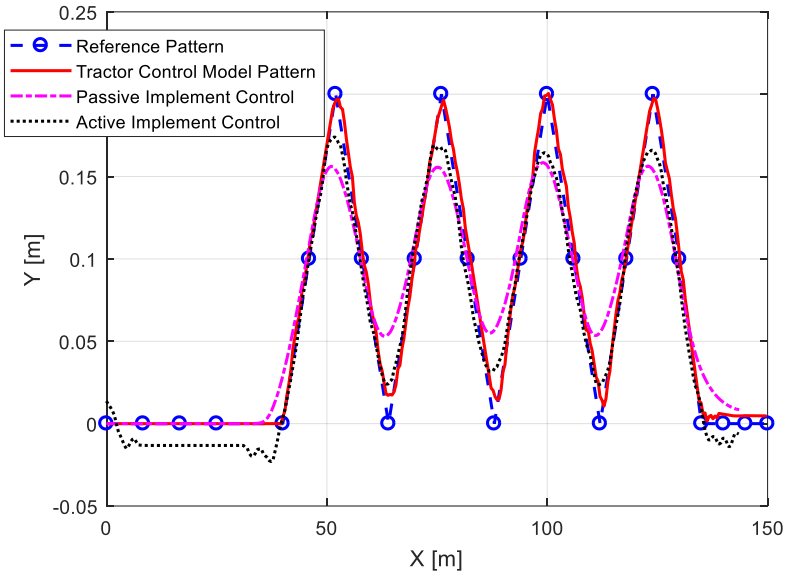

Figure 4.14. Tractor and towed implement behaviors in tracking a zigzag trajectory in passive and active control conditions at 9 m/s. X: the longitudinal direction and forward motion of the tractor and towed implement, Y: the lateral direction of motion.

Table 4.7. One-tail *t-test* results to test $H_0 : Avg.(e_{t,x}) \leq \pm 4$ cm, $Avg.(e_{t,y}) \leq \pm 3$ cm for the tractor following a zigzag trajectory at 95% level of confidence for df=∞.

Speed [m/s]	$e_{t,x}$ [cm]			$e_{t,y}$ [cm]			Decision
	Mean	Standard deviation	*t-calculated*	Mean	Standard deviation	*t-calculated*	
1	0.32	0.09	-1452	0.24	0.0867	-1229.4	Fail to reject H_0
3	0.35	0.08	-1632	0.30	0.1161	-899.6	Fail to reject H_0
5	0.41	0.12	-1155	0.34	0.0862	-1191	Fail to reject H_0
7	0.48	0.10	-1244	0.36	0.1358	-751.4	Fail to reject H_0
9	0.51	0.11	-1131	0.47	0.1838	-531.6	Fail to reject H_0

Table 4.8. One-tail *t-test* results to test $H_0 : Avg.(e_{t,x}) \leq \pm 4$ cm, $Avg.(e_{t,y}) \leq \pm 3$ cm for the implement in passive condition following a zigzag trajectory at 95% level of confidence for df=∞.

Speed [m/s]	$e_{c,x}$ [cm]			$e_{c,y}$ [cm]			Decision
	Mean	Standard deviation	*t-calculated*	Mean	Standard deviation	*t-calculated*	
1	3.86	1.0693	-5.03	3.06	0.9498	2.68	Reject H_0
3	3.80	1.3029	-5.75	3.09	0.9799	3.65	Reject H_0
5	3.90	1.2670	-2.75	3.04	1.0158	1.69	Reject H_0
7	4.04	1.3748	1.28	3.07	1.1329	2.40	Reject H_0
9	4.05	1.3894	1.47	3.12	1.1476	4.15	Reject H_0

Table 4.9. One-tail *t-test* results to test $H_0 : Avg.(e_{t,x}) \leq \pm 4$ cm, $Avg.(e_{t,y}) \leq \pm 3$ cm for the implement in active condition following a zigzag trajectory at 95% level of confidence for df=∞.

Speed [m/s]	$e_{c,x}$ [cm]			$e_{c,y}$ [cm]			Decision
	Mean	Standard deviation	*t-calculated*	Mean	Standard deviation	*t-calculated*	
1	0.3	0.0569	-2519	1.99	0.63	-61.72	Fail to reject H_0
3	0.5	0.1723	-785.4	2.21	0.75	-40.51	Fail to reject H_0
5	0.64	0.2043	-636.03	2.32	0.71	-36.54	Fail to reject H_0
7	0.69	0.2805	-456.07	2.59	0.67	-23.55	Fail to reject H_0
9	0.9	0.2894	-413.56	2.84	0.72	-8.48	Fail to reject H_0

4.4.2. Analysis of the Fuzzy Logic Controller for Tracking a Sinusoidal Trajectory

Similar to zigzag trajectory, Figure 4.15-Figure 4.19 show that the actual trajectory that the tractor tracked was pretty close to the sinusoidal reference trajectory. However, compared with zigzag trajectory, the towed implement had a better performance for following the sinusoidal trajectory in passive condition, and deviations from the reference trajectory were not significantly different from the error ranges. In the active control condition, although the controller improved the performance of the implement, the average lateral and longitudinal errors did not improve significantly compared to passive control condition (Table 4.11and Table

4.12). Simulation results of sinusoidal trajectory highlighted the effect of trajectory pattern on the accuracy of implement trajectory tracking. According to these simulation for trajectories with smooth changes in the direction of motion, the passive controlled implement could follow the trajectory with sufficient accuracy.

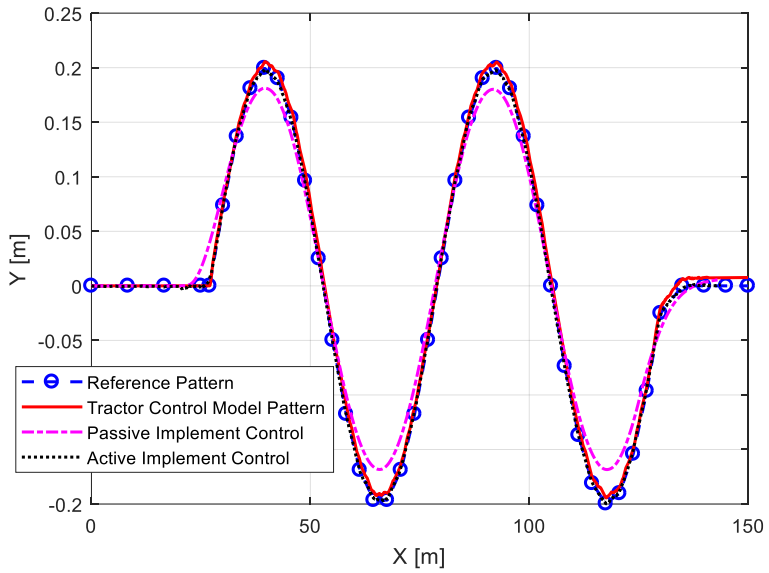

Figure 4.15. Tractor and towed implement behaviors in tracking a sinusoidal trajectory in passive and active control conditions at 1 m/s. X: the longitudinal direction and forward motion of the tractor and towed implement, Y: the lateral direction of motion.

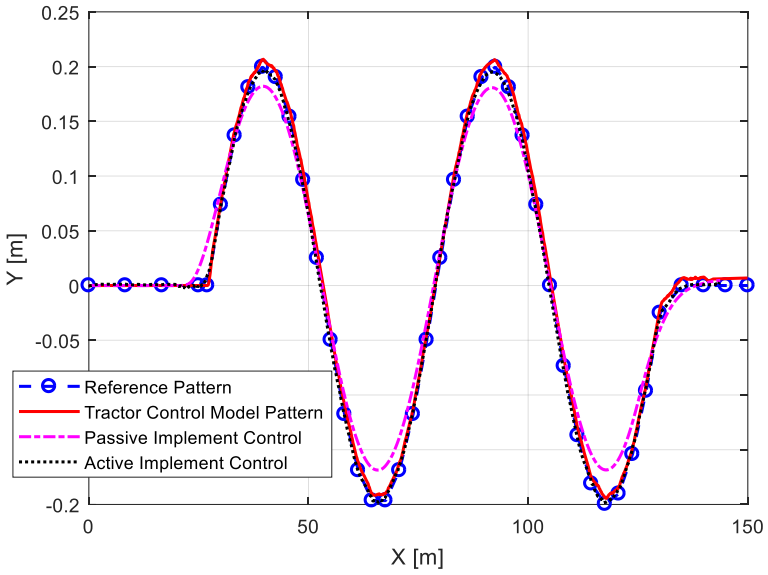

Figure 4.16. Tractor and towed implement behaviors in tracking a sinusoidal trajectory in passive and active control conditions at 3 m/s. X: the longitudinal direction and forward motion of the tractor and towed implement, Y: the lateral direction of motion.

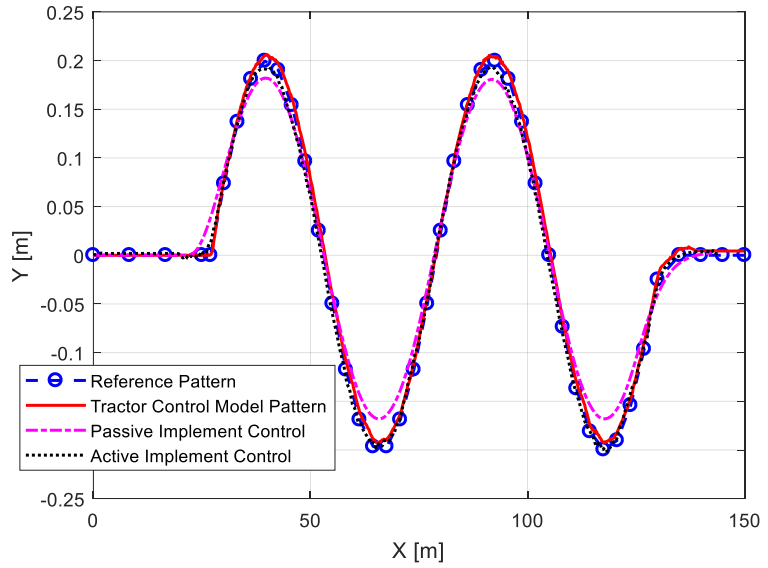

Figure 4.17. Tractor and towed implement behaviors in tracking a sinusoidal trajectory in passive and active control conditions at 5 m/s. X: the longitudinal direction and forward motion of the tractor and towed implement, Y: the lateral direction of motion.

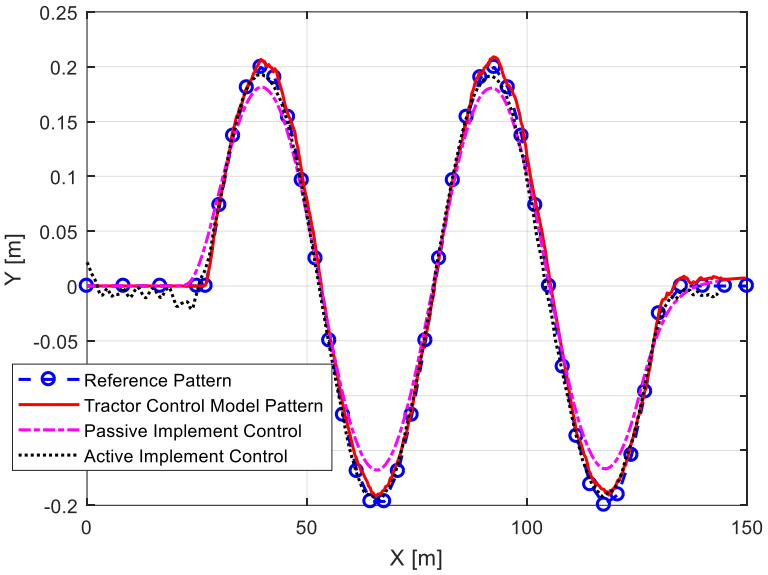

Figure 4.18. Tractor and towed implement behaviors in tracking a sinusoidal trajectory in passive and active control conditions at 7 m/s. X: the longitudinal direction and forward motion of the tractor and towed implement, Y: the lateral direction of motion.

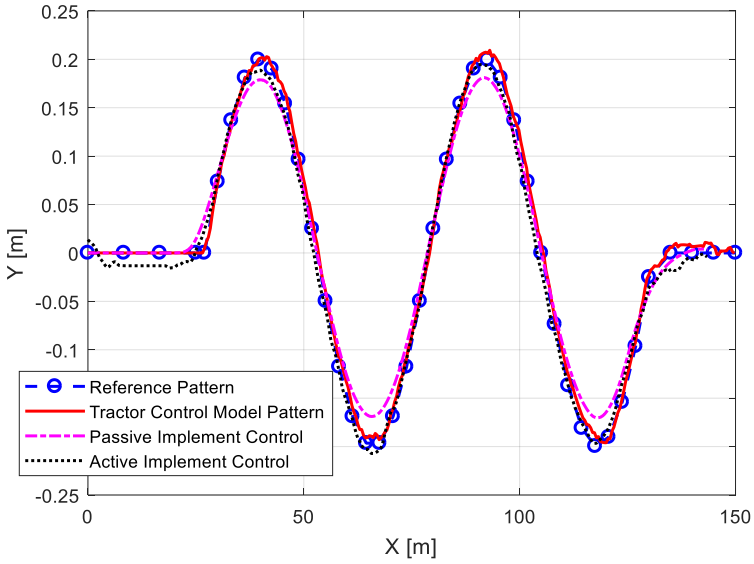

Figure 4.19. Tractor and towed implement behaviors in tracking a sinusoidal trajectory in passive and active control conditions at 9 m/s. X: the longitudinal direction and forward motion of the tractor and towed implement, Y: the lateral direction of motion.

Table 4.10. One-tail *t-test* results to test $H_0 : Avg.(e_{t,x}) \leq \pm 4$ cm, $Avg.(e_{t,y}) \leq \pm 3$ cm for the tractor following a sinusoidal trajectory at 95% level of confidence for df=∞.

Speed [m/s]	$e_{t,x}$ [cm]			$e_{t,y}$ [cm]			Decision
	Mean	Standard deviation	*t-calculated*	Mean	Standard deviation	*t-calculated*	
1	0.75	0.14	-870.9	1.41	0.30	-203.70	Fail to reject H_0
3	1.00	0.11	-989.1	1.38	0.33	-184.40	Fail to reject H_0
5	1.04	0.25	-440.9	1.54	0.25	-217.80	Fail to reject H_0
7	1.30	0.29	-356.2	1.96	0.25	-156.6	Fail to reject H_0
9	1.42	0.3	-323.7	2.45.	0.31	-67.24	Fail to reject H_0

Table 4.11. One-tail *t-test* results to test $H_0 : Avg.(e_{t,x}) \leq \pm 4$ cm, $Avg.(e_{t,y}) \leq \pm 3$ cm for the implement in passive condition following a sinusoidal trajectory at 95% level of confidence for df=∞.

Speed [m/s]	$e_{c,x}$ [cm]			$e_{c,y}$ [cm]			Decision
	Mean	Standard deviation	*t-calculated*	Mean	Standard deviation	*t-calculated*	
1	2.67	0.43	-117.83	1.4909	0.35	-165.45	Fail to reject H_0
3	2.90	0.56	-75.40	2.2472	0.20	-144.26	Fail to reject H_0
5	3.02	0.53	-70.57	2.6995	0.05	-198.92	Fail to reject H_0
7	3.14	0.60	-54.06	2.6467	0.31	-43.60	Fail to reject H_0
9	3.53	0.60	-29.30	2.9941	0.28	-0.79	Fail to reject H_0

Table 4.12. One-tail *t-test* results to test $H_0 : Avg.(e_{t,x}) \leq \pm 4$ cm, $Avg.(e_{t,y}) \leq \pm 3$ cm for the implement in active condition following a sinusoidal trajectory at 95% level of confidence for df=∞.

Speed [m/s]	$e_{c,x}$ [cm]			$e_{c,y}$ [cm]			Decision
	Mean	Standard deviation	*t-calculated*	Mean	Standard deviation	*t-calculated*	
1	1.80	0.69	-123.04	1.25	0.42	-156.87	Fail to reject H_0
3	1.98	0.67	-115.06	1.48	0.45	-127.56	Fail to reject H_0
5	2.16	0.75	-93.83	1.63	0.4	-107.97	Fail to reject H_0
7	2.38	0.87	-71.35	1.92	0.57	-72.41	Fail to reject H_0
9	3.00	0.64	-59.06	2.14	0.71	-46.31	Fail to reject H_0

4.4.3. Analysis of the Fuzzy Logic Controller for Tracking a Step Trajectory

Compared with the zigzag and sinusoidal trajectories, the controller was only able to adjust the position of the tractor at slower speeds up to 5 m/s (Table 4.13). According to Table 4.13 the ability of the controller to control the tractor motion at high speeds (7 and 9 m/s) degraded with significant overshoots and fluctuations at headlands. These fluctuations were due to the changes of slip angle at 7 and 9 m/s, which were greater than 0.5 rad (28.6°). A similar behavior was observed for zigzag and sinusoidal trajectories, with a difference that the fluctuations in tractor motion only happened at the end of simulations at high speeds (Figure 4.13 and Figure 4.18). In passive control condition, the lateral and longitudinal errors of the towed implement in following the step trajectory at 7 and 9 m/s were significantly beyond the error ranges. The controller improved the trajectory tracking of the implement in active condition up to 7 m/s. Similar to the zigzag and sinusoidal trajectories at higher speeds the controller had difficulties in adjusting the implement position at the outset (Figure 4.23 and Figure 4.24).

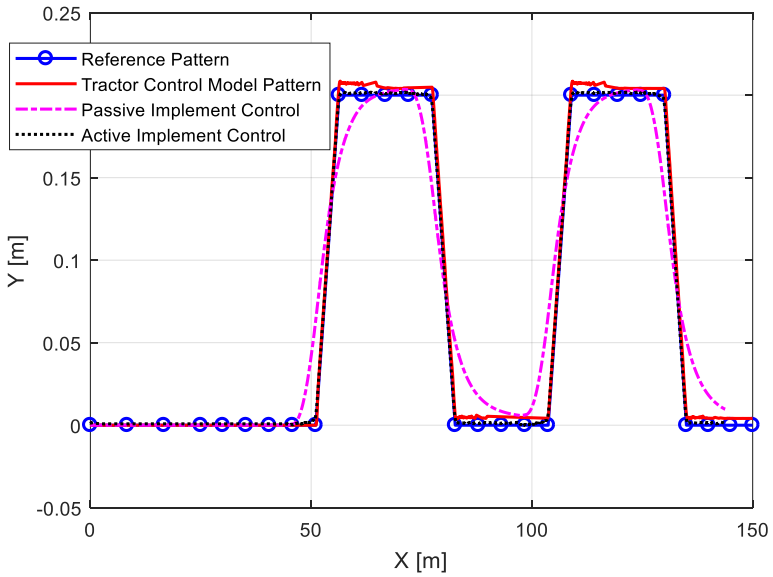

Figure 4.20. Tractor and towed implement behaviors in tracking a step trajectory in passive and active control conditions at 1 m/s. X: the longitudinal direction and forward motion of the tractor and towed implement, Y: the lateral direction of motion.

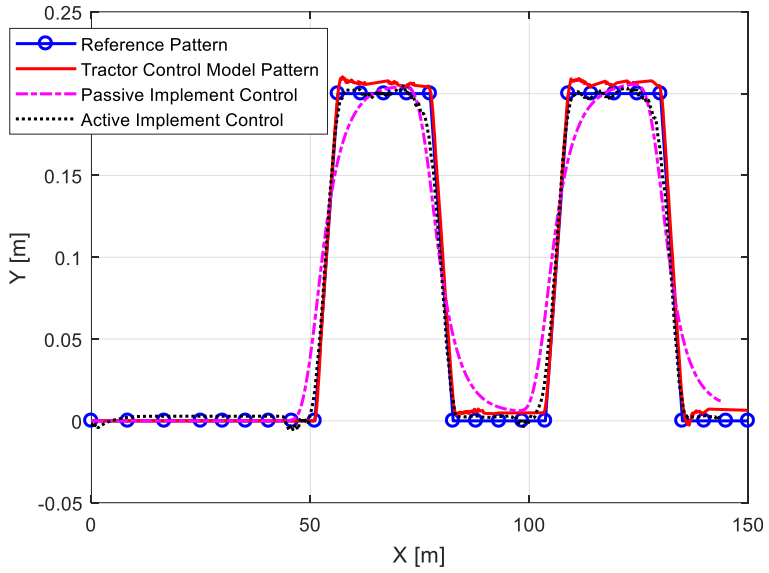

Figure 4.21. Tractor and towed implement behaviors in tracking a step trajectory in passive and active control conditions at 3 m/s. X: the longitudinal direction and forward motion of the tractor and towed implement, Y: the lateral direction of motion.

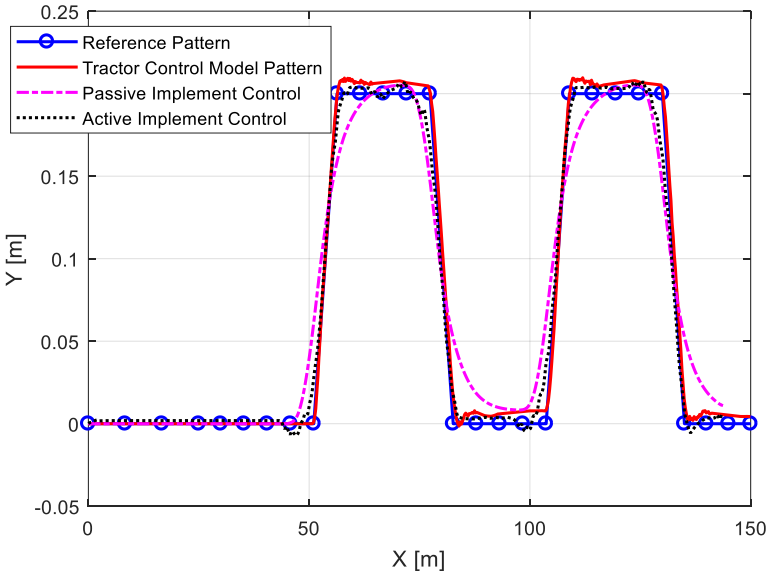

Figure 4.22. Tractor and towed implement behaviors in tracking a step trajectory in passive and active control conditions at 5 m/s. X: the longitudinal direction and forward motion of the tractor and towed implement, Y: the lateral direction of motion.

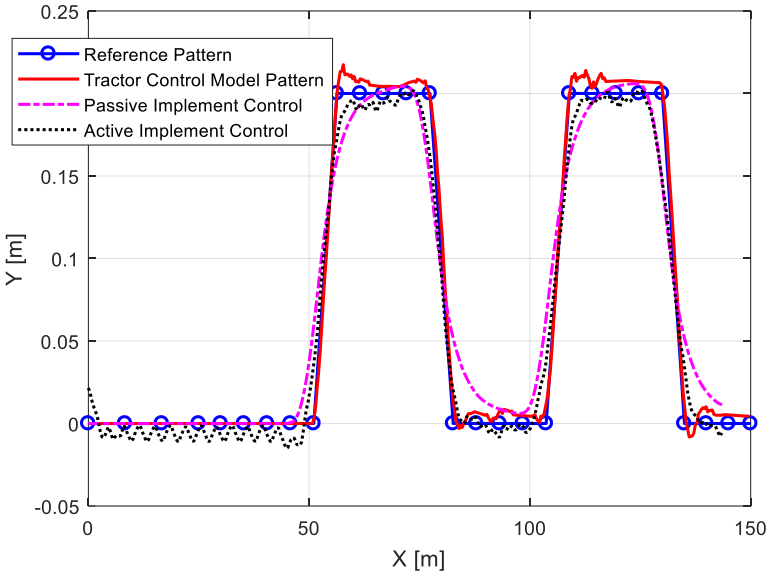

Figure 4.23. Tractor and towed implement behaviors in tracking a step trajectory in passive and active control conditions at 7 m/s. X: the longitudinal direction and forward motion of the tractor and towed implement, Y: the lateral direction of motion.

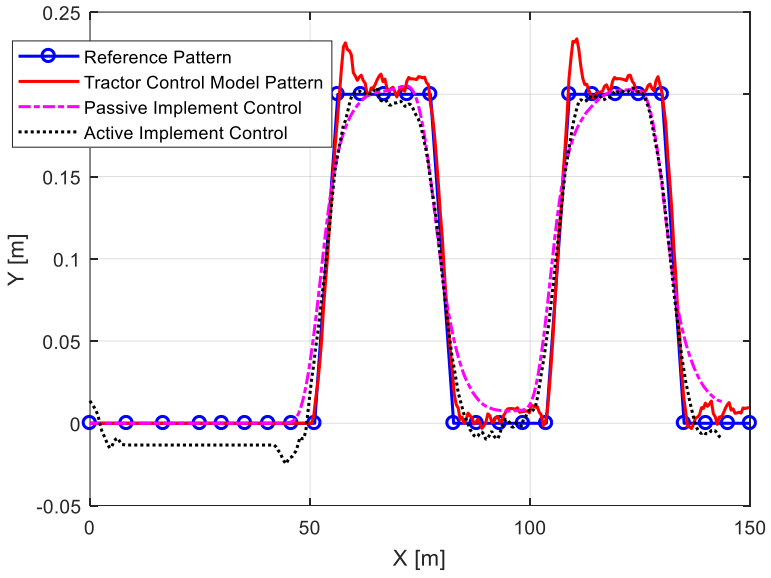

Figure 4.24. Tractor and towed implement behaviors in tracking a step trajectory in passive and active control conditions at 9 m/s. X: the longitudinal direction and forward motion of the tractor and towed implement, Y: the lateral direction of motion.

Table 4.13. One-tail *t-test* results to test $H_0 : Avg.(e_{t,x}) \leq \pm 4$ cm, $Avg.(e_{t,y}) \leq \pm 3$ cm for the tractor following a step trajectory at 95% level of confidence for df=∞.

Speed [m/s]	$e_{t,x}$ [cm]			$e_{t,y}$ [cm]			Decision
	Mean	Standard deviation	*t-calculated*	Mean	Standard deviation	*t-calculated*	
1	3.97	0.58	-1.43	2.89	0.53	-7.77	Fail to reject H_0
3	3.999	0.63	-0.03	2.96	0.49	-3.07	Fail to reject H_0
5	4.01	0.60	1.12	2.99	0.40	-0.46	Fail to reject H_0
7	4.03	0.73	2.07	3.02	0.52	1.53	Reject H_0
9	4.051	0.77	2.5389	3.02	0.46	2.12	Reject H_0

Table 4.14. One-tail *t-test* results to test $H_0 : Avg.(e_{t,x}) \leq \pm 4$ cm, $Avg.(e_{t,y}) \leq \pm 3$ cm for the implement in passive condition following a step trajectory at 95% level of confidence for df=∞.

Speed [m/s]	$e_{c,x}$ [cm]			$e_{c,y}$ [cm]			Decision
	Mean	Standard deviation	*t-calculated*	Mean	Standard deviation	*t-calculated*	
1	3.03	0.47	-79.15	2.85	0.54	-10.49	Fail to reject H_0
3	3.39	0.46	-50.58	2.91	0.56	-6.10	Fail to reject H_0
5	3.54	0.54	-32.30	2.99	0.06	-0.0923	Fail to reject H_0
7	3.77	0.48	-17.81	3.00	0.02	1.62	Reject H_0
9	3.88	0.58	-7.6689	3.04	0.66	2.4989	Reject H_0

Table 4.15. One-tail *t-test* results to test $H_0 : Avg.(e_{t,x}) \leq \pm 4$ cm, $Avg.(e_{t,y}) \leq \pm 3$ cm for the implement in active condition following a step trajectory at 95% level of confidence for df=∞.

Speed [m/s]	$e_{c,x}$ [cm]			$e_{c,y}$ [cm]			Decision
	Mean	Standard deviation	*t-calculated*	Mean	Standard deviation	*t-calculated*	
1	3.34	0.31	-80.44	2.81	0.17	-42.39	Fail to reject H_0
3	3.50	0.34	-55.13	2.85	0.20	-28.13	Fail to reject H_0
5	3.70	0.46	-24.23	2.91	0.17	-19.18	Fail to reject H_0
7	4.00	0.53	0.70	3.00	0.66	0.19	Fail to reject H_0
9	4.03	0.53	2.41	3.02	0.48	2.31	Reject H_0

4.4.4. Analysis of the Fuzzy Logic Controller for Tracking a Mixed Trajectory

The simulation results of tracking a mixed trajectory in both active and passive conditions at various speeds are displayed in Figure 4.25-Figure 4.29. Data analyses showed that the controller was successful in controlling the movements of the tractor within the defined boundaries. The errors of the towed implement in the passive condition for following the mixed trajectory were significantly beyond the error thresholds. The controller improved the implement motions in active control condition at 1-5 m/s. Similar to the zigzag trajectory, the trajectory tracking accuracy of the implement at 7 and 9 m/s in active control condition was not significantly different from the passive condition. This observation confirmed that the performance of the controller particularly at higher traveling speeds depended on the complexity of the tracking trajectory.

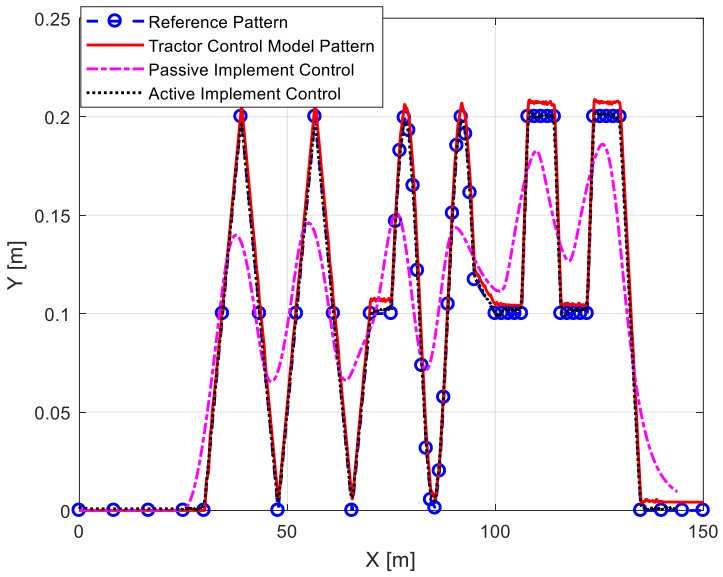

Figure 4.25. Tractor and towed implement behaviors in tracking a mixed trajectory in passive and active control conditions at 1 m/s. X: the longitudinal direction and forward motion of the tractor and towed implement, Y: the lateral direction of motion.

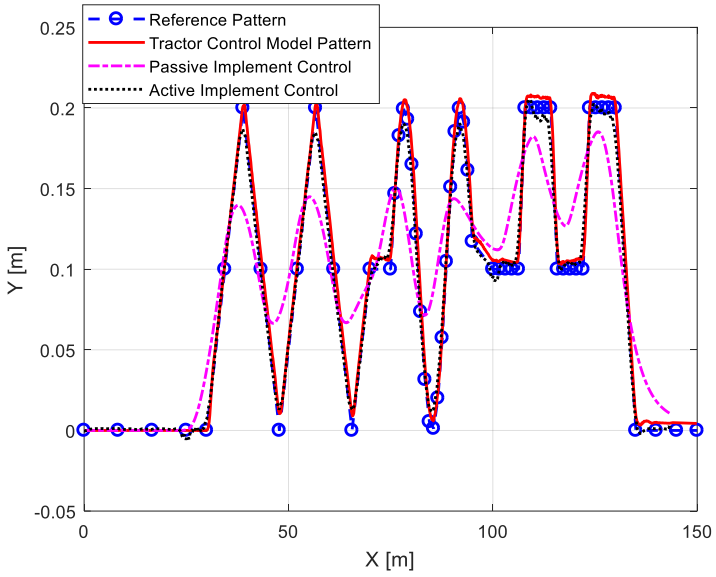

Figure 4.26. Tractor and towed implement behaviors in tracking a mixed trajectory in passive and active control conditions at 3 m/s. X: the longitudinal direction and forward motion of the tractor and towed implement, Y: the lateral direction of motion.

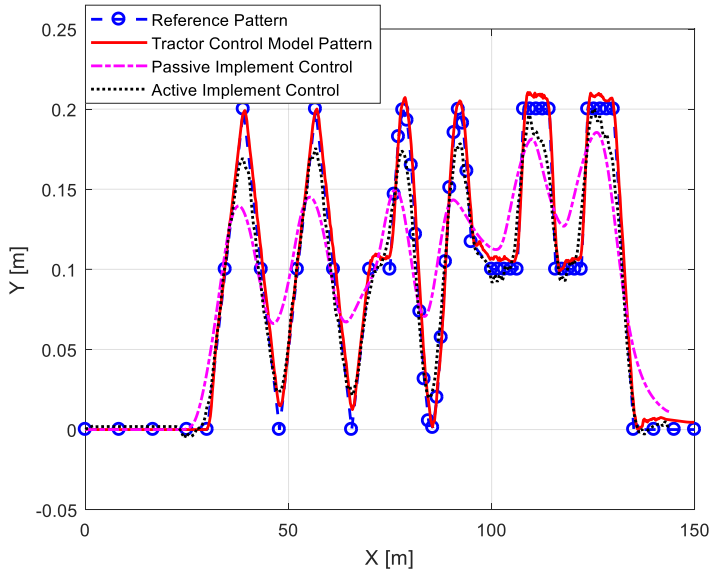

Figure 4.27. Tractor and towed implement behaviors in tracking a step trajectory in passive and active control conditions at 5 m/s. X: the longitudinal direction and forward motion of the tractor and towed implement, Y: the lateral direction of motion.

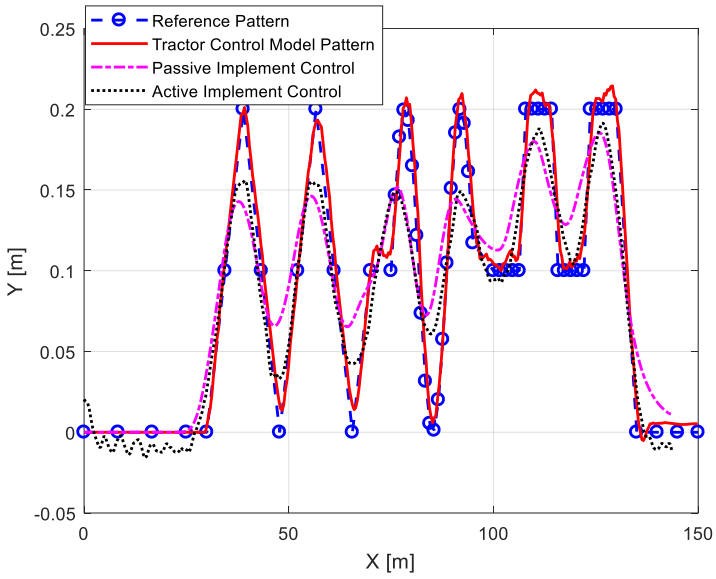

Figure 4.28. Tractor and towed implement behaviors in tracking a step trajectory in passive and active control conditions at 7 m/s. X: the longitudinal direction and forward motion of the tractor and towed implement, Y: the lateral direction of motion.

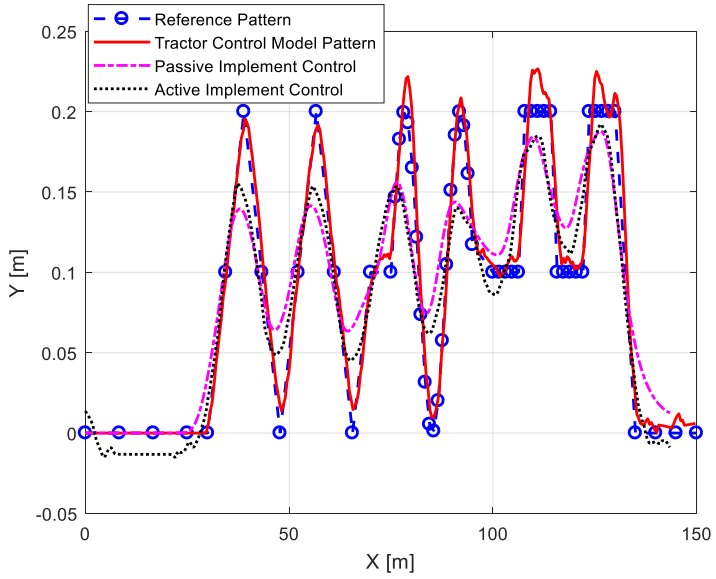

Figure 4.29. Tractor and towed implement behaviors in tracking a step trajectory in passive and active control conditions at 9 m/s. X: the longitudinal direction and forward motion of the tractor and towed implement, Y: the lateral direction of motion.

Table 4.16. One-tail *t-test* results to test $H_0 : Avg.(e_{t,x}) \leq \pm 4$ cm, $Avg.(e_{t,y}) \leq \pm 3$ cm for the tractor following a step trajectory at 95% level of confidence for df=∞.

Speed [m/s]	$e_{t,x}$ [cm]			$e_{t,y}$ [cm]			Decision
	Mean	Standard deviation	*t-calculated*	Mean	Standard deviation	*t-calculated*	
1	0.60	0.22	-579.9	0.92	0.17	-454.34	Fail to reject H_0
3	1.07	0.41	-273.9	1.16	0.20	-333.28	Fail to reject H_0
5	1.28	0.46	-225.8	1.42	0.29	-207.58	Fail to reject H_0
7	1.95	0.60	-131.4	2.00	0.34	-111.69	Fail to reject H_0
9	3.06	0.84	-42.8	2.61	0.52	-28.55	Fail to reject H_0

Table 4.17. One-tail *t-test* results to test $H_0 : Avg.(e_{t,x}) \leq \pm 4$ cm, $Avg.(e_{t,y}) \leq \pm 3$ cm for the implement in passive condition following a step trajectory at 95% level of confidence for=∞.

Speed [m/s]	$e_{c,x}$ [cm]			$e_{c,y}$ [cm]			Decision
	Mean	Standard deviation	*t-calculated*	Mean	Standard deviation	*t-calculated*	
1	4.16	0.96	6.46	3.09	0.40	9.42	Reject H_0
3	4.38	0.96	15.56	3.22	0.47	18.66	Reject H_0
5	4.73	1.02	27.79	3.73	0.47	59.93	Reject H_0
7	5.30	1.09	46.12	3.82	0.40	78.46	Reject H_0
9	5.78	1.08	64.07	4.01	0.50	77.00	Reject H_0

Table 4.18. One-tail *t-test* results to test $H_0 : Avg.(e_{t,x}) \leq \pm 4$ cm, $Avg.(e_{t,y}) \leq \pm 3$ cm for the implement in active condition following a step trajectory at 95% level of confidence for df=∞.

Speed [m/s]	$e_{c,x}$ [cm]			$e_{c,y}$ [cm]			Decision
	Mean	Standard deviation	*t-calculated*	Mean	Standard deviation	*t-calculated*	
1	1.83	0.56	-148.27	1.66	0.54	-95.26	Fail to reject H_0
3	2.03	0.62	-121.09	1.94	0.56	-72.96	Fail to reject H_0
5	2.46	0.70	-85.04	2.24	0.53	-54.77	Fail to reject H_0
7	4.34	0.90	14.64	3.10	0.78	5.13	Reject H_0
9	5.12	1.39	31.23	4.08	0.89	46.92	Reject H_0

The results of the simulations showed the controller was able to control the movements of the tractor at conventional traveling speeds (> 7 m/s) for all the tested trajectories. The accuracy

of controller in steering the towed implement reduced significantly due to increasing the tractor traveling speed, particularly for following complex trajectories. Oscillations and overshoots at high speeds were due to the non-negligible changes of slip angle (> 0.5 rad). These results showed the kinematic bicycle model used in this study was not capable of representing the system dynamics at high speeds.

The accuracy of the towed implement trajectory tracking in both passive and active conditions was measured as the percentage of the positions in which the towed implement was kept inside the defined boundaries (Table 4.19). These measurements show the effect of the fuzzy logic controller in improving the implement trajectory tracking. According to Table 4.19, regardless of the trajectory type and traveling speed, the controller improved the overall accuracy of the trajectory tracking for the implement.

Table 4.19. Towed implement accuracies (%) for following different trajectories at different speeds for passive and active control conditions.

	Passive					Active				
Speed [m/s]	1	3	5	7	9	1	3	5	7	9
Trajectory										
Zigzag	55	53	53	52	52	96	84	75	71	67
Sinusoidal	85	82	81	77	76	97	97	95	91	88
Step	75	72	66	58	57	98	95	92	67	67
Mixed	53	50	47	45	43	98	93	72	48	44

In other studies, with different types of controllers (Backman et al., 2009; Kayacan et al., 2016), the maximum speed at which the controllers had a good performance was 4.47 m/s. The result of data analyses showed that in simple trajectories (e.g. sinusoidal) the fuzzy logic controller designed in this study had a good performance up to 7 m/s. However, similar to the previous studies, the best performance of the controller was achieved at lower speeds (1-5 m/s) regardless of the trajectory complexity. In more complex patterns (e.g. mixed) the performance

of controller degraded considerably, and at higher speeds (7-10 m/s) there was no significant differences between the accuracy of trajectory tracking in active and passive control conditions. Considering the running speed and the trajectory type, the best performance of the controller was obtained for zigzag and sinusoidal trajectories at 1-5 m/s.

4.5. Conclusion

The simulation results showed that regardless of the trajectory type and the running speeds, the controller was successful in steering a tractor and towed implement at low speeds (less than 7 m/s). Significant fluctuations and overshoots were observed in tractor motion at higher running speeds (higher than 7 m/s). These fluctuations were due to the significant changes of the slip angle at high speeds. The controller steered the implement best when following the sinusoidal and zigzag trajectories up to 7 m/s, while no major improvements were achieved for mixed trajectory. The traveling speed of the tractor was considered a major limitation to the performance of the controller. Considering the common running speeds of the agricultural operations and deviation from straight row patterns in a field, the performance of the controller was satisfactory. At higher speeds and complex trajectories, a dynamic modeling of the tractor and towed implement, and more accurate tuning of the fuzzy logic rules, could improve the accuracy of the controller.

The developed kinematic bicycle model only provided a mathematical description of the vehicle motion without considering the forces that affect the motion and the equations of motion are based purely on geometric relationships governing the system. However, at high speeds (> 5 m/s) slip angles of front and rear wheels and subsequently the lateral forces generated by the tires are no longer negligible and affect the dynamic of the system significantly. Although most agricultural operations are conducted at low speeds and accelerations, kinematic bicycle model

also cannot represent a heavy loaded tractor and towed implement driving through uneven and unstructured agricultural field conditions. Thus, the development of dynamic model of the tractor and towed implement considering the lateral tire forces. In addition, the main drawback of fuzzy logic controllers is that there is no systematic technique to tune the controller to achieve a desired set point. The trial-and-error method is the common approach used to tune a fuzzy logic controller until a satisfactory result is obtained. Further studies can be conducted to consider the effect of terrain and tire friction on the performance of the controller.

5. DESIGN AND DEVELOPMENT OF A HARDWARE IN-THE-LOOP SYSTEM TO ANALYZE THE PERFORMANCE OF A FUZZY LOGIC CONTROLLER FOR STEERING AGRICULTURAL TOWED IMPLEMENTS

5.1. Abstract

Agricultural vehicles could benefit from using fluid power to actuate a steering system for controlling a towed implement. The required force to change the implement and to turn the wheels is provided by hydraulic cylinders. Auto-steering control of the implement can be achieved through an electrically controlled directional hydraulic valve that controls the position of a cylinder rod. Therefore, a controller generates electrical signals to control the electrohydraulic valve and thus the steering. In this study, a fuzzy logic controller was designed to create the required steering signals to control the position of an implement using an electrohydraulic valve. A set of 81 logic rules was defined to correct the position of a towed implement in different operating conditions. To validate the performance of the controller in real conditions, the designed control algorithm was implemented in a hardware-in-loop electrohydraulic system. Two different trajectories (step and sinusoidal trajectories) and four different traveling speeds (1, 3, 5, and 7 m/s) were selected to evaluate the capability of the controller at different conditions. The performance of the control algorithm depended on both the traveling speed and the complexity of the trajectory. The result obtained from this research showed the fuzzy logic controller was capable of keeping the towed implement within the boundary of crop rows with an average error of 5 cm. This study provides some fundamental insight into designing high-performance electrohydraulic control systems for auto steering of towed implements.

5.2. Introduction

Agricultural vehicles often work on different types of terrains and soils, ranging from asphalt to soft topsoil in the field. In the case of automatic or autonomous navigation, steering controllers should be able to provide appropriate steering action in response to the variation in equipment operation state, traveling speed, tire cornering stiffness, ground conditions, and many other parameters influencing steering dynamics. Also, the design of the actuator should provide a stable and fast response. For this purpose, most modern agricultural vehicles employ some form of hydraulic steering system to meet all the mentioned requirements. The controller first translates the vehicle's position deviation signals into a voltage signal; an actuator then converts the voltage signal to an appropriate mechanical adjustment in the angular displacement of the implement. The voltage signal is used to open a valve forcing the hydraulic cylinder in the steering circuit to change the angular displacement of the front or rear axle and side shift the equipment relative to the tractor or the plant rows.

Before the implementation of a controller in a real machine, it is common to study its performance via computer simulations. In order to simulate the performance of the system in the real world, it is necessary to develop a mathematical model of the system and its running environment. In agricultural vehicles, the hydraulic valve-cylinder system is usually used to implement automated steering control. Due to high-nonlinearity of hydraulic systems, the modeling of such systems is complex with high levels of uncertainty. However, it is feasible to fabricate a system in which the hydraulic components of the system are physically integrated to the controller's elements. This method always leads to a more reliable design of the control system because any mathematical model, no matter how accurate it is, will always approximate reality. This method used is named hardware in-the-loop (HIL), and is an efficient method of

designing and verifying a controller when it is difficult or impossible to model the controller system with an acceptable precision.

The method for designing a fuzzy logic control system to steer agricultural intelligent vehicles was discussed extensively in Delavarpour et al., (2020b), and the performance of the controller was simulated and studied for different reference trajectories at different speeds. To further validate the accuracy of the designed fuzzy logic controller, it is crucial to analyze the performance of the controller in a real-world setting. This study focuses on the evaluation of the execution of the steering commands generated by the fuzzy logic controller to follow a trajectory. For this purpose, a HIL was developed to simulate and analyze the performance of the fuzzy logic controller. The dynamic behavior of an electrohydraulic valve was analyzed and the effectiveness of the controller to control the valve as an intermediate step to control a towed implement was examined. Figure 5.1 represents the concept of the HIL used in this study and includes hardware and software parts of the system. To design this system, a Linear Variable Differential Transformer (LVDT) position sensor, as a part of the hardware side of HIL, was used to estimate the position of the cylinder rod, and provided the feedback signal required to close the control loop.

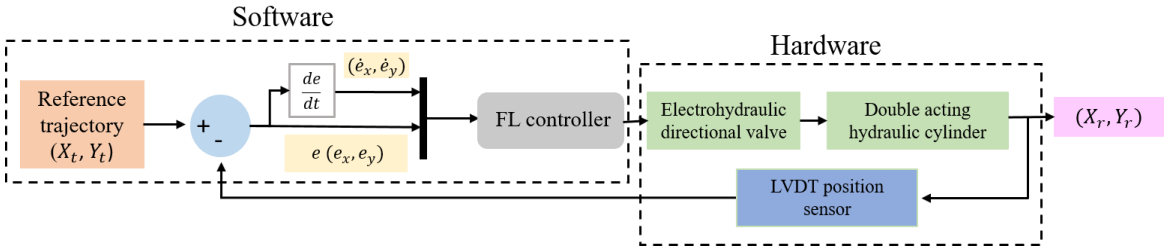

Figure 5.1. Control system block diagram representing the concept of the hardware in-the-loop system.

5.3. Materials and Methods

5.3.1. Design and Development of the Hydraulic Unit for the HIL System

In agricultural fields, the vehicles typically should follow the straight crop rows with minimal deviation from the row line and the angular displacements to keep a vehicle exactly between the crop rows are small in magnitude (less than 10˚or 0.17 rad). Thus, there is a direct relationship between vehicle steering linkage and the displacement of the hydraulic cylinder rod that actuates it. Controlling the position of cylinder rod is equivalent to controlling the angle turned by the steering wheel of a manually steered vehicle. Consequently, there is a linear relationship between the displacement of the cylinder rod and the actual angle turned by the steering wheel. In this study, a hydraulic test unit was designed to take the steering controller signals from the fuzzy logic controller and convert the output voltage signal to a mechanical adjustment of the cylinder rod. The schematic of the hydraulic circuit representing the HIL system is shown in Figure 5.2.

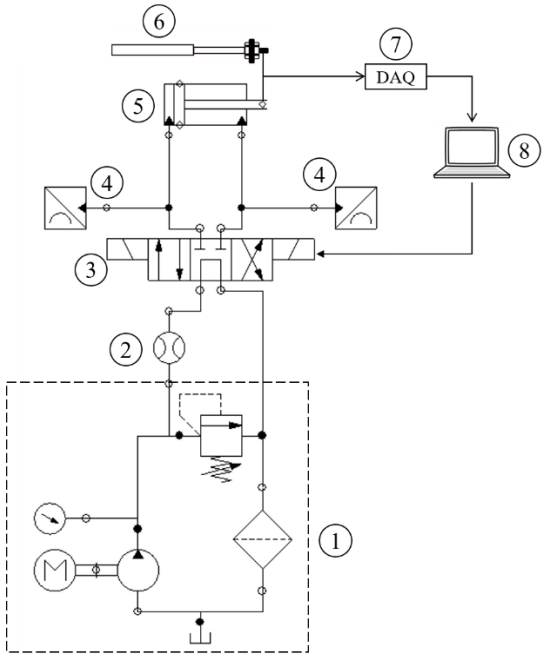

Figure 5.2. Schematic representation of the integrated electrohydraulic valve and steering system. 1. Hydraulic power pack, 2. Flowmeter, 3. Electrohydraulic directional valve, 4. Pressure transducer, 5. Double acting hydraulic cylinder, 6. LVDT position sensor, 7. Data acquisition board, 9. Control unit.

The hydraulic unit, shown in Figure 5.3, consists of a hydraulic power pack (Dayton Electric MFG. CO. Chicago, USA), an electrohydraulic directional valve (Yuken KOGYO CO., LTD, JAPAN), a differential double-acting cylinder with a rod of 11-cm in length (Surplus Center, Lincoln, NE, USA), a LVDT position sensor (P3 America-Precision Positioning Products, San Diego, CA, USA), and a data acquisition system (DATAQ Instruments, Akron, Ohio, USA). Two pressure transducers (Omega Engineering INC, Norwalk, CT, USA) were connected to the inlet and outlet ports of the hydraulic cylinder to check the oil pressure continuously. The pressure transducers were calibrated using a deadweight gauge tester (Chandler Engineering, Tulsa, OK, USA) shown in Figure 5.4. The flowrate of the hydraulic oil was measured using a flow measurement device (Owatonna Tool Company, Owatonna, MN, USA) shown in Figure 5.5. According to the flow gauge, the maximum flow rate of the hydraulic power pack was 9 GPM.

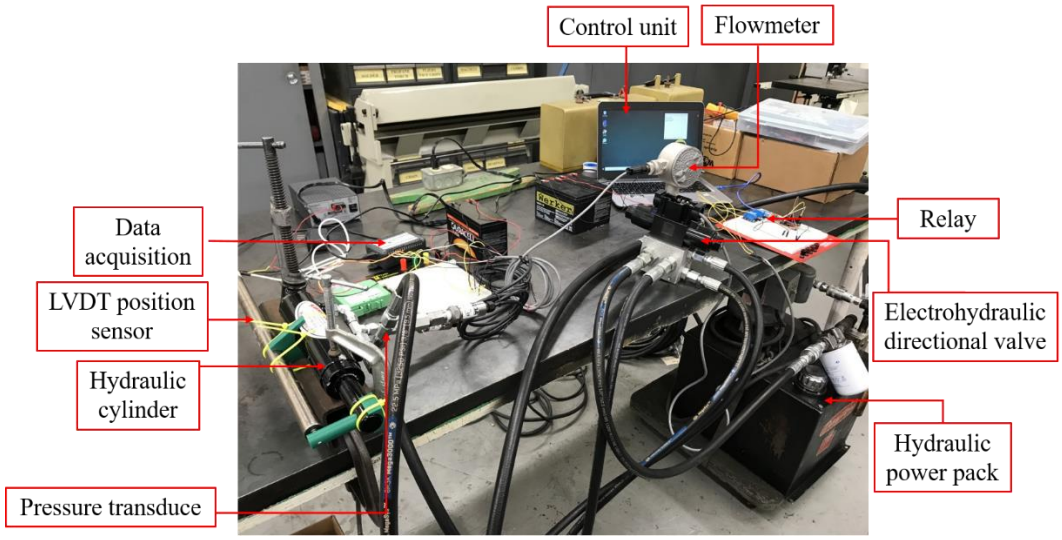

Figure 5.3. Hydraulic test unit for the hardware in-the-loop system.

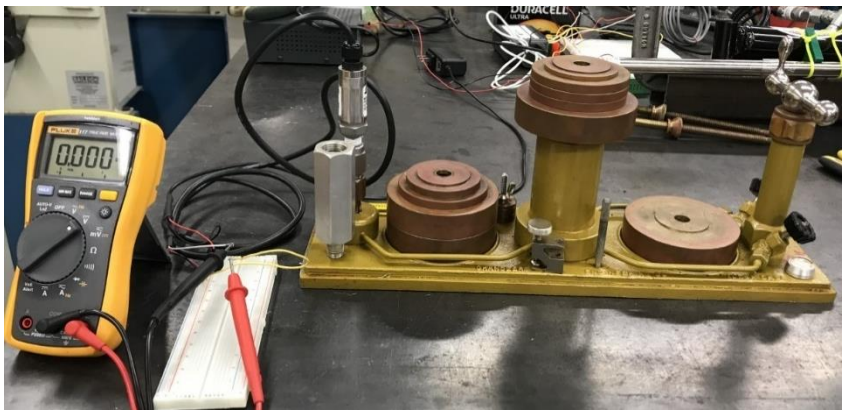

Figure 5.4. Deadweight gauge tester to calibrate the pressure transducers used in the HIL system.

Figure 5.5. Flowrate measurement of the hydraulic power pack.

The electrohydraulic directional valve, the pressure transducers, and the LVDT position sensor were energized using 12 VCD voltage. The electrohydraulic valve was an open center,

three position, four-way, directional solenoid valve. The required force to actuate the valve was obtained electrically using a microcontroller board (Arduino UNO, ELEGOO, China). Two 5V relay modules (Songle Relay, China) actuated flow path from the hydraulic power pack to the cylinder and a return line from the cylinder to the fluid reservoir. The relays were wired normally open and switched the power 'ON' when the coil was activated. The microcontroller energized one of the relays for 't' seconds with respect to the request of the fuzzy logic controller to adjust the cylinder rod position. The activated relay delays the operation of its contact for 't' seconds and a timer brings back its contacts immediately to their normal positions when the coil is de-energized 'OFF'. The Arduino UNO microcontroller was programmed in MATLAB to control the direction of flow into the hydraulic circuit.

5.3.2. Controller Adjustments and Selection of Input and Output Variables

The goal of the feedback control system was to create an actuating signal to make the actuator follows the desired control command promptly and accurately. The design and development of the fuzzy logic controller used in this study is explained in Delavarpour et al., (2020b). The inputs to this controller were the vehicle's lateral and longitudinal errors from the reference trajectory ($\varepsilon_x, \varepsilon_y$) and the change rates of these errors ($\dot{\varepsilon}_x, \dot{\varepsilon}_y$) to estimate an angular displacement for the vehicle.

Adjustments were required to adapt the fuzzy logic controller in Delavarpour et al., (2020b) in the designed HIL of this study. Thus, before implementing the fuzzy logic control loop in the HIL system, it was necessary to modify the controller to determine the input to a relay based on the reference trajectory in every instant of the experiment. The output of the controller was modified to generate a voltage signal to activate the electrohydraulic valve

proportional to the estimated errors and errors changing rate and to change the position of the implement accordingly in the range of [-30˚,30˚].

To find the appropriate modifications, the response of the electrohydraulic valve to different input signals was studied. The time required to extend or retract the rod to a certain position and the length of the rod after responding to a command were recorded. An LVDT position sensor was attached to the cylinder to measure the position of the rod, and to provide the feedback signal required to close the control loop. The cylinder rod displacement for steering actuation was defined from the middle point of the rod stroke, and therefore the maximum position error was always less than 5.5 cm, one half of the rod stroke (11 cm). When the rod retracted, the requested angular displacement was negative, and when it extended, the requested angular displacement was positive. The initial result of these experiments demonstrated that the cylinder cannot extend and retract symmetrically and it retracts a longer length than it extends for the same time delay. The reason behind this observation is that the internal surface areas of the cylinder at the rod end and the blind end are different. Principally, the area of the rod end is smaller than the area of the blind end. Thus, for the same flow rate, a cylinder retracts faster compared with the extension course. This could lead to an overshoot phenomenon for following a reference trajectory and correction should be introduced to the controller to limit the rod position when it retracts. Table 5.1 shows the required average time delays to retract and extend the cylinder rod to certain degrees. In order to estimate the required time delay to energize relays with respect to the magnitude and direction of the estimated angular displacement, look-up tables were added to the fuzzy logic controller.

Table 5.1. Required time delay to energize a relay to retract or extend the cylinder rod to a certain positions and degrees.

Cylinder rod position (cm)	Angular displacement of the hitch (degrees)	Time delay to retract the rods (sec)	Time delays to extend the rod (sec)
1	5	0.01	0.015
2	10	0.05	0.065
3	20	1	1.03
4	25	2	2.05
5	30	3	3.08

5.3.3. Experimental Design and Statistical Analysis

The modified fuzzy logic algorithm was implemented on the HIL hydraulic simulator. The differences between the desired trajectory (X_t ,Y_t) and the followed trajectory by the vehicle (X_r ,Y_r) were calculated at four different speeds of 1, 3, 5, and 7 m/s. Since straight rows are the most common trajectories in agricultural operations, two simple reference trajectories (sinusoidal and step trajectories) were selected to analyze the performance of the controller for both straight line and curvilinear geometries (Figure 5.6). The experiments were repeated three times. The average lateral and longitudinal errors between the reference trajectory and the trajectory followed by the vehicle (ε_x, ε_y) were calculated to provide a quantitative evaluation of the fuzzy controller performance. Very small errors (ε_x, ε_y) are expected when the angular displacement of the vehicle followed by the rod is very close to the voltage signals. Errors will start to increase when the rod cannot keep up with the generated input. The errors (ε_x, ε_y) were used to calculate the Euclidean error to the reference trajectory points.

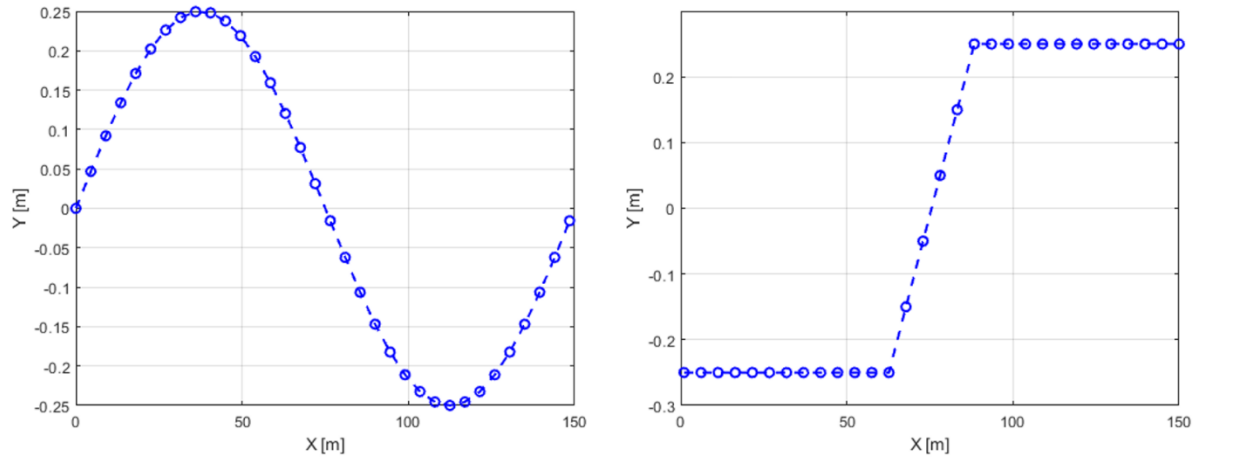

Figure 5.6. Designed trajectory to test the performance of the fuzzy logic controller in HIL system, (a) sinusoidal trajectory, (b) step trajectory.

In order to provide a sufficient number of data points for each traveling speed, different sampling frequencies were selected. It was desired to study approximately 12,000 points per each experiment and the sampling frequencies at each speed were calculated accordingly. One-tailed *t*-tests were conducted to test whether the accuracy of the controller in steering the vehicle is sufficient to keep the Euclidean errors (*e*) less than the permissible error range at the 95% level of confidence. Considering the dimensions of the designed hydraulic hitch drive and the rows spacing of 76 cm, the permissible Euclidean error value of the vehicle from reference trajectory points was considered as ±5 cm. The summary of controller's accuracy testing hypothesis is:

$H_0 : e \leq \pm 5cm$

H_A : Euclidean error greater than the defined values in H_0

5.4. Test Results and Discussion

5.4.1. Step Trajectory Tracking

The results of experiments to test the accuracy of the fuzzy logic controller for tracking a step trajectory in a HIL system at 7 m/s speed is displayed in Figure 5.7. The same trend was observed for the other traveling speeds. The differences between the angles commanded by the

controller and actuation angles realized due to the changes in the rod position for the straight sections of the trajectory had a significant fluctuation of ±0.05 rad (±2.86˚). The angles from changes in cylinder rod position were within the acceptable limits of angular displacement. The negligible variations from requested angular displacement were due to either transient response or noises on the measurements. Also, the small inertia of the system was a potential limiting factor in the performance of the hydraulic cylinder. For the part between the straight sections of the trajectory, the controller generated larger angles at all traveling speeds. Although, the angles were greater in value, the difference between the requested and the actual angular displacement decreased significantly. This showed that the designed hydraulic system performed better in generating greater angular displacements. Additionally, as the vehicle speed increased, the angular displacement range generated by the controller increased. At 1 m/s the angular displacement range was between -0.2 to 0.18 rad (-11.5˚ to 10.3˚) and it increased to -0.25 to 0.26 rad (-14.32˚ to 15˚) at 7 m/s.

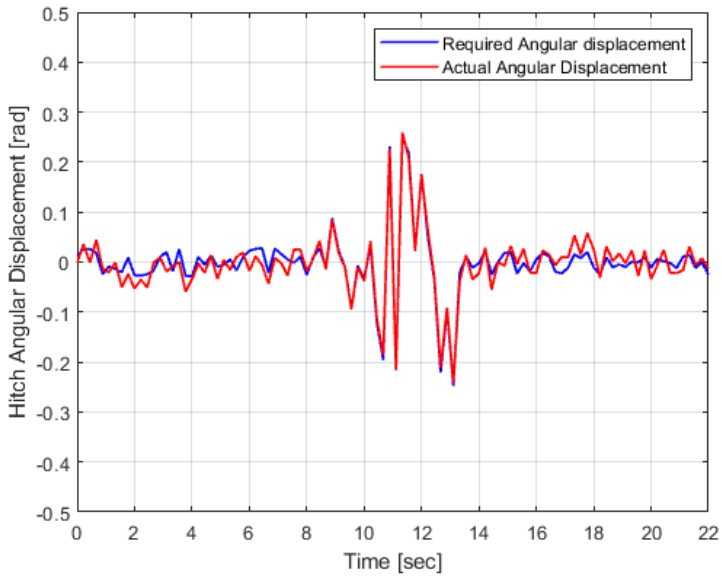

Figure 5.7. Difference between the required angular displacement generated by the controller and the actual angular displacement due to the changes in rod position for following a step trajectory at 7 m/s.

Figure 5.8 shows that the actual trajectory that the vehicle tracked was pretty close to the reference trajectory at higher angular displacement compared with straight paths at 7 m/s. The same behavior was also observed for the other speeds tested. Although at higher speed the Euclidean error values increased, this error was kept within ±5cm at all speeds (Table 5.2). Consequently, the accuracy of the controller along with the design of HIL system was sufficient to steer the vehicle through the step trajectory.

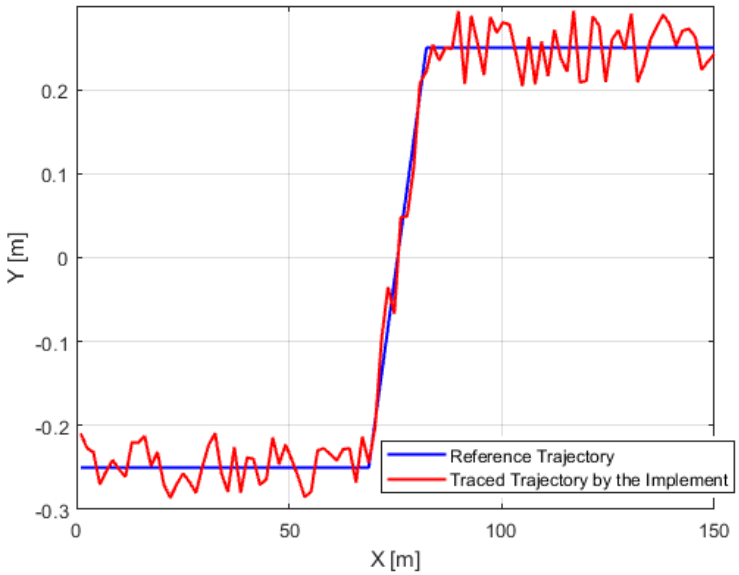

Figure 5.8. Step trajectory tracking in HIL system at 7 m/s. X: the longitudinal direction and forward motion of the tractor and towed implement, Y: the lateral direction of motion.

Table 5.2. One-tail *t-test* results to test $H_0 : e \leq \pm 5$ cm for the tractor following a step trajectory at 95% level of confidence for df=∞.

Speed [m/s]	e [cm]			Decision
	Mean	Standard deviation	*t-calculated*	
1	2.00	0.57	-835.28	Fail to reject H_0
3	3.99	0.90	-449.31	Fail to reject H_0
5	4.05	1.13	-374.49	Fail to reject H_0
7	4.85	1.18	-354.16	Fail to reject H_0

5.4.2. Sinusoidal Trajectory Tracking

The accuracies of the fuzzy logic controller for tracking a sinusoidal trajectory in a HIL system at 7 m/s is shown in Figure 5.9. The desired angular displacement was achieved in a sinusoidal trajectory by changing the cylinder rod position. The angle ranges at all traveling speeds were within the acceptable limits of angular displacement. At 1 m/s speed it was kept within ±0.2 rad (±11.5˚) and it increased to ±0.3 (±17˚) at V=7 m/s. The increase of the angle range at higher speeds was expected due to the insufficient time to respond to the generated signal and reach the desired rod position. This also resulted in higher deviation from the reference trajectory at higher speeds (Table 5.3). Similar to step trajectory, following small angles, which were the results of short extension or retraction of the cylinder rod, included negligible deviations from requested angular displacement. The designed hydraulic system performed better in generating larger angular displacement. As the speed increased, the angular displacement range generated by the controller increased. At 1 m/s the angular displacement range was between -0.2 to 0.18 rad (-11.5˚ to 10.3˚) and it increased to -0.3 to 0.3 rad (-17.2˚ to 17.2˚) at 7 m/s. Figure 5.10 compares the actual tracked trajectory and the reference trajectory at 7 m/s. Similar to straight line trajectory, Euclidean error was kept within ±5 cm at all speeds for step trajectories (Table 5.3), however, the maximum Euclidean error increased to 6.2 cm at 7 m/s.

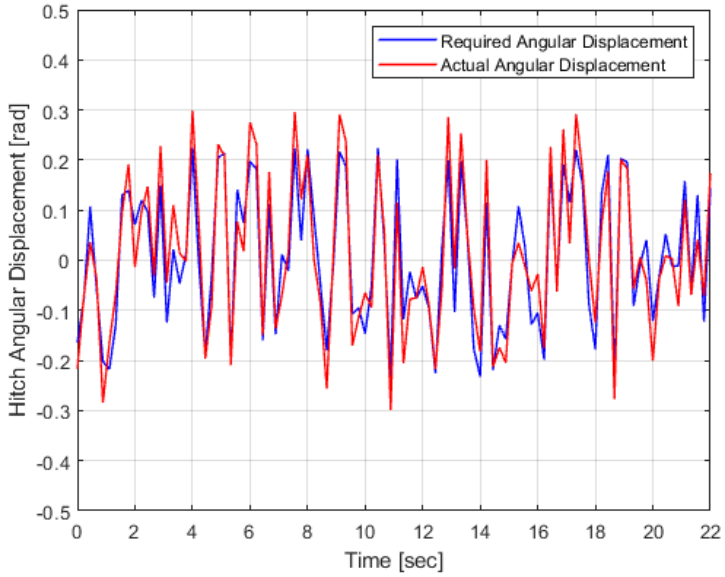

Figure 5.9. Difference between the required angular displacement generated by the controller and the actual angular displacement due to the changes in rod length for following a sinusoidal trajectory at 7 m/s.

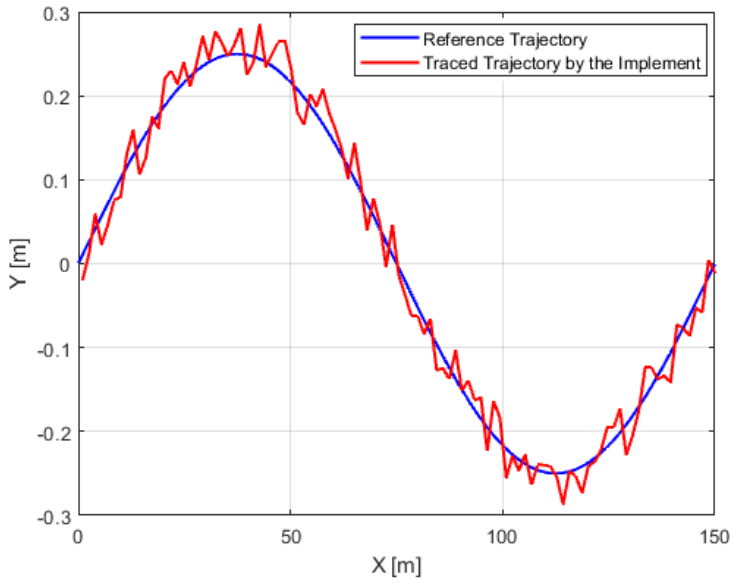

Figure 5.10. Sinusoidal trajectory tracking in HIL system at 7 m/s. X: the longitudinal direction and forward motion of the tractor and towed implement, Y: the lateral direction of motion.

Table 5.3. One-tail *t-test* results to test $H_0 : e \leq \pm 5$ cm for the tractor following a step trajectory at 95% level of confidence for df=∞.

Speed [m/s]	e [cm]			Decision
	Mean	Standard deviation	*t-calculated*	
1	2.50	1.43	-190.25	Fail to reject H_0
3	3.51	2.01	-80.84	Fail to reject H_0
5	4.01	2.30	-46.90	Fail to reject H_0
7	5.00	2.88	0.19	Fail to reject H_0

5.5. Conclusion

The hydraulic cylinder successfully followed the controller signals with sufficient accuracy. The symmetrical behavior in extension and retraction of the hydraulic cylinder showed the controller was tuned appropriately to respond to negative and positive angular displacements. Small extension or retraction of the cylinder rod resulted in negligible deviations from the requested angular displacement. These deviations from requested angles were due to the transient response, the noises on the measurements, and the inherent inertia of the hydraulic cylinder. For the selected speeds and trajectories, the angular displacements remained in the range of ±10˚ and never hit the constraint of maximum achievable angle, which was ±30˚. This observation showed that the design of the HIL system along with the fuzzy logic controller were sufficient to correct tracking errors. The trajectories traced by the hydraulic cylinder closely resembled the reference trajectories. This was the desired outcome to achieve a satisfactory control of the hydraulic cylinder. The test results showed that the automatic steering control system designed for navigating towed implement has good tracking performance with a fast response, thus meeting the navigation control requirement of agricultural equipment to a certain extent.

FUTURE WORK

The research studies and methodologies in this dissertation covered all steps involved in development of an autonomous agricultural machines relatively using different methods. However, future research is required to further improve the applicability of these systems. Here are a few suggestions for future research:

- Implementing the guidance systems (the tactile and ultrasonic sensors) and the fuzzy logic controller on a towed implement and conducting field experiments. This research currently does not consider field experiments.
- Analyzing the safety level while steering a towed implement using these local guidance sensors and the fuzzy logic controller.
- Developing a controller using the dynamic model of the tractor and towed implement and compare the accuracy of this controller to the controller with the kinematic bicycle model.
- Considering effects of disturbances like bumps and terrains on the performance of the controller.
- Analyzing the performance of the guidance sensors, controller, and the hydraulic actuation for following uphill or downhill slopes.

REFERENCE

Allou, S., Zennir, Y., & Belmeguenai, A. (2017). Fuzzy logic controller for autonomous vehicle path tracking. *2017 18th International Conference on Sciences and Techniques of Automatic Control and Computer Engineering (STA)*, 328–333. https://doi.org/10.1109/STA.2017.8314969

Alonso-Garcia, S., Gomez-Gil, J., & Arribas, J. I. (2011). Evaluation of the use of low-cost GPS receivers in the autonomous guidance of agricultural tractors. *Spanish Journal of Agricultural Research*, *9*(2), 377–388. https://doi.org/10.5424/sjar/20110902-088-10

Ang, K. H., Chong, G., & Li, Y. (2005). PID control system analysis, design, and technology. *IEEE Transactions on Control Systems Technology*, *13*(4), 559–576. https://doi.org/10.1109/TCST.2005.847331

Astolfi, A., Bolzern, P., & Locatelli, A. (2004). Path-tracking of a tractor-trailer vehicle along rectilinear and circular paths: A Lyapunov-based approach. *IEEE Transactions on Robotics and Automation*, *20*(1), 154–160. https://doi.org/10.1109/TRA.2003.820928

Backman, J., Oksanen, T., & Visala, A. (2009). Parallel guidance system for tractor-trailer system with active joint. *Precision Agriculture '09*, 615–622.

Backman, J., Oksanen, T., & Visala, A. (2012). Navigation system for agricultural machines: Nonlinear Model Predictive path tracking. *Computers and Electronics in Agriculture*, *82*, 32–43. https://doi.org/10.1016/j.compag.2011.12.009

Bhondave, B., Ganesan, T., Varma, N., Renu, R., & Sabarinath, N. (2017). Design and Development of Electro Hydraulics Hitch Control for Agricultural Tractor. *SAE International Journal of Commercial Vehicles*, *10*(1), 405–410. https://doi.org/10.4271/2017-26-0227

Brooks, R. R., & Iyengar, S. S. (1997). *Multi-Sensor Fusion: Fundamentals and Applications With Software* (Har/Dskt edition). Prentice Hall.

Cariou, C., Lenain, R., Thuilot, B., & Martinet, P. (2010a). Autonomous maneuver of a farm vehicle with a trailed implement: Motion planner and lateral-longitudinal controllers. *2010 IEEE International Conference on Robotics and Automation*. https://www.academia.edu/28081732/Autonomous_maneuver_of_a_farm_vehicle_with_a_trailed_implement_motion_planner_and_lateral_longitudinal_controllers

Cariou, C., Lenain, R., Thuilot, B., & Martinet, P. (2010b). Path following of a vehicle-trailer system in presence of sliding: Application to automatic guidance of a towed agricultural implement. *2010 IEEE/RSJ International Conference on Intelligent Robots and Systems*, 4976–4981. https://doi.org/10.1109/IROS.2010.5652673

Chen, Z., Yao, B., & Wang, Q. (2013). Accurate Motion Control of Linear Motors With Adaptive Robust Compensation of Nonlinear Electromagnetic Field Effect. *IEEE/ASME Transactions on Mechatronics*, *18*(3), 1122–1129. https://doi.org/10.1109/TMECH.2012.2197217

Cheung, W. W. L., Pitcher, T. J., & Pauly, D. (2005). A fuzzy logic expert system to estimate intrinsic extinction vulnerabilities of marine fishes to fishing. *Biological Conservation*, *124*(1), 97–111. https://doi.org/10.1016/j.biocon.2005.01.017

Chosa, T., Omine, M., Itani, K., & Ehsani, R. (2011). Evaluation of the Dynamic Accuracy of a GPS Receiver: Is dynamic accuracy the same as static accuracy? *Engineering in Agriculture, Environment and Food*, *4*(2), 54–61. https://doi.org/10.1016/S1881-8366(11)80021-2

Delavarpour, N., Eshkabilov, S., Bon, T., Nowatzki, J., & Bajwa, S. (2019). The Performance Analysis of Tactile and Ultrasonic Sensors for Planting, Fertilizing, and Cultivating Cover Crops. *2019 Boston, Massachusetts July 7- July 10, 2019*. 2019 Boston, Massachusetts July 7- July 10, 2019. https://doi.org/10.13031/aim.201901247

Delavarpour, N., Eshkabilov, S., Bon, T., Nowatzki, J., & Bajwa, S. (2020a). Performance Comparison of Two Guidance Systems for Agricultural Equipment Navigation. *Advances in Design, Simulation and Manufacturing II*, 541–551. https://doi.org/10.1007/978-3-030-22365-6_54

Delavarpour, N., Eshkabilov, S., Bon, T., Nowatzki, J., & Bajwa, S. (2020b). The Tractor-Cart System Controller with Fuzzy Logic Rules. *Applied Sciences*, *10*(15), 5223. https://doi.org/10.3390/app10155223

Durrant-Whyte, H. F. (1990). Sensor Models and Multisensor Integration. In I. J. Cox & G. T. Wilfong (Eds.), *Autonomous Robot Vehicles* (pp. 73–89). Springer. https://doi.org/10.1007/978-1-4613-8997-2_7

Electro-hydraulic systems, potentialities and limits—Power Transmission World. (n.d.). Retrieved March 14, 2022, from https://www.powertransmissionworld.com/7810-2/

Engeberg, E. D., & Meek, S. G. (2013). Adaptive Sliding Mode Control for Prosthetic Hands to Simultaneously Prevent Slip and Minimize Deformation of Grasped Objects. *IEEE/ASME Transactions on Mechatronics*, *18*(1), 376–385. https://doi.org/10.1109/TMECH.2011.2179061

Eriksson, L., Oksanen, T., & Mikkola, K. (2009). PID controller tuning rules for integrating processes with varying time-delays. *Journal of the Franklin Institute*, *346*(5), 470–487. https://doi.org/10.1016/j.jfranklin.2009.01.003

Falcone, P., Borrelli, F., Asgari, J., Tseng, H. E., & Hrovat, D. (2007). Predictive Active Steering Control for Autonomous Vehicle Systems. *IEEE Transactions on Control Systems Technology*, *15*(3), 566–580. https://doi.org/10.1109/TCST.2007.894653

Feng, L., He, Y., & Zhang, Q. (2005). Tractor-implement dynamic trajectory model for automated navigation applications. *Third International Conference on Information Technology and Applications (ICITA'05)*, *1*, 330–335.

Franklin, G. F., Powell, J. D., & Emami-Naeini, A. (2019). *Feedback control of dynamic systems* (Eighth edition). Pearson.

Galar, D., & Kumar, U. (2017). Chapter 1—Sensors and Data Acquisition. In D. Galar & U. Kumar (Eds.), *EMaintenance* (pp. 1–72). Academic Press. https://doi.org/10.1016/B978-0-12-811153-6.00001-4

Gomez-Gil, J., Alonso-Garcia, S., Gómez-Gil, F. J., & Stombaugh, T. (2011). A Simple Method to Improve Autonomous GPS Positioning for Tractors. *Sensors (Basel, Switzerland)*, *11*(6), 5630–5644. https://doi.org/10.3390/s110605630

Gouda, M. M., Danaher, S., & Underwood, C. P. (2000). Fuzzy Logic Control Versus Conventional PID Control for Controlling Indoor Temperature of a Building Space. *IFAC Proceedings Volumes*, *33*(24), 249–254. https://doi.org/10.1016/S1474-6670(17)36900-8

Gray, K. (2002). Obstacle detection sensor technology. *Proceedings of the Automation Technology for Off-Road Equipment*, 442–450. Scopus.

Guerrero, J. M., Ruz, J. J., & Pajares, G. (2017). Crop rows and weeds detection in maize fields applying a computer vision system based on geometry. *Computers and Electronics in Agriculture*, *142*, 461–472. https://doi.org/10.1016/j.compag.2017.09.028

Gupta, S., Khosravy, M., Gupta, N., Darbari, H., & Patel, N. (2019). Hydraulic system onboard monitoring and fault diagnostic in agricultural machine. *Brazilian Archives of Biology and Technology*, *62*.

Hodo, D. W., Hung, J. Y., Bevly, D. M., & Millhouse, D. S. (2007). Analysis of Trailer Position Error in an Autonomous Robot-Trailer System With Sensor Noise. *2007 IEEE International Symposium on Industrial Electronics*, 2107–2112. https://doi.org/10.1109/ISIE.2007.4374933

Hoover, A., & Olsen, B. D. (2000). Sensor network perception for mobile robotics. *Proceedings 2000 ICRA. Millennium Conference. IEEE International Conference on Robotics and Automation. Symposia Proceedings (Cat. No.00CH37065)*, *1*, 342–347 vol.1. https://doi.org/10.1109/ROBOT.2000.844080

Omega Engineering. (n.d.). *How does a Fuzzy Logic Controller work?* Https://Www.Omega.Co.Uk/. Retrieved March 16, 2022, from https://www.omega.co.uk/technical-learning/pid-fuzzy-logic-adaptive-control.html

Kayacan, E., Ramon, H., & Saeys, W. (2016). Robust Trajectory Tracking Error Model-Based Predictive Control for Unmanned Ground Vehicles. *IEEE/ASME Transactions on Mechatronics*, *21*(2), 806–814. https://doi.org/10.1109/TMECH.2015.2492984

Keymasi Khalaji, A., & Moosavian, S. A. A. (2014). Robust Adaptive Controller for a Tractor–Trailer Mobile Robot. *IEEE/ASME Transactions on Mechatronics*, *19*(3), 943–953. https://doi.org/10.1109/TMECH.2013.2261534

King, P. J., & Mamdani, E. H. (1977). The application of fuzzy control systems to industrial processes. *Automatica*, *13*(3), 235–242. https://doi.org/10.1016/0005-1098(77)90050-4

Lee, J.-H., Chung, W., Kim, M., & Song, J.-B. (2004). A Passive Multiple Trailer System with Off-axle Hitching. *International Journal of Control, Automation, and Systems*, *2*(3), 289–297.

Leng, Z., & Minor, M. A. (2017). Curvature-Based Ground Vehicle Control of Trailer Path Following Considering Sideslip and Limited Steering Actuation. *IEEE Transactions on Intelligent Transportation Systems*, *18*(2), 332–348. https://doi.org/10.1109/TITS.2016.2572208

Li, M., Imou, K., Wakabayashi, K., & Yokoyama, S. (2009). Review of research on agricultural vehicle autonomous guidance. *International Journal of Agricultural and Biological Engineering*, *2*(3), 1–16. https://doi.org/10.25165/ijabe.v2i3.160

Lin, C.-C., & Lal Tummala, R. (1994). Adaptive sensor integration for mobile robot navigation. *Proceedings of 1994 IEEE International Conference on MFI '94. Multisensor Fusion and Integration for Intelligent Systems*, 85–91. https://doi.org/10.1109/MFI.1994.398469

Lindner, P. (2018). Hydraulic Drive Axle for Agricultural Trailers. *ATZoffhighway Worldwide*, *11*(1), 20–23.

Liu, J., Tan, J., Mao, E., Song, Z., & Zhu, Z. (2016). Proportional directional valve based automatic steering system for tractors. *Frontiers of Information Technology & Electronic Engineering*, *17*(5), 458–464. https://doi.org/10.1631/FITEE.1500172

M. Min, R. Ehsani, & M. Salyani. (2008). Dynamic Accuracy of GPS Receivers in Citrus Orchards. *Applied Engineering in Agriculture*, *24*(6), 861–868. https://doi.org/10.13031/2013.25356

Hatten Electric Service & Bak-Vol. (2016). *Major Advantages & Disadvantages of Electric*. Retrieved March 14, 2022, from https://connect2local.com/l/152273/c/176968/major-advantages---disadvantages-of-electric-motors

Masoudi, H., Noguchi, N., Omid, M., Alimardani, R., Mohtasebi, S., Ishii, K., & Bagheri-Shooraki, S. (2009, August 10). *Evaluation of ultrasonic sensors as guidance sensors for greenhouse applications robot*. https://doi.org/10.13140/2.1.4700.2563

Meng, Q., Hao, X., Zhang, Y., & Yang, G. (2018). Guidance Line Identification for Agricultural Mobile Robot Based on Machine Vision. *2018 IEEE 3rd Advanced Information Technology, Electronic and Automation Control Conference (IAEAC)*, 1887–1893. https://doi.org/10.1109/IAEAC.2018.8577651

Meng, Q., Qiu, R., He, J., Zhang, M., Ma, X., & Liu, G. (2015). Development of agricultural implement system based on machine vision and fuzzy control. *Computers and Electronics in Agriculture*, *112*, 128–138. https://doi.org/10.1016/j.compag.2014.11.006

Nakamura, Y., Ezaki, H., Tan, Y., & Chung, W. (2000). Design of steering mechanism and control of nonholonomic trailer systems. *Proceedings 2000 ICRA. Millennium Conference. IEEE International Conference on Robotics and Automation. Symposia Proceedings (Cat. No.00CH37065)*, *1*, 247–254 vol.1. https://doi.org/10.1109/ROBOT.2000.844066

Golden Harvest. (n.d.). *Narrow Corn Rows Increasing Yield Potential in Northern Latitudes*. Retrieved March 16, 2022, from https://www.goldenharvestseeds.com/agronomy/articles/corn-row-spacing

Oksanen, T., & Backman, J. (2013). Guidance system for agricultural tractor with four wheel steering. *IFAC Proceedings Volumes*, *46*(4), 124–129. https://doi.org/10.3182/20130327-3-JP-3017.00030

Pradalier, C., & Usher, K. (2007). A simple and efficient control scheme to reverse a tractor-trailer system on a trajectory. *Proceedings 2007 IEEE International Conference on Robotics and Automation*, 2208–2214. https://doi.org/10.1109/ROBOT.2007.363648

Ryu, J.-C., Agrawal, S. K., & Franch, J. (2008). Motion Planning and Control of a Tractor With a Steerable Trailer Using Differential Flatness. *Journal of Computational and Nonlinear Dynamics*, *3*(3). https://doi.org/10.1115/1.2908178

S. I. Cho & N. H. Ki. (1999). AUTONOMOUS SPEED SPRAYER GUIDANCE USING MACHINE VISION AND FUZZY LOGIC. *Transactions of the ASAE*, *42*(4), 1137–1143. https://doi.org/10.13031/2013.20130

Thelen, M. (2014). *Safely moving farm equipment on public roads can be a challenge*. MSU Extension. Retrieved March 14, 2022, from https://www.canr.msu.edu/news/safely_moving_farm_equipment_on_public_roads_can_be_a_challenge

Silva, J. F., & Pinto, S. F. (2018). 35—Linear and Nonlinear Control of Switching Power Converters. In M. H. Rashid (Ed.), *Power Electronics Handbook (Fourth Edition)* (pp. 1141–1220). Butterworth-Heinemann. https://doi.org/10.1016/B978-0-12-811407-0.00039-8

Stombaugh, T. (1997). Automatic navigation of agricultural vehicles at higher speeds. *PhD. Diss. Urbana, IL.: University of Illinois at Urbana-Champaign*.

Subramanian, V. (2005). *Autonomous vehicle guidance using machine vision and laser radar for agricultural applications*. University of Florida.

Subramanian, V., Burks, T. F., & Dixon, W. E. (2009). Sensor fusion using fuzzy logic enhanced kalman filter for autonomous vehicle guidance in citrus groves. *Transactions of the ASABE*, *52*(5), 1411–1422.

Thamrin, N. M., Arshad, N. H. M., Adnan, R., Sam, R., Razak, N. A., Misnan, M. F., & Mahmud, S. F. (2013). Tree detection profile using a single non-intrusive ultrasonic sensor for inter-row tracking application in agriculture field. *2013 IEEE 9th International Colloquium on Signal Processing and Its Applications*, 310–313.

Tillett, N. D. (1991). Automatic guidance sensors for agricultural field machines: A review. *Journal of Agricultural Engineering Research*, *50*, 167–187.

Visser, A., & Groen, F. C. A. (1999). Organisation and design of autonomous systems. Textbook, Faculty of Mathematics. *Computer Science, Physics and Astronomy, University of Amsterdam, Kruislaan*, *403*.

Wu, D., Zhang, Q., & Reid, J. F. (2001). Adaptive steering controller using a Kalman estimator for wheel-type agricultural tractors. *Robotica*, *19*(5), 527–533.

Wu, T. (2017). *Solutions for tractor-trailer path following at low speed*.

Xue, J., Zhang, L., & Grift, T. E. (2012). Variable field-of-view machine vision based row guidance of an agricultural robot. *Computers and Electronics in Agriculture*, *84*, 85–91.

Yin, J., Zhu, D., Liao, J., Zhu, G., Wang, Y., & Zhang, S. (2019). Automatic Steering Control Algorithm Based on Compound Fuzzy PID for Rice Transplanter. *Applied Sciences*, *9*(13), 2666. https://doi.org/10.3390/app9132666

Zhang, M., Ma, W., Liu, Z., & Liu, G. (2013). Fuzzy-adaptive control method for off-road vehicle guidance system. *Mathematical and Computer Modelling*, *58*(3–4), 551–555.

Zhao, P., Chen, J., Song, Y., Tao, X., Xu, T., & Mei, T. (2012). Design of a Control System for an Autonomous Vehicle Based on Adaptive-PID. *International Journal of Advanced Robotic Systems*, *9*(2), 44. https://doi.org/10.5772/51314

Zhou, S., Zhao, H., Chen, W., Miao, Z., Liu, Z., Wang, H., & Liu, Y.-H. (2019). Robust path following of the tractor-trailers system in GPS-denied environments. *IEEE Robotics and Automation Letters*, *5*(2), 500–507.

APPENDIX A. MATLAB CODE

This is a sample code used in chapter 4 and includes the fuzzy logic control design.

```
clearvars; close all; clc;


%% Predefined values
V = 2; % Running speed of tractor [m/s]
L = 150; %Total length of motion [m]
t = L/V; %[s]
dt = 0.05; %The time of passing each step per speed
dL = V*dt/t; %Length of each step [m]
N = round(L/dL);


%% Tractor and implement constant values
Lr = 1.700;    %Distance from tractor front wheel to its center of gravity [m]
Lf = 1.200;    %Distance from tractor rear wheel to its center of gravity [m]
Lc = 4; %Distance from implement center of gravity to the hitch point [m]
a = 0.500; %Distance from tractor center of gravity to the hitch point [m]
R = 0.1; %Hitch arm length [m]
Lt = (Lf+Lr); %Wheel base [m]


XT(1)=0; YT(1)=0; %Tractor initial location
XC(1) = -(Lr+a+R+Lc); YC(1) = 0; %Implement initial location
delta_t=(Lr+a+R+Lc)/V; %time difference between tractor CG and implement CG
```

```
%% Pattern generating
%Straight Part
L1 =linspace(0, L/6, 4); %The x-axis points
Y1 = [0 0 0 0];
Track_Shape1 = Y1;
%Zigzag Part
L2 = linspace((L/6)+5, (L/2)-5, 10); %The x-axis points
Y2 = [0 0.1 0.2 0.1];
Track_Shape2 = [Y2 Y2 0 0.1];
% Sinusoidal Part
L3 = linspace((L/2), L-55, 20); %The x-axis points
[P2, t2] = gensig('sine', 2, 3, 0.155);
Track_Shape3 = (P2+1)/10;
% Square Part
L4 = linspace(L-50, L-20, 20); %The x-axis points
[P3, t3] = gensig('square', 2, 4, 0.21);
Track_Shape4 = (P3+1)/10;
%Straight Part
L5 = linspace(L-15, L, 4); %The x-axis points
Y5 = [0 0 0 0];
Track_Shape5 = Y5;
% Generating the mixed pattern
L6 = [L1 L2 L3 L4 L5];
```

```
Track_Shape = [Track_Shape1 Track_Shape2 Track_Shape3' Track_Shape4'
Track_Shape5];
plot(L6, Track_Shape, 'b--o','linewidth', 1.5);
xlabel('X [m]');
ylabel('Y [m]');  hold on;

%% Reference line x-y
Xref = linspace(0, L, N);
Yref = interp1(L6, Track_Shape, Xref);
t1 = linspace(0, t, N);
XT_REF = [t1' Xref'];
YT_REF = [t1' Yref'];

%% Reference pattern for implement
t4= t1'-delta_t;
XCref = zeros(numel(t1),1);
YCref = zeros(numel(t1),1);
for jj = 1:numel(t4)
    if t4(jj) < 0
        XCref(jj) = 0;
        YCref(jj) = 0;
    else
        [minval index] = min(abs(t4(jj)-t1'));
```

```
        XCref(jj) = Xref(index);
        YCref(jj) = Yref(index);
    end
end
XC_REF = [t1' ,XCref];
YC_REF = [t1' ,YCref];

%% Fuzzy logic
controller = readfis('FUZZFILE.fis');
controller2 = readfis('newfuncfuzz.fis');
[t5, O] = sim('tylorexpansion');
u = ucontrol.Data;
XC = XC.Data;
YC = YC.Data;
NO_Control_Xc = NO_Control_Xc.Data;
NO_Control_Yc = NO_Control_Yc.Data;

coverage = zeros(1,numel(XC));
XCEr = zeros(1,numel(XC));
for k = 1:numel(XC)-1
    YCEr(k) = YC(k)-YCref(k);
    XCEr(k) = XC(k)-XCref(k);
```

```
    if abs(YCEr(k)) < 0.01 && abs(XCEr(k)) <0.1
        coverage(k) = 1;
    else
        coverage(k) = 0;
    end
end
n = find(coverage == 1);
C_P = numel(n)*100/numel(coverage)

%% tractor & implement CG plot
M = movmean(O(:,2),6);
M1 = movmean(YC,6);
M2 = movmean(NO_Control_Yc,6);
plot(O(:,1), M, 'r-','linewidth', 1.5); hold on
plot(NO_Control_Xc, M2, 'm-.','linewidth', 1.5); hold on
plot(XC, M1, 'k:', 'linewidth', 1.5)
legend('Reference Pattern' ,'Tractor Control Model Pattern','Passive Implement Control',
'Active Implement Control')
xlim([-0 L]);
grid on
hold off
alpha=alpha.Data;
```

APPENDIX B. FUZZY LOGIC CONTROLLER RULES

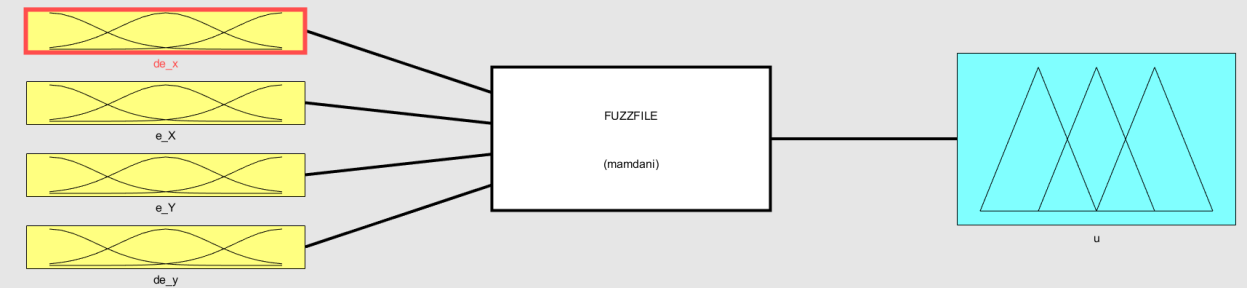

Figure B1. 'FUZZFILE.fis' Membership Function for the tractor used in MATLAB code given in APPENDIX A

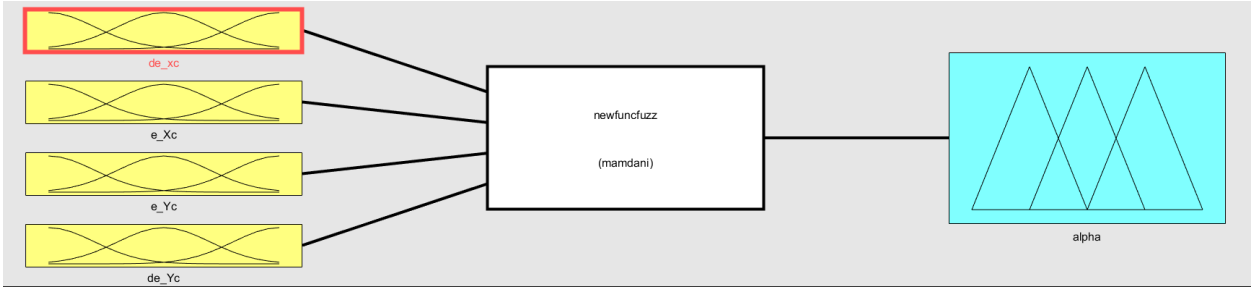

Figure B2. 'newfuncfuzz.fis' Membership Function for the towed implement used in MATLAB code given in APPENDIX A